

UNCLASSIFIED

AD NUMBER
AD880069
NEW LIMITATION CHANGE
TO Approved for public release, distribution unlimited
FROM Distribution authorized to U.S. Gov't. agencies and their contractors; Critical Technology; AUG 1970. Other requests shall be referred to Air Force Armament Laboratory, ATTN: ADLRD, Eglin AFB, FL 32542.
AUTHORITY
AFATL ltr dtd 4 Oct 1972

THIS PAGE IS UNCLASSIFIED

② 230

AFATL-TR-70-87

880069

AD No. _____
DEC FILE COPY

**FOLLOW-ON STUDIES
ON THE
BALLISTIC IMPACT
OF COMPOSITE MATERIALS**

DEPARTMENT OF ENGINEERING SCIENCE AND MECHANICS
UNIVERSITY OF FLORIDA

TECHNICAL REPORT AFATL-TR-70-87

AUGUST 1970

DTIC
RECEIVED
FEB 16 1971
RECEIVED
E

This document is subject to special export controls and each transmittal to foreign governments or foreign nationals may be made only with prior approval of the Air Force Armament Laboratory (ADLRD), Eglin AFB, Florida 32542.

AIR FORCE ARMAMENT LABORATORY

AIR FORCE SYSTEMS COMMAND • UNITED STATES AIR FORCE

EGLIN AIR FORCE BASE, FLORIDA

Follow-On Studies
on the
Ballistic Impact
of Composite Materials

R. L. Sierakowski

G. E. Nevill, Jr.

C. A. Ross

E. R. Jones

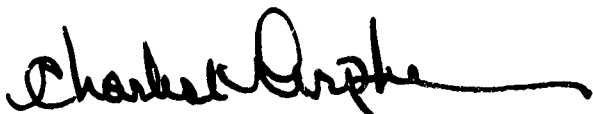
This document is subject to special export controls and each transmittal to foreign governments or foreign nationals may be made only with prior approval of the Air Force Armament Laboratory (ADLRD), Eglin AFB, Florida 32542.

FOREWORD

This final report documents research accomplished during the period July 1969 to July 1970 by the Department of Engineering Science and Mechanics of the University of Florida, Gainesville, Florida, under Contract F08635-68-C-0115 with the Air Force Armament Laboratory, Eglin Air Force Base, Florida. Mr. Leonard L. Wilson (ADLRD) was program monitor for the Armament Laboratory.

Information in this report is embargoed under the Department of State International Traffic In Arms Regulations. This report may be released to foreign governments by departments or agencies of the U. S. Government subject to approval of the Air Force Armament Laboratory (ADLRD), Eglin AFB, Florida 32542, or higher authority within the Department of the Air Force. Private individuals or firms require a Department of State export license.

This technical report has been reviewed and is approved.



CHARLES K. ARPKE, Lt Colonel, USAF
Chief, Technology Division

ABSTRACT

The dynamic compressive and wave propagation behavior of unidirectional reinforced composite specimens has been investigated. Studies have been conducted on both metal matrix and non-metal matrix reinforced systems. Emphasis has been placed on fabricating high quality and reproducible specimens from each of these primary groups. In addition, tests have been conducted on specimens received from industrial sources which are of current practical interest. Mechanical properties tests have been conducted using a conventional Tinius Olsen and Split Hopkinson Pressure Bar System in order to investigate composite strain rate sensitivity and load carrying capability. Further, failure/fracture studies have been conducted by projecting the various composite specimens at a rigid elastic target. Analytical criteria have been utilized in order to establish predictable bounds on composite failure/fracture characteristics for potential application to terminal ballistics design. Satisfactory failure/fracture predictors have been defined for both brittle and ductile matrix composites. Correlation and verification of established criteria has been obtained from terminal ballistics behavior of composite specimens as observed from photographic recordings of the impact event. Finally, studies of wave propagation, attenuation, and dispersement have been conducted in order to establish criteria for evaluating energy transfer and absorption properties of composites as well as varying wave speeds for failure by controlled fragmentation.

This document is subject to special export controls and each transmittal to foreign governments or foreign nationals may be made only with prior approval of the Air Force Armament Laboratory (ADLRD), Eglin AFB, Florida 32542.

TABLE OF CONTENTS

Section	Title	Page
I	Introduction	1
II	Mechanical Properties	3
III	Failure/Fracture Studies	46
IV	Wave Propagation Studies	60
	Appendix	74
	References	77

LIST OF FIGURES

Figure	Title	Page
1	Fabricated Steel Epoxy-Test Specimens Varying Volume Fractions and Wire Sizes	4
2	Stress-Strain Curves for Steel-Epoxy Composites $V_f = 10\%$ Wire Diameter = 0.004 Inch	6
3	Stress-Strain Curves for Steel-Epoxy Composites $V_f = 10\%$ Wire Diameter = 0.008 Inch	7
4	Stress-Strain Curves for Steel-Epoxy Composites $V_f = 10\%$ Wire Diameter = 0.016 Inch	8
5	Stress-Strain Curves for Steel-Epoxy Composites $V_f = 26\%$ Wire Diameter = 0.004 Inch	9
6	Stress-Strain Curves for Steel-Epoxy Composites $V_f = 26\%$ Wire Diameter = 0.008 Inch	10
7	Stress-Strain Curves for Steel-Epoxy Composites $V_f = 26\%$ Wire Diameter = 0.016 Inch	11
8	Stress-Strain Curves for Steel-Epoxy Composites $V_f = 40\%$ Wire Diameter = 0.004 Inch	12
9	Stress-Strain Curves for Steel-Epoxy Composites $V_f = 40\%$ Wire Diameter = 0.008 Inch	13
10	Stress-Strain Curves for Steel-Epoxy Composites $V_f = 40\%$ Wire Diameter = 0.016 Inch	14
11	Dynamic Stress-Strain Curves (a) Epoxy $V_f = 0\%$ (b) $V_f = 26\%$ Wire Diameter = 0.004 Inch (c) $V_f = 26\%$ Wire Diameter = 0.008 Inch (d) $V_f = 26\%$ Wire Diameter = 0.016 Inch	15

LIST OF FIGURES (Continued)

Figure	Title	Page
12	Dynamic Stress-Strain Curves (a) E-glass fiberglass (b) $V_f = 10\%$ Wire Diameter = 0.008 Inch (c) $V_f = 26\%$ Wire Diameter = 0.008 Inch (d) $V_f = 40\%$ Wire Diameter = 0.008 Inch	15
13	Predicted and Measured Compressive Strengths for Steel-Epoxy Composites	16
14	Steel-Epoxy Composites, Failure Modes	17
15	Maximum Stress Versus Wire Diameter for Steel-Epoxy Composites	18
16	Stress Versus Strain Rate with Varying Strain, Steel-Epoxy Composites $V_f = 26\%$ Wire Diameter = 0.004 Inch	20
17	Stress Versus Strain Rate with Varying Strain, Steel-Epoxy Composites $V_f = 26\%$ Wire Diameter = 0.008 Inch	21
18	Stress Versus Strain Rate with Varying Strain, Steel-Epoxy Composites $V_f = 26\%$ Wire Diameter = 0.016 Inch	22
19	Stress Versus Volume Fraction at One Percent Strain for High and Low Strain Rates Wire Diameter = 0.004 Inch	23
20	Stress Versus Volume Fraction at One Percent Strain for High and Low Strain Rates Wire Diameter = 0.008 Inch	24
21	Stress Versus Volume Fraction at One Percent Strain for High and Low Strain Rates Wire Diameter = 0.016 Inch	25

LIST OF FIGURES (Continued)

Figure	Title	Page
22	Maximum Stress Versus Strain Rate for Steel-Epoxy Composites Varying Volume Fraction Wire Diameter = 0.004 Inch	26
23	Maximum Stress Versus Strain Rate for Steel-Epoxy Composites Varying Volume Fraction Wire Diameter = 0.008 Inch	27
24	Maximum Stress Versus Strain Rate for Steel-Epoxy Composites Varying Volume Fraction Wire Diameter = 0.016 Inch	28
25	Al ₃ Ni Microstructures (a) Solidification Rate 11 Cm/Inch (b) Solidification Rate 0.6 Cm/Inch	30
26	Stress-Strain Curve for Aluminum-Nickel Composite, Whisker-Type Reinforcement	32
27	Stress-Strain Curve for Aluminum-Nickel Composite, Plate-Like Reinforcement	33
28	Hopkinson Bar Stress-Strain Curves for Aluminum-Nickel Composites (a) Whisker-Type Reinforcement (b) Plate-Like Reinforcement (c) Matrix Material, Pure Aluminum	34
29	Aluminum-Nickel Composites Failure Modes for Given Strain Rates	34
30	Deformation Behavior of Aluminum-Nickel Composites, Hopkinson Bar Test	35
31	Stress Versus Strain Rate at One Percent Strain Aluminum-Nickel Composite and Pure Aluminum	36

LIST OF FIGURES (Continued)

Figure	Title	Page
32	Winding Mandrel for Tungsten-Copper Specimens	38
33	Crucible and Winding Mandrel, with Spacers, for Fabrication of Tungsten-Copper Specimens by Liquid Infiltration	39
34	Cross Section View of Tungsten-Copper Specimens	41
35	Dynamic Stress-Strain Curves, Tungsten-Copper (a) Tungsten-Copper 0.125 Inch Diameter Rod Reinforcement (b) Tungsten-Copper 0.250 Inch Diameter Rod Reinforcement (c) Tungsten-Copper $V_f = 10\%$ Wire Diameter = 0.004 Inch (d) Tungsten-Copper $V_f = 10\%$ Wire Diameter = 0.008 Inch	42
36	Dynamic Stress-Strain Curves (a) Tungsten 0.25 Inch Rod Diameter (b) Cold Drawn Copper (c) Boron-Epoxy $V_f = 65\%$ Filament Diameter = 0.004 Inch (d) Graphite-Epoxy $V_f = 50\%$ Morganite I Filament Diameter = 0.0003 Inch	42
37	Critical Fracture Velocity Versus Wire Diameter for Steel Epoxy-Composites $V_f = 10\%, 26\%, 40\%$	47
38	Critical Plastic Flow Velocity Versus Wire Diameter for Steel-Epoxy Composites $V_f = 10\%, 26\%, 40\%$	48

LIST OF FIGURES (Continued)

Figure	Title	Page
39	Dynamic Target Impact Behavior of Aluminum-Nickel (a) Whisker Type Reinforcement, Impact Velocity = 19,050 In/Second (b) Plate-Like Reinforcement, Impact Velocity = 16,000 In/Second	50
40	Dynamic Deformation at Various Impact Velocities Aluminum-Nickel Composites End View $V_f = 11\%$	51
41	Dynamic Deformation at Various Impact Velocities Aluminum-Nickel Composites End View $V_f = 11\%$	51
42	Dynamic Target Impact Behavior of Tungsten-Copper Composites	52
43	Dynamic Deformation at Various Impact Velocities Tungsten-Copper Filament Composites $V_f = 10\%$ (a) Side View (b) End View	54
44	Dynamic Deformation at Various Impact Velocities Tungsten-Copper Rod Reinforced Composites $V_f = 10\%$ (a) Side View (b) End View	55
45	Dynamic Stress Versus Volume Fraction for Tungsten-Copper Composites	56
46	Dynamic Deformation at Various Impact Velocities Graphite-Epoxy and Boron-Epoxy	57
47	Dynamic Deformation Summary	57
48	Aluminum Mold Used for Fabrication of Steel-Epoxy Composite Rods	62
49	End View of Fabricated Composite Rods	63'

LIST OF FIGURES (Continued)

Figure	Title	Page
50	Experimental Test Setup for Wave Propagation Studies	64
51	Experimental Wave Propagation Results (a) Epoxy (b) Steel (c) Steel-Epoxy Rod $V_f = 10\%$ Wire Diameter = 0.008 inch (d) Steel-Epoxy Rod $V_f = 10\%$ Wire Diameter = 0.016 inch	65
52	Experimental Wave Propagation Results (a) Steel-Epoxy Rod $V_f = 26\%$ Wire Diameter = 0.008 inch (b) Steel-Epoxy Rod $V_f = 26\%$ Wire Diameter = 0.016 inch (c) Steel-Epoxy Rod $V_f = 40\%$ Wire Diameter = 0.016 inch	66
53	Experimental Wave Propagation Results (a) Epoxy (b) Steel (c) Steel-Epoxy Rod $V_f = 10\%$ Wire Diameter = 0.008 inch (d) Steel-Epoxy Rod $V_f = 10\%$ Wire Diameter = 0.016 inch	66
54	Experimental Wave Propagation Results (a) Steel-Epoxy Rod $V_f = 26\%$ Wire Diameter = 0.008 inch (b) Steel-Epoxy Rod $V_f = 26\%$ Wire Diameter = 0.016 inch (c) Steel Epoxy Rod $V_f = 40\%$ Wire Diameter = 0.016 inch	67
55	Rule of Mixtures Prediction for Composite Wave Velocities	69
56	Rule of Mixtures Prediction for Composite Attenuation	70

LIST OF FIGURES (Concluded)

Figure	Title	Page
I-1	Composite Plate Mounted for Impact Test	75
I-2	Fracture Pattern of Penetrated Composite Plate	76

LIST OF TABLES

Table	Title	Page
I	Volume Fractions and Wire Sizes Tested	4
II	Fabrication Methods for Stable Systems	37
III	Wave Speeds of Test Specimens	67
IV	Wave Attenuation for Test Specimens	69

SECTION I

INTRODUCTION

The studies reported herein are a continuation of the investigation of dynamic compressive and wave propagation behavior of unidirectional reinforced composite specimens.

As demonstrated by recent articles appearing in technical journals, the analysis and applications of composite materials for various aircraft systems is a current and active area. Further, the ability to custom design composite material properties by varying the reinforcement arrays and volume fraction for static applications is being incorporated into design procedures. Composite dynamic behavior is less fully explored and is discussed in Reference 1. In order to assess the important parameters associated with one technologically important problem area, ballistic performance, a continued effort to define and optimize important composite material properties affecting dynamic response characterization has been pursued.

The present program is a continued effort to systematically determine and evaluate the dynamic properties and fracture behavior of several representative filamentary and whisker reinforced composites. The particular composites studied are steel reinforced epoxy, E-glass fiberglass, aluminum-nickel reinforced aluminum, tungsten reinforced copper, boron-epoxy and graphite-epoxy. Geometrical variations among selected specimens included variable fiber diameter, fiber spacing and volume percent of reinforcement. Included in the results is tabulated data on the dynamic properties of the composites tested, fracture characteristics including velocity, attenuation, and dispersion.

The present experimental program has involved three basic types of testing procedures. To determine mechanical properties data for the composite materials, tests have been performed involving low strain rate compression (in the order of 10^{-5} to 10^{-3} /sec) using a Tinius Olsen Testing Machine, and high strain rate testing (in the order of 10^3 /sec) using a Split Hopkinson Pressure Bar system. For determining fracture characteristics

of the composite specimens, a series of ballistic impact tests using an air gun assembly has been utilized to fire composite specimens at a massive elastic target. An image converting camera has been used to record the impact event and establish visual observation of specimen delamination and fracture. The third test program conducted has involved wave propagation studies including measurements of velocity of wave transmittal, attenuation, and dispersion characteristics. To obtain this information, a series of long bar impact tests has been conducted. The air gun assembly has been used to fire an impacting projectile at essentially freely suspended three-foot long thin bar composite specimens instrumented to record appropriate dynamic properties.

Specific information obtained from this program includes a quantitative evaluation of composite strain rate sensitivity, geometric effects such as reinforcement size, spacing and density, constituent property relations, specimen fracture energies, wave velocities, and wave attenuation characteristics. In addition, qualitative information on the nature and characteristics of specimen delamination and fracture and wave dispersion have been obtained.

SECTION II

MECHANICAL PROPERTIES

In order to establish information for potential correlation with the fracture and wave propagation studies, a series of mechanical property tests has been conducted on various composite specimens in the compression mode following the procedures described in Reference 1. These tests have utilized a Tinius Olsen Testing Machine for low strain rates and a Split Hopkinson Pressure Bar for high rates. The use of this equipment for the test program is discussed in Reference 1. Care has been exercised in all of these tests to insure minimum end friction effects by lubricating the specimen end surfaces with molybdenum disulfide grease. In addition, care was taken to accept results only from specimens which displayed no premature debonding or splitting-type failures. Materials property data obtained by these test techniques is further described for each of the respective test specimens in the following paragraphs.

2.1 Steel-Epoxy

A comprehensive description of the fabrication and test results for this series of specimens has been reported on in References 1 and 2. This model system was selected for extensive study as a representative and readily controlled and fabricated model or simulation of advanced type composites. The flexibility of this system in terms of fabrication procedures as well as variability of the constituent component properties to include both brittle and ductile type reinforcements is possible. A further discussion of this model system and its properties is presented in Reference 3.

In References 1 and 2 data is reported for a series of wire sizes and volume percent reinforcements. The present program has involved a more detailed study of the mechanical properties of such uniaxially reinforced specimens using additional ductile fibers of varying size and volume percent.

For ease in comparing results, some of the data reported in Reference 1 is repeated in this report. Table I lists the combinations of wire size and volume percent of reinforcement tested. Some typical cross sections of specimens tested are shown in Figure 1.

TABLE I. VOLUME FRACTIONS AND WIRE SIZES TESTED

Volume Percent	10	26	40
Wire Size	0.004 in.	0.004 in.	0.004 in.
	0.008	0.008	0.008
	0.016	0.016	0.016

STEEL-EPOXY
TYPICAL CROSS-SECTIONS
 Vol. Fract. in % Wire Dia. in inches

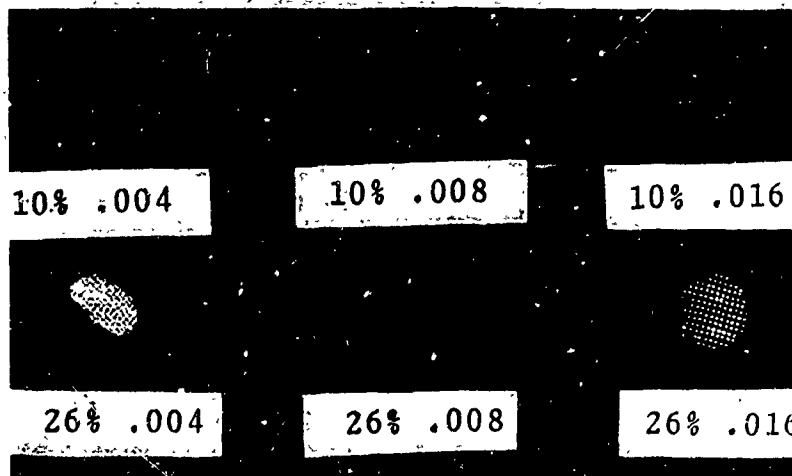


Figure 1. Fabricated Steel-Epoxy Test Specimens Varying Volume Fractions and Wire Sizes V_f in % and Wire Diameter in Inches

In Figures 2 through 10, the stress-strain curves associated with each of the wire sizes and volume fractions are shown plotted with strain rate as a parameter. Also shown in Figures 11 and 12 are some typical dynamic stress-strain curves obtained from the Hopkinson Pressure Bar. Each curve represents the average results of at least three samples tested at the corresponding strain rate. From the results obtained, the following observations are noted. First, composite strength is observed to increase over 50 to 100 percent in going from quasi-static to intermediate strain rates. Secondly, the influence of varying wire size on specimen load carrying capability for a fixed volume percent at the high strain rates appears small. In the low strain rate region, however, it is observed that the smaller wire sizes for corresponding volume percent of reinforcing material produce higher stress values. Further, increasing the volume percent of filaments results in higher load carrying capacity for the specimens in the low strain rate region. In addition, the high volume percent reinforced specimens are observed to respond in a more elastic manner to failure.

In order to correlate the low strain rate data with proposed models of compressive failure, a comparison was made with the buckling type criteria established in Reference 4. The experimental results are shown plotted in Figure 13 in conjunction with the theoretically proposed buckling criteria. As has been found, for example, by other investigators, ^(5,6,7,8) the experimental data falls considerably below the theoretical. The reason for this discrepancy can be attributed to the inherent theoretical model, which is based on two dimensional planar buckling of plate-like elements on an elastic foundation. Such failure modes are high energy modes and do not coincide with the observed failure characteristics of compression specimens as documented in Figure 14. In fact, for the ductile-type reinforcements tested in the present work, the principal failure modes appeared as a symmetrical failure mode characterized by localized matrix shear accompanied by fiber bending/buckling. In some cases out-of-plane helical deformation as described in Reference 3 was obtained and can be observed in Figure 14.

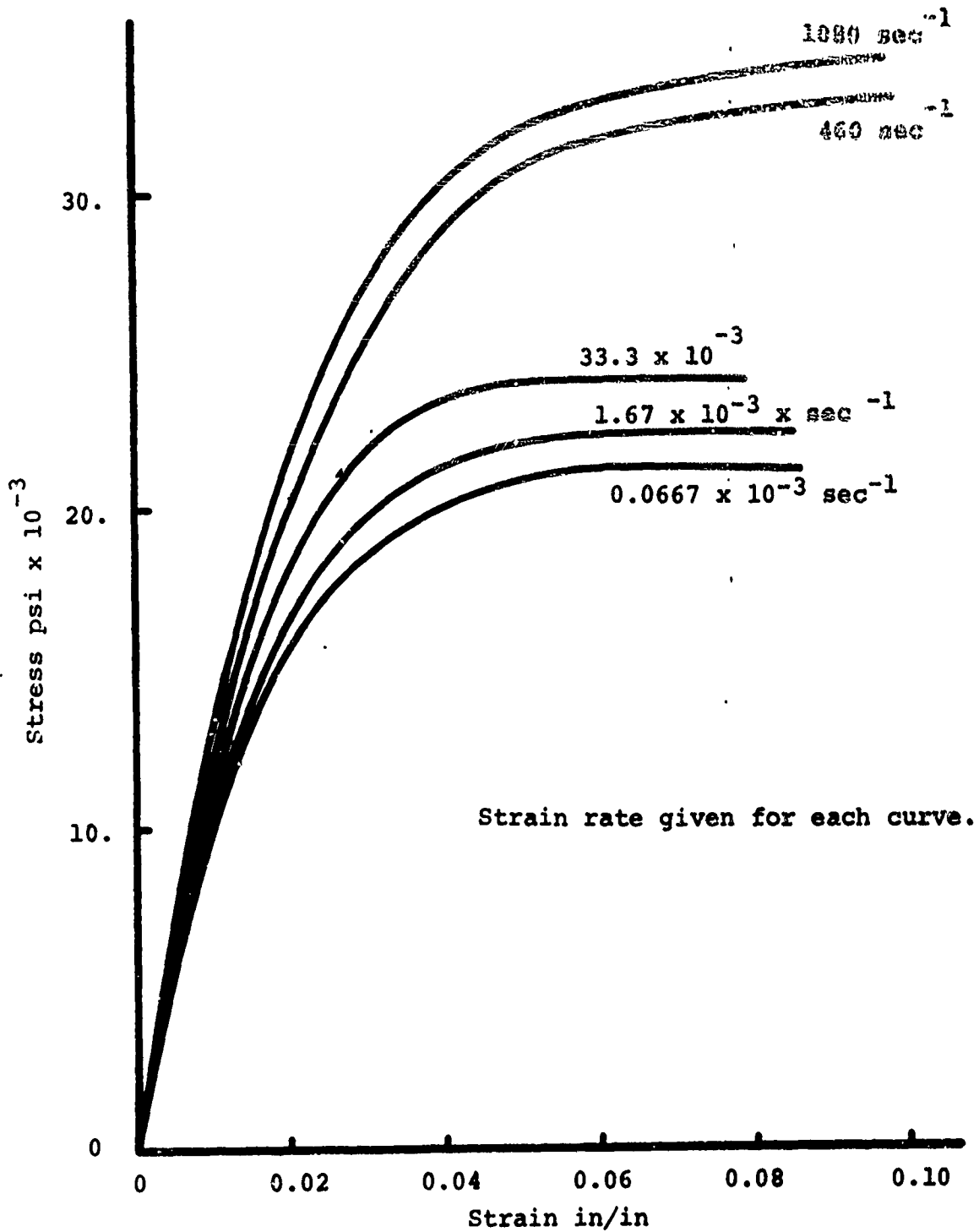


Figure 2. Stress-Strain Curves for Steel-Epoxy Composites
 $V_f = 10\%$ Wire Diameter = 0.004 Inch

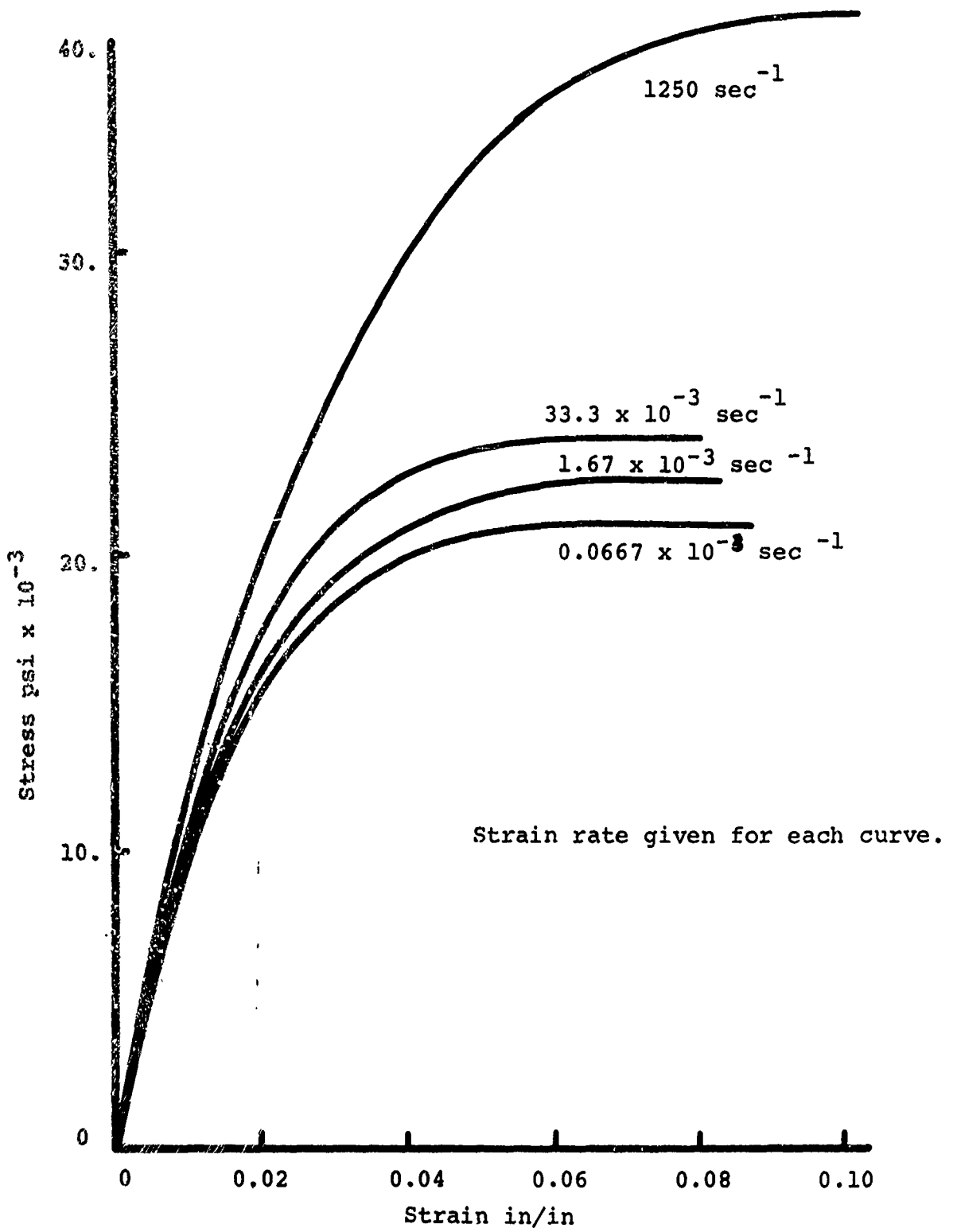


Figure 3. Stress-Strain Curves for Steel-Epoxy Composites
 $V_f = 10\%$ Wire Diameter = 0.008 Inch

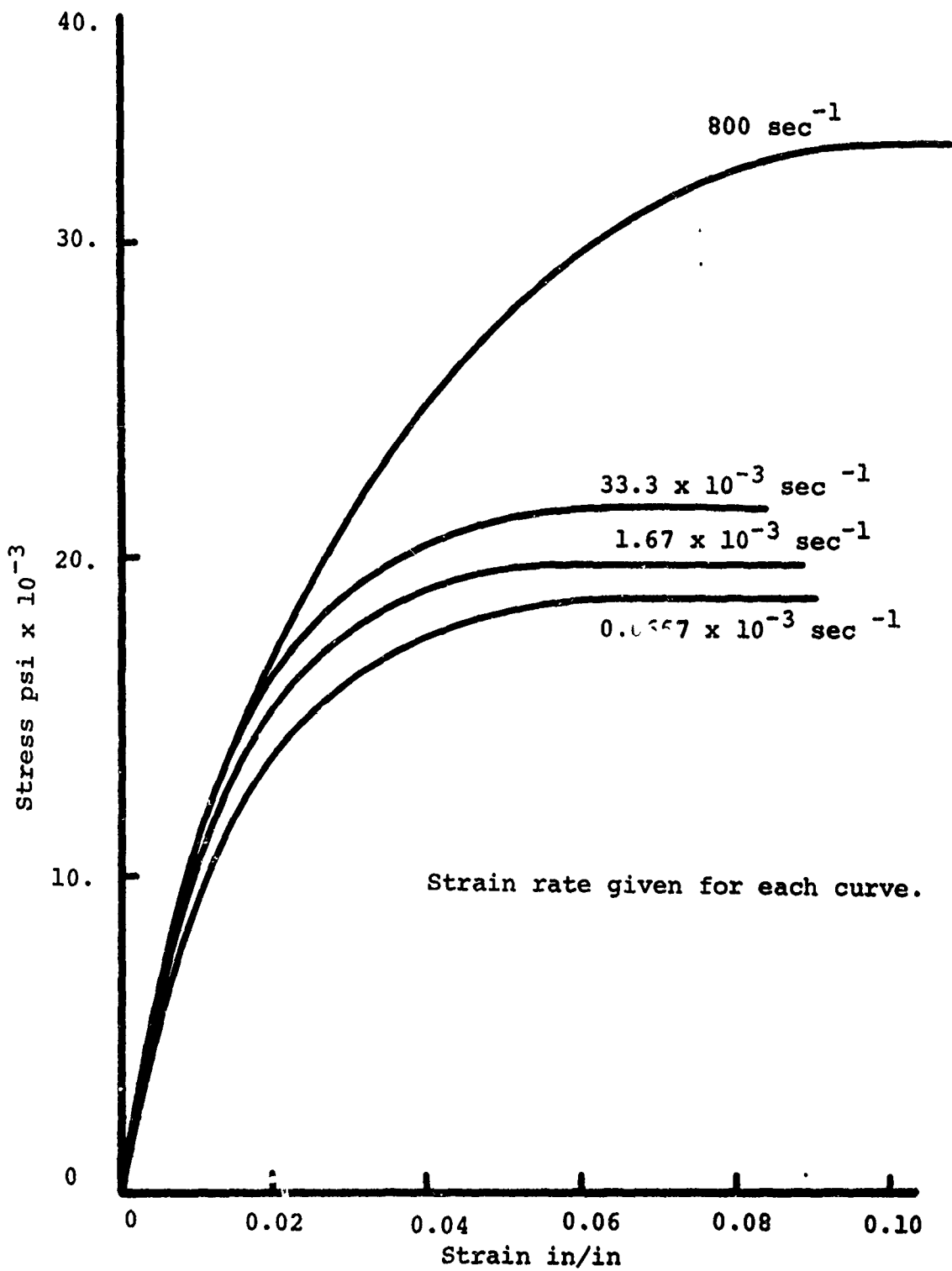


Figure 4. Stress-Strain Curves for Steel-Epoxy Composites
 $V_f = 10\%$ Wire Diameter - 0.016 Inch

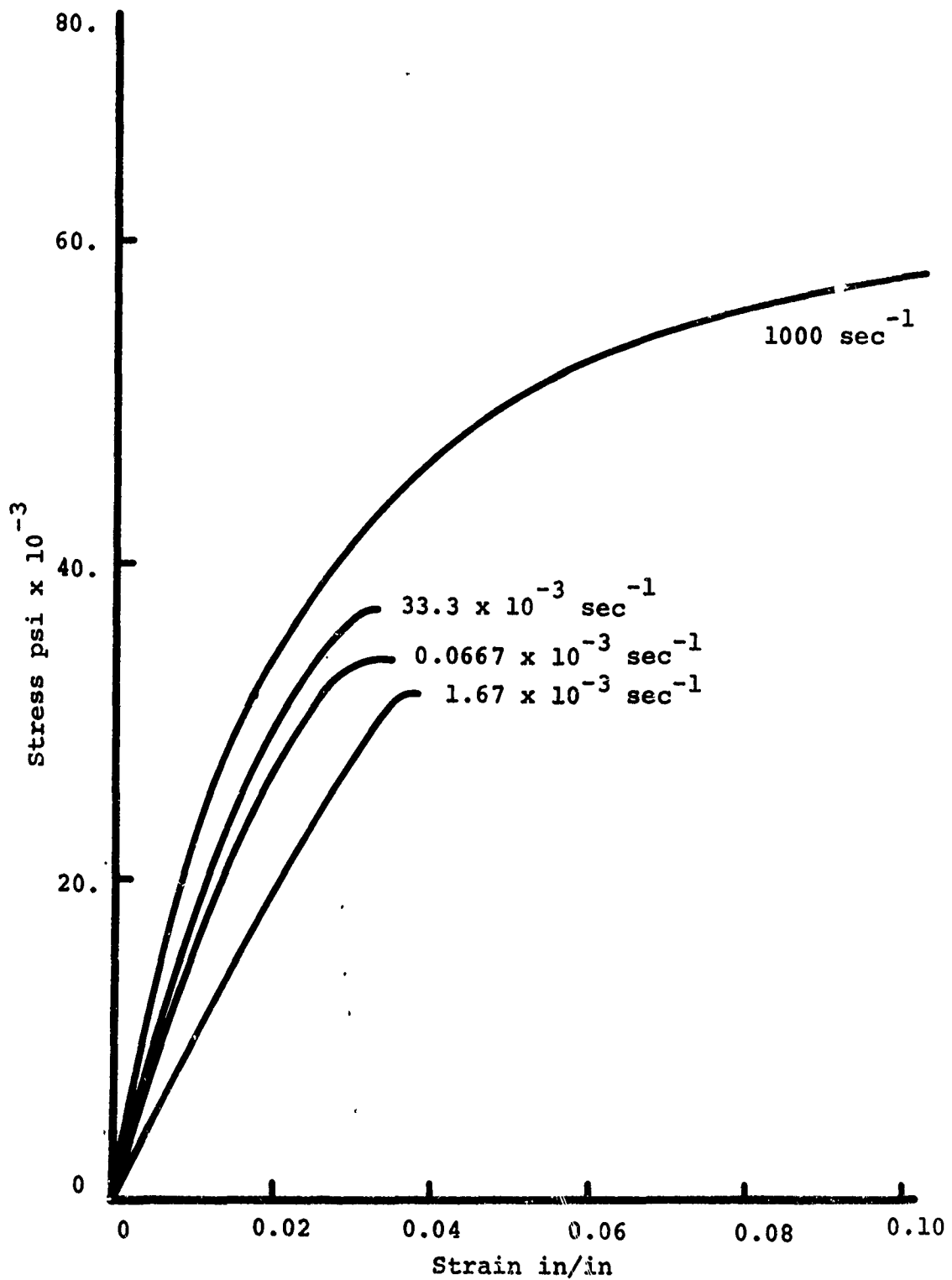


Figure 5. Stress-Strain Curves for Steel-Epoxy Composites
 $V_f = 26\%$ Wire Diameter = 0.004 Inch

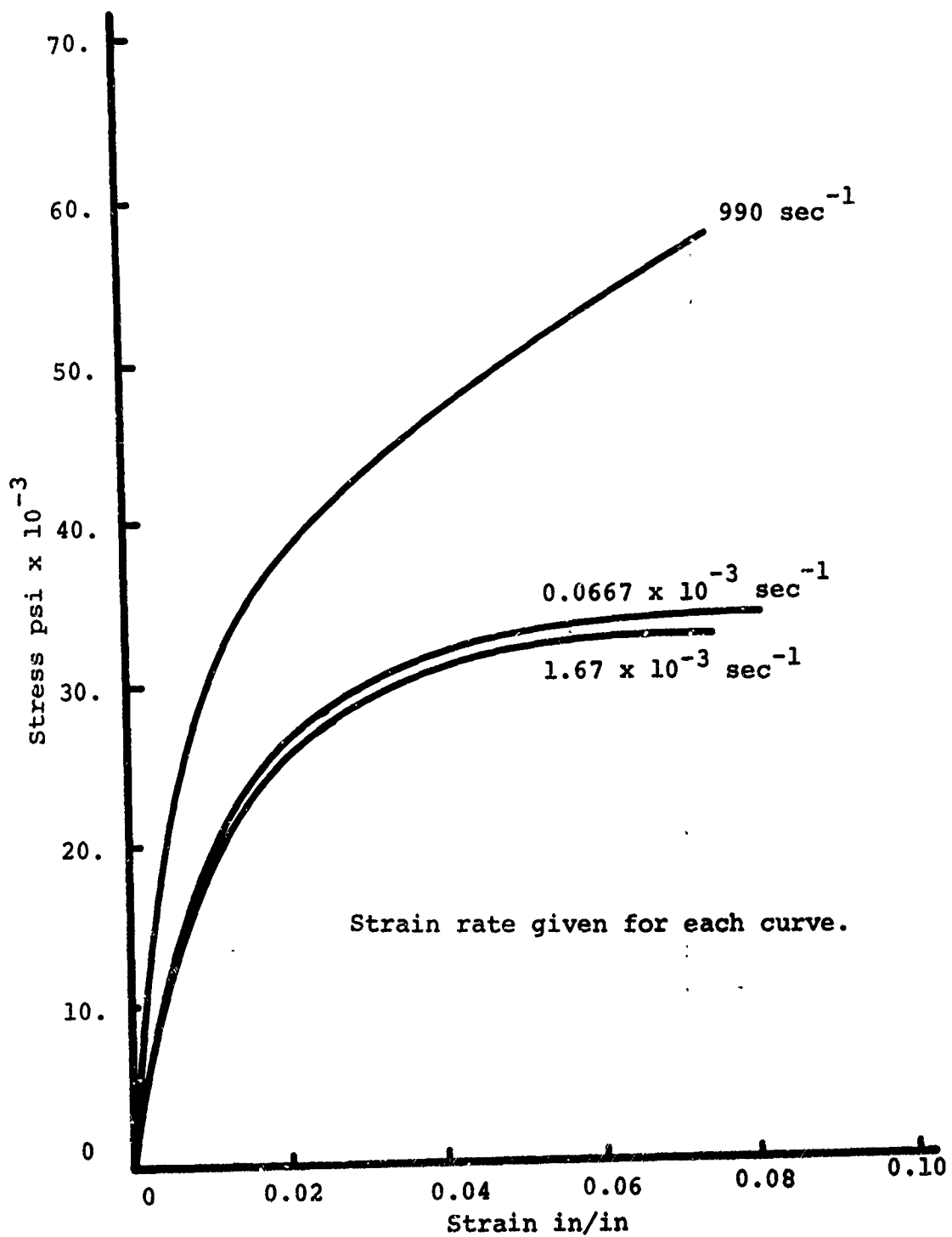


Figure 6. Stress-Strain Curves for Steel-Epoxy Composites
 $V_f = 26\%$ Wire Diameter = 0.008 Inch

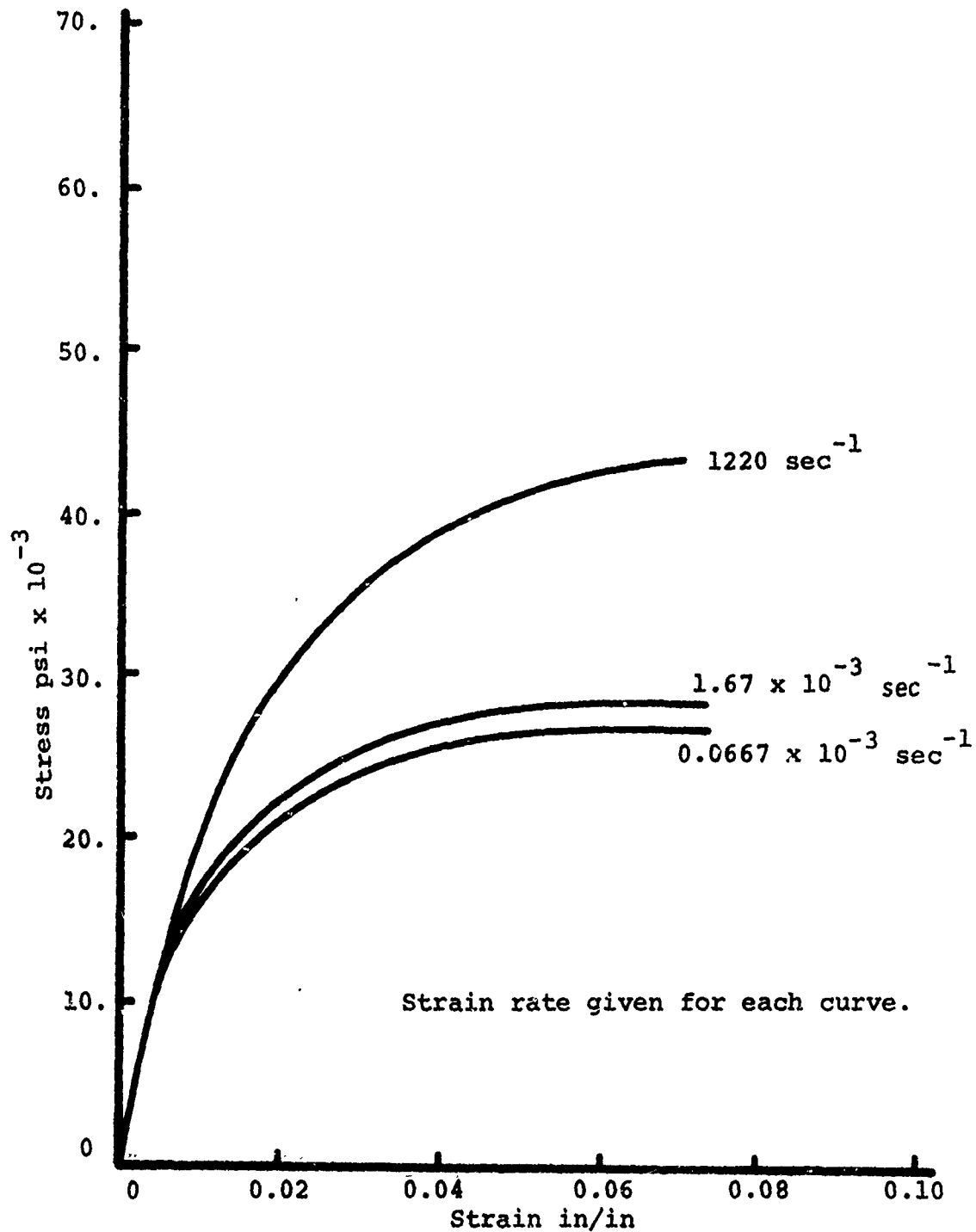


Figure 7. Stress-Strain Curves for Steel-Epoxy Composites
 $V_f = 25\%$ Wire Diameter = 0.016

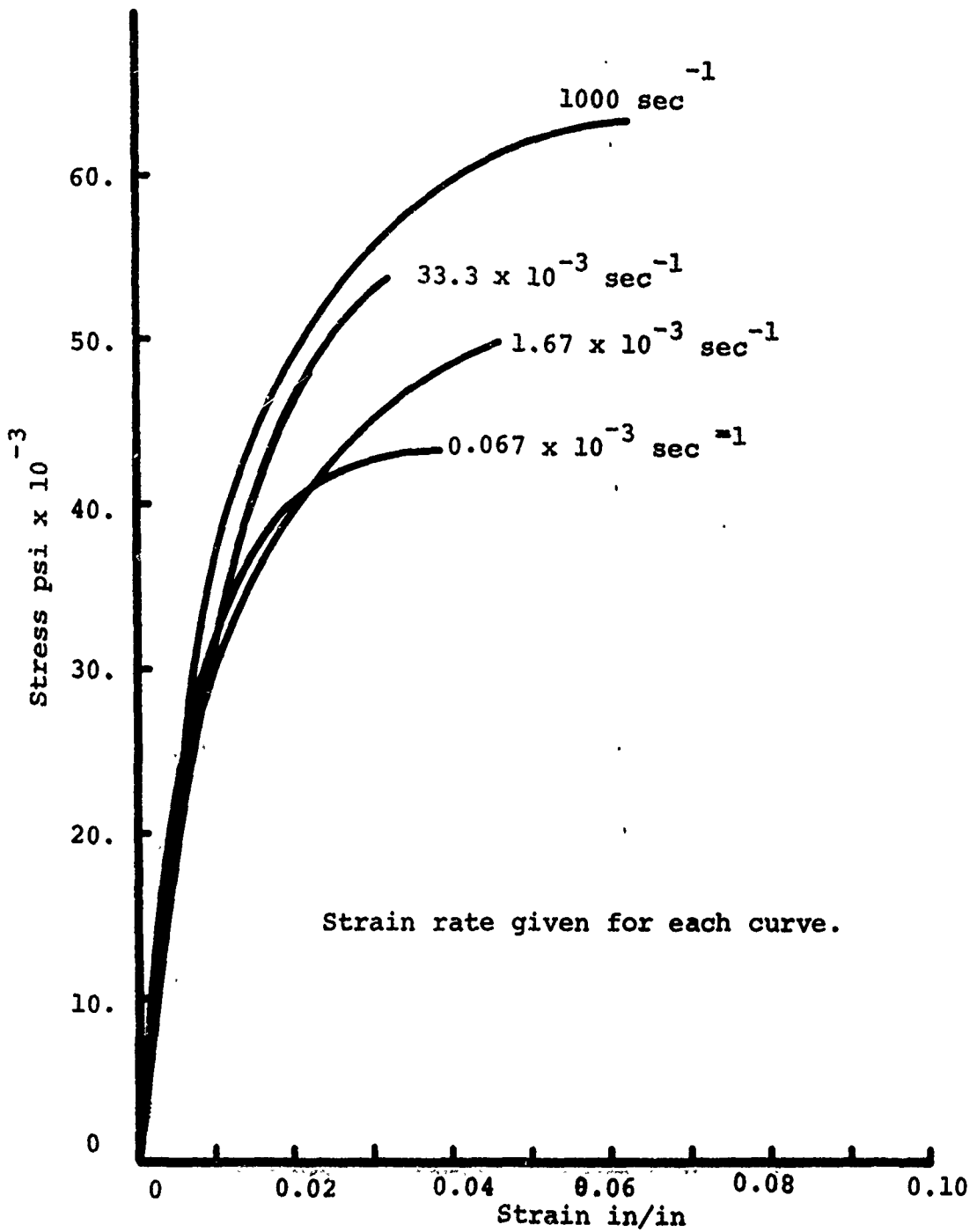


Figure 8. Stress-Strain Curves for Steel-Epoxy Composites $V_f = 40\%$ Wire Diameter = 0.004 Inch

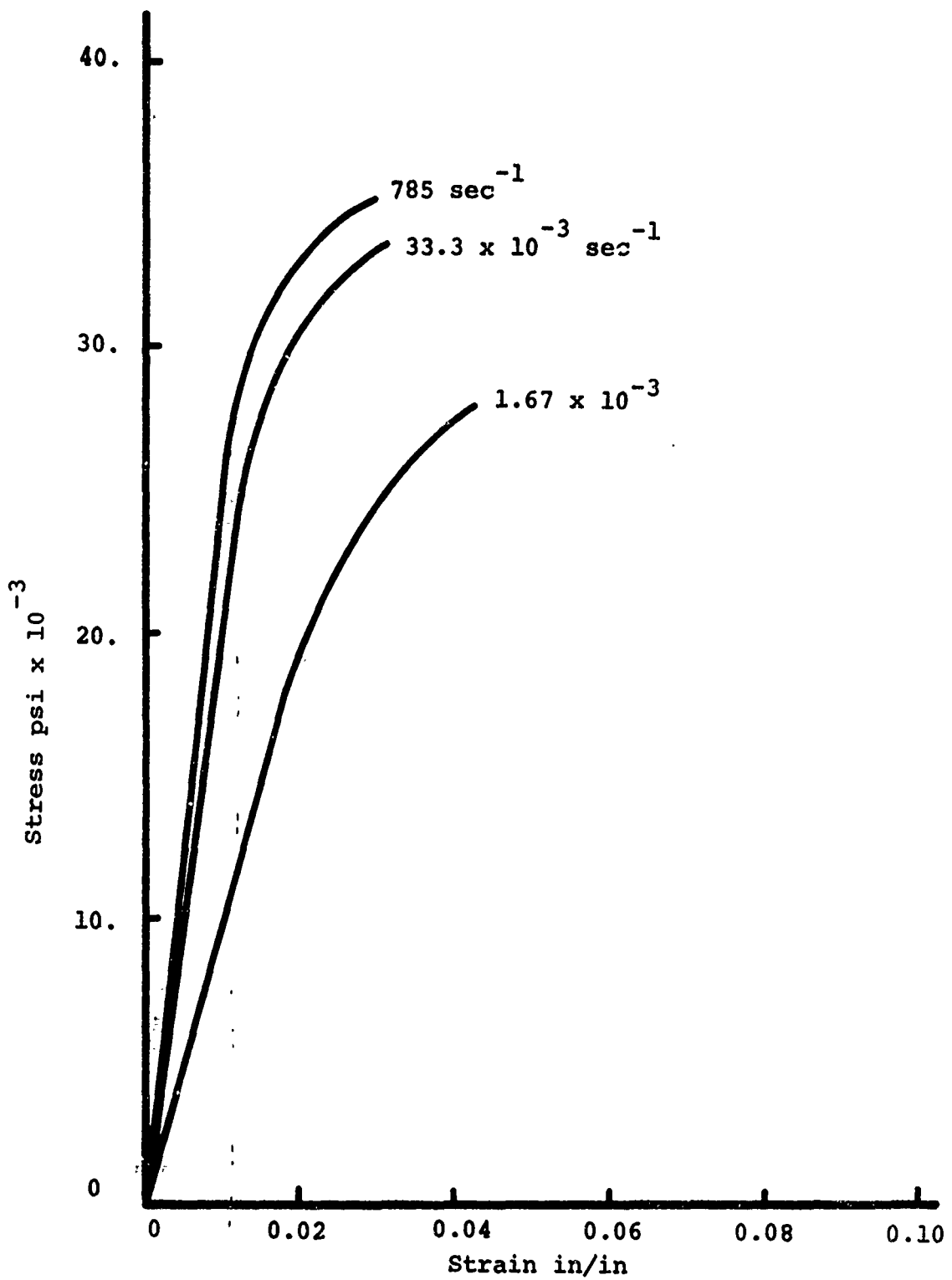


Figure 9. Stress-Strain Curves for Steel-Epoxy Composites $V_f = 40\%$ Wire Diameter = 0.008 Inch.

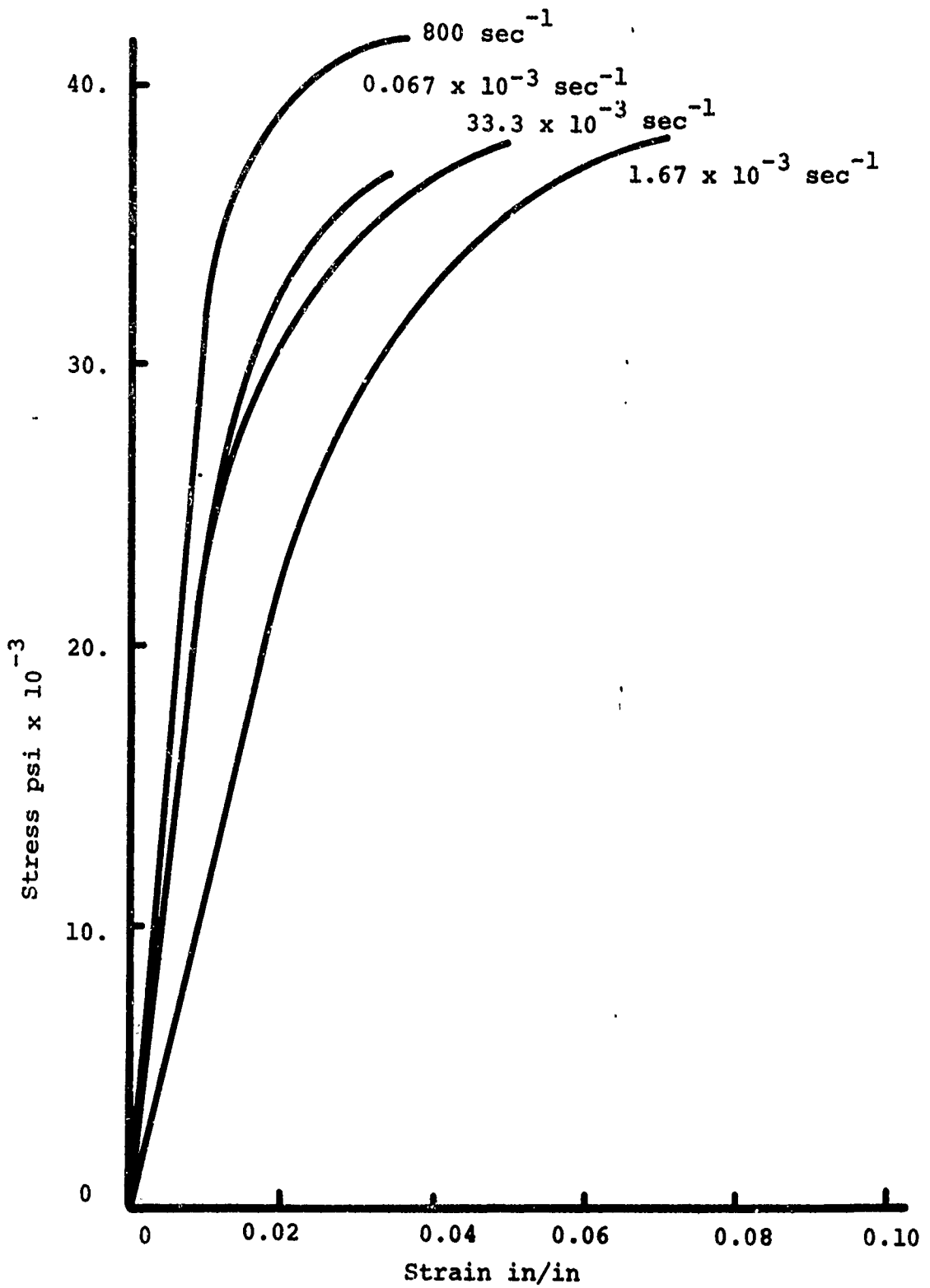


Figure 10. Stress-Strain Curves for Steel-Epoxy Composites $V_f = 40\%$ Wire Diameter = 0.016 Inch

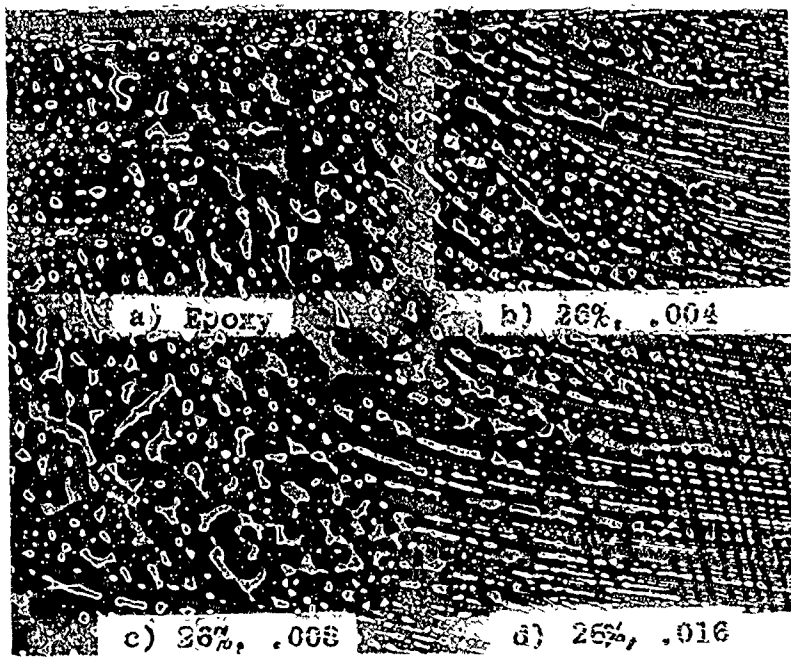


Figure 11. Dynamic Stress-Strain Curves V_f
in Percent and Wire Diameter in Inches

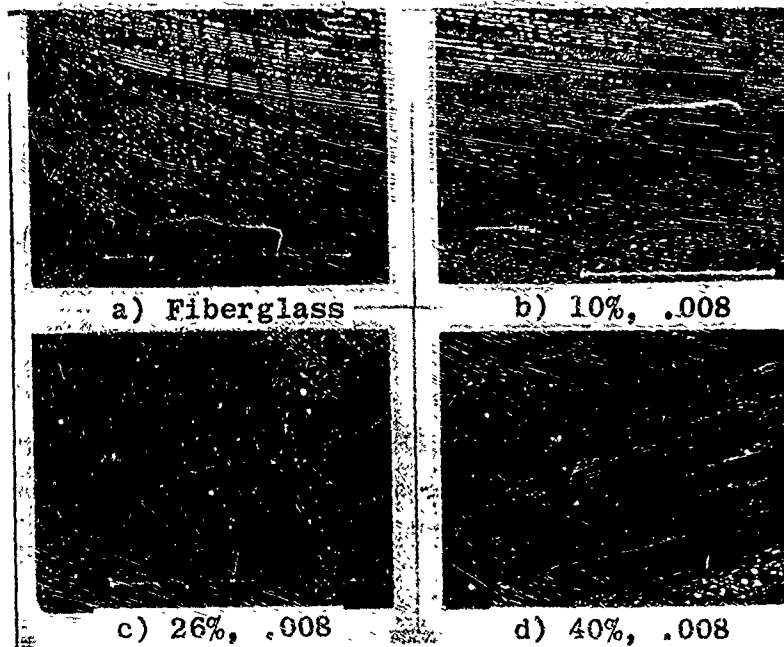


Figure 12. Dynamic Stress-Strain Curves V_f
in Percent and Wire Diameter in Inches

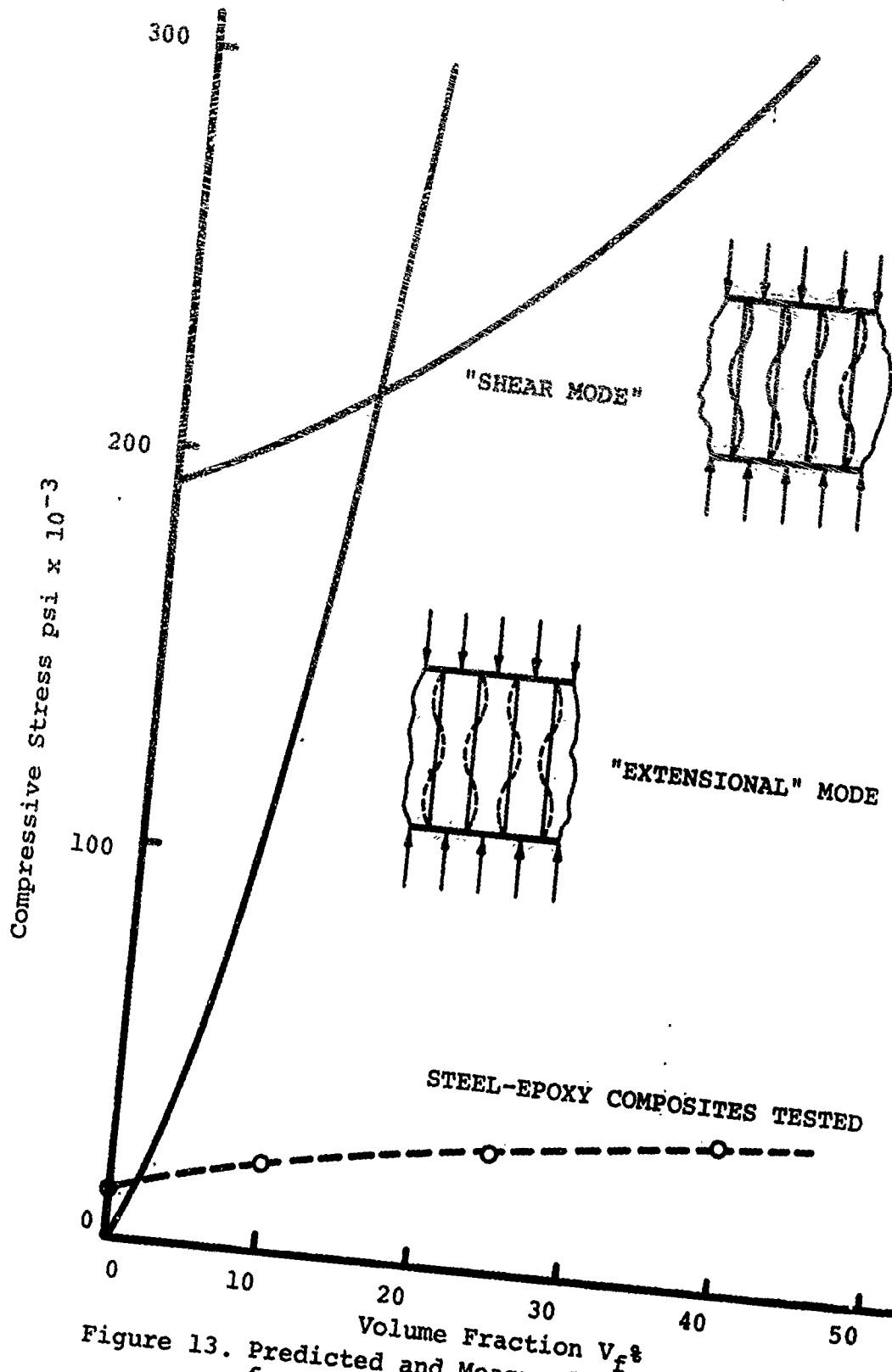


Figure 13. Predicted and Measured Compressive Strengths for Steel-Epoxy Composites.

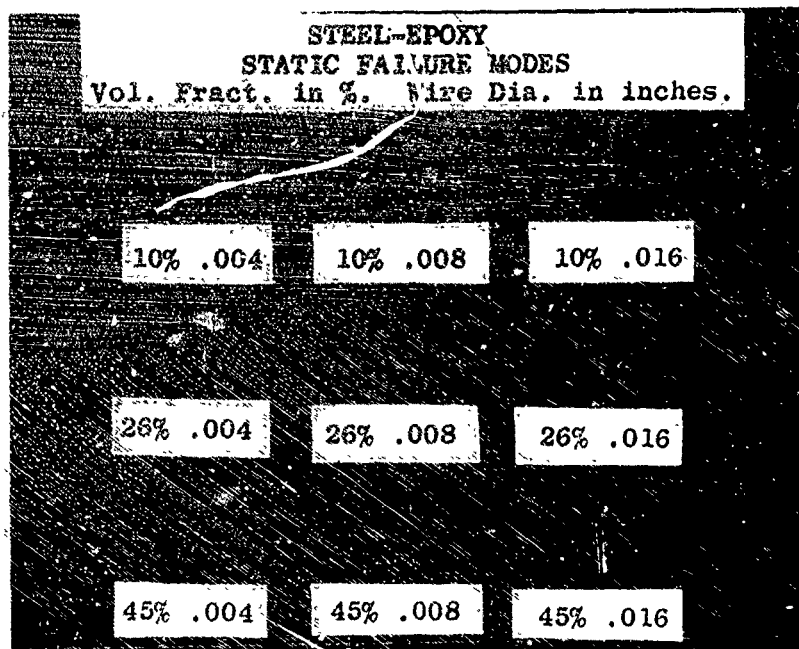


Figure 14. Steel-Epoxy Composites, Failure Modes

Some further relations to proposed and existing models have been noted. It appears that, in general, the models proposed are based on two-dimensional buckling considerations for a continuous and perfect elastic support. Thus, matrix shear is an important design parameter. Experimental data obtained for reinforced metal matrix systems with plate-like reinforcements appear to follow such models modified to incorporate a perfectly plastic or work-hardening matrix^(6,8). For epoxy-type systems the results are less favorable, indicating distinct failure discrepancies between metal and non-metal matrix systems. These differences can perhaps be attributed to the inherent load transfer mechanisms existing for these types of composite materials. This is further documented by visual observation of the varying stages of steel-epoxy response to compressive loads which consists of specimen barrelling followed by localized matrix shear. Again, this response characteristic has been observed in Reference 3.

An interesting observation of the data obtained occurs if the rule of mixtures is used to calculate the compressive failure load, neglecting matrix influence. Although somewhat subjective, the calculations indicate approximately a constant value of the fiber buckling stress for a fixed volume percent reinforcement.

The results reported here coincide closely with those presented in Reference 3 where studies on both ductile and brittle types of reinforcements with unordered filament packing are described. Comparing the results obtained in Reference 3 with those presented here, similarity in the observed compressive failure characteristics is noted. This is further indicated in Figure 15, which shows the maximum stress versus wire diameter with volume percent reinforcement as a parameter. Results are presented for comparable volume percents and rate of testing with the data included in Reference 3. The increased strength characteristics as a function of decreasing filament size and volume percent reinforcement is noted. This can be attributed to the greater amount of surface bonding area between filament and matrix. In addition, the stress difference is observed to decrease with increasing volume percent for a constant wire size.

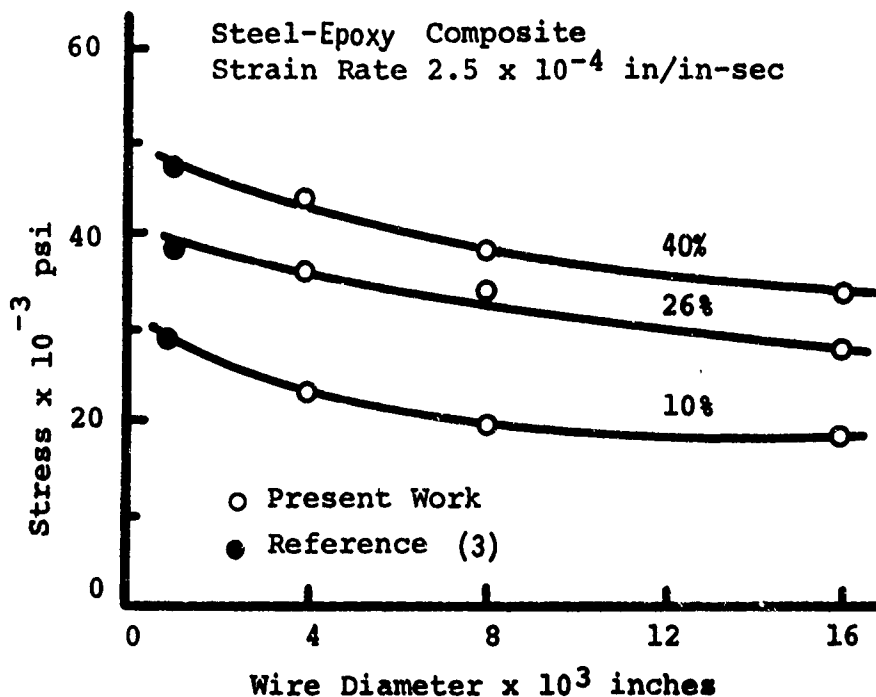


Figure 15. Maximum Stress Versus Wire Diameter for Steel-Epoxy Composites

In Figures 16 through 18, plots of stress versus strain rate for constant volume percent reinforcement with varying wire size and strain are shown. For comparative purposes, the base matrix material properties and those of steel reported in Reference 9 are presented. The latter material is of the same type as the wire used in the present test series. It appears that for a given volume percent reinforcement the stress increases with strain and strain rate, the influence of the latter becoming more significant in the high strain rate region. In the normally quasi-static loading region, the influence of rate sensitivity is less apparent. This can perhaps be attributed to the matrix material capability of absorbing a gradual load transfer from the reinforcing filaments. This effect is more readily apparent in Figures 19 through 21 which show a plot of stress versus volume percent reinforcement for constant strain (1%) and varying wire size. The two respective ranges of strain rate data are shown for both high and low strain rate values. For high volume fractions the material strain rate dependence is readily apparent. Figures 22 through 24 summarize much of the previous data obtained by showing maximum stress versus strain rate for varying wire sizes and volume percent of reinforcing material. It is observed that for the smaller wire sizes (0.004", 0.008") the twenty-six volume percent reinforcement exhibits the greatest rate sensitivity. The ten percent reinforced system for various wire sizes shows rate dependency characteristics more closely associated with that of the epoxy while the forty percent system follows more closely the strain rate characteristics of the reinforcing steel. Also, the smaller wire sizes (0.004", 0.008") for higher volume fractions of reinforcing material show less strain rate sensitivity. This may be attributed to the influence of interfiber spacing in which the higher volume fraction of small wires have greater matrix shear strains than larger wires. Therefore, the matrix fractures earlier at the high strain rates for the smaller wires due to the high density of fiber packing, thus resulting in lower maximum stresses. In summary of these latter results, it appears that for intermediate volume percents (26%) of reinforcement, regardless of wire size, the material specimens exhibit properties and characteristics less affected by the basic characteristics of the constituent elements.

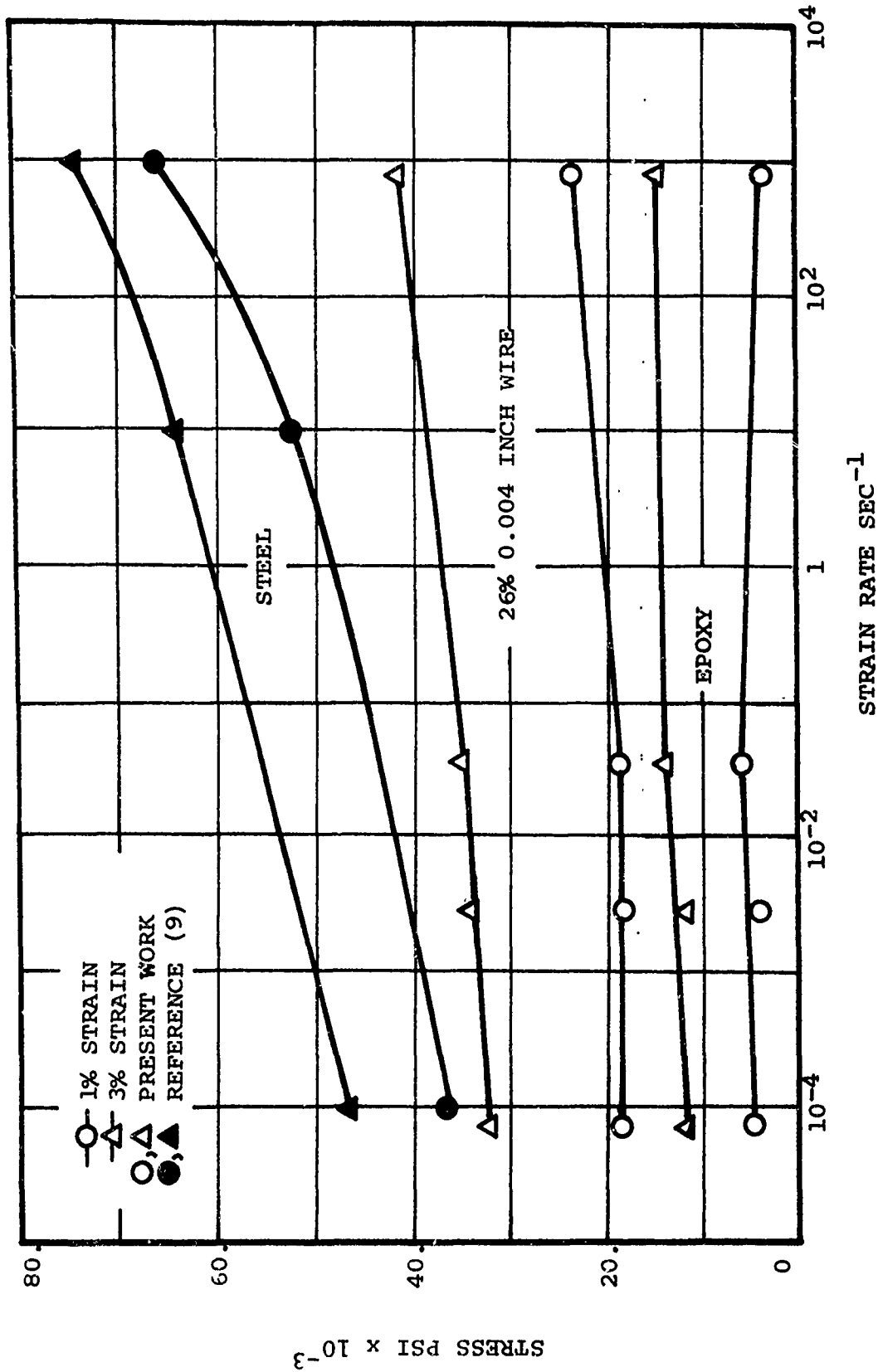


Figure 16. Stress Versus Strain Rate with Varying Strain, Steel-Epoxy Composites $V_f = 26\%$ Wire Diameter = 0.004 Inch

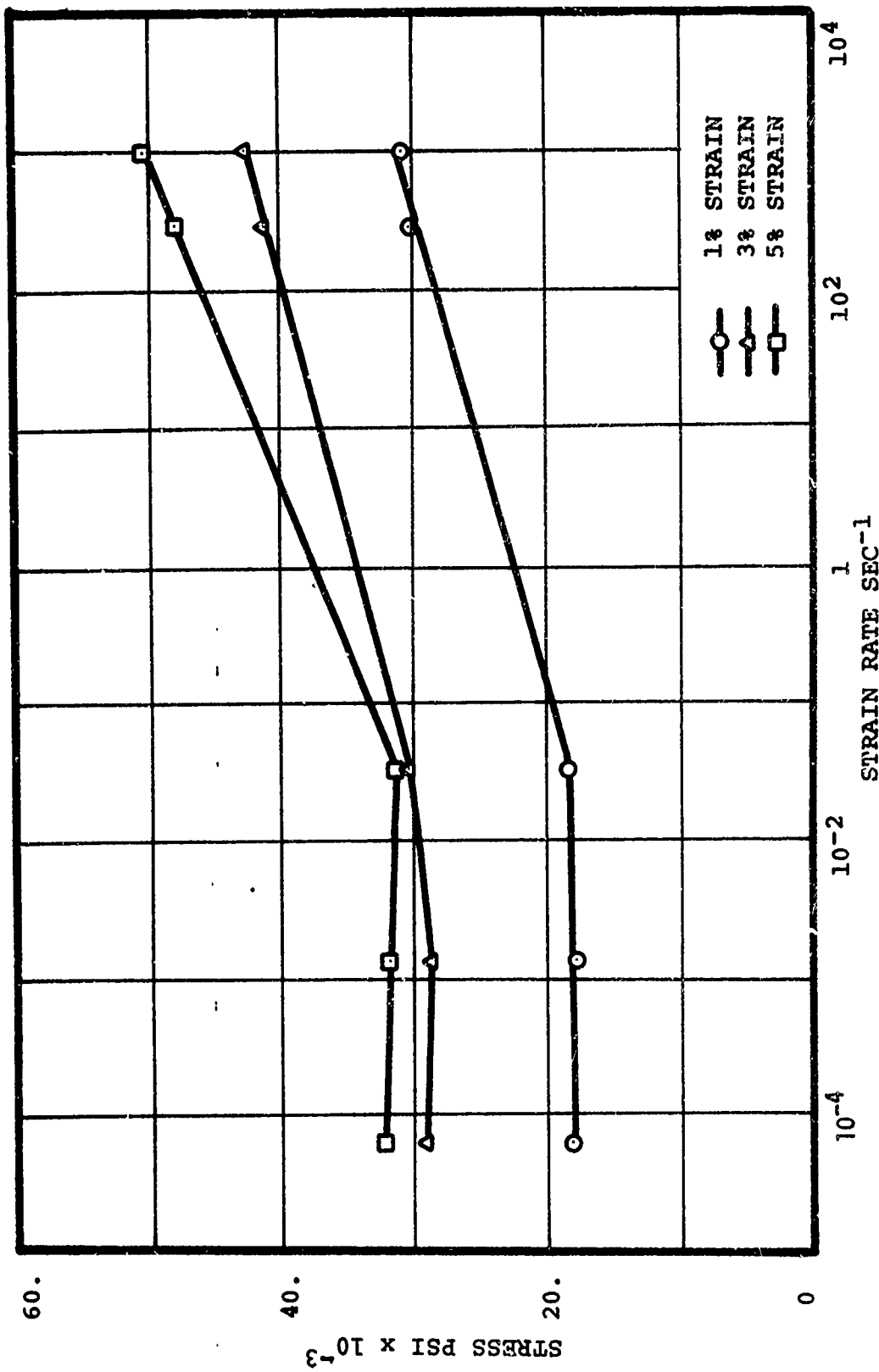


Figure 17. Stress versus Strain Rate with Varying Strain, Steel-Epoxy Composites $V_f = 26\%$ Wire Diameter = 0.008 Inch.

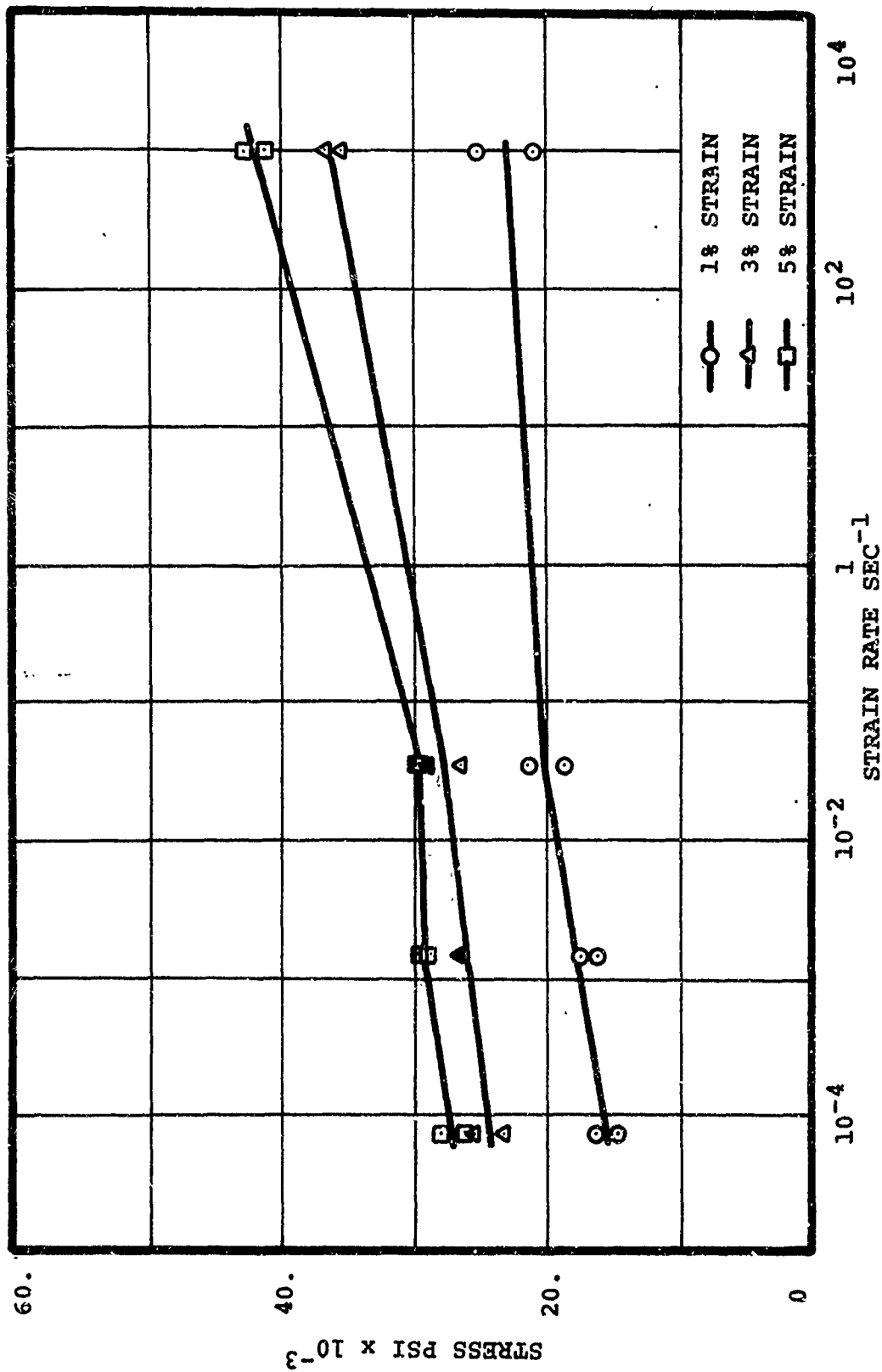


Figure 18. Stress versus Strain Rate with Varying Strain,
Steel-Epoxy Composites $V_f = 26\%$ Wire Diameter = 0.016 Inch

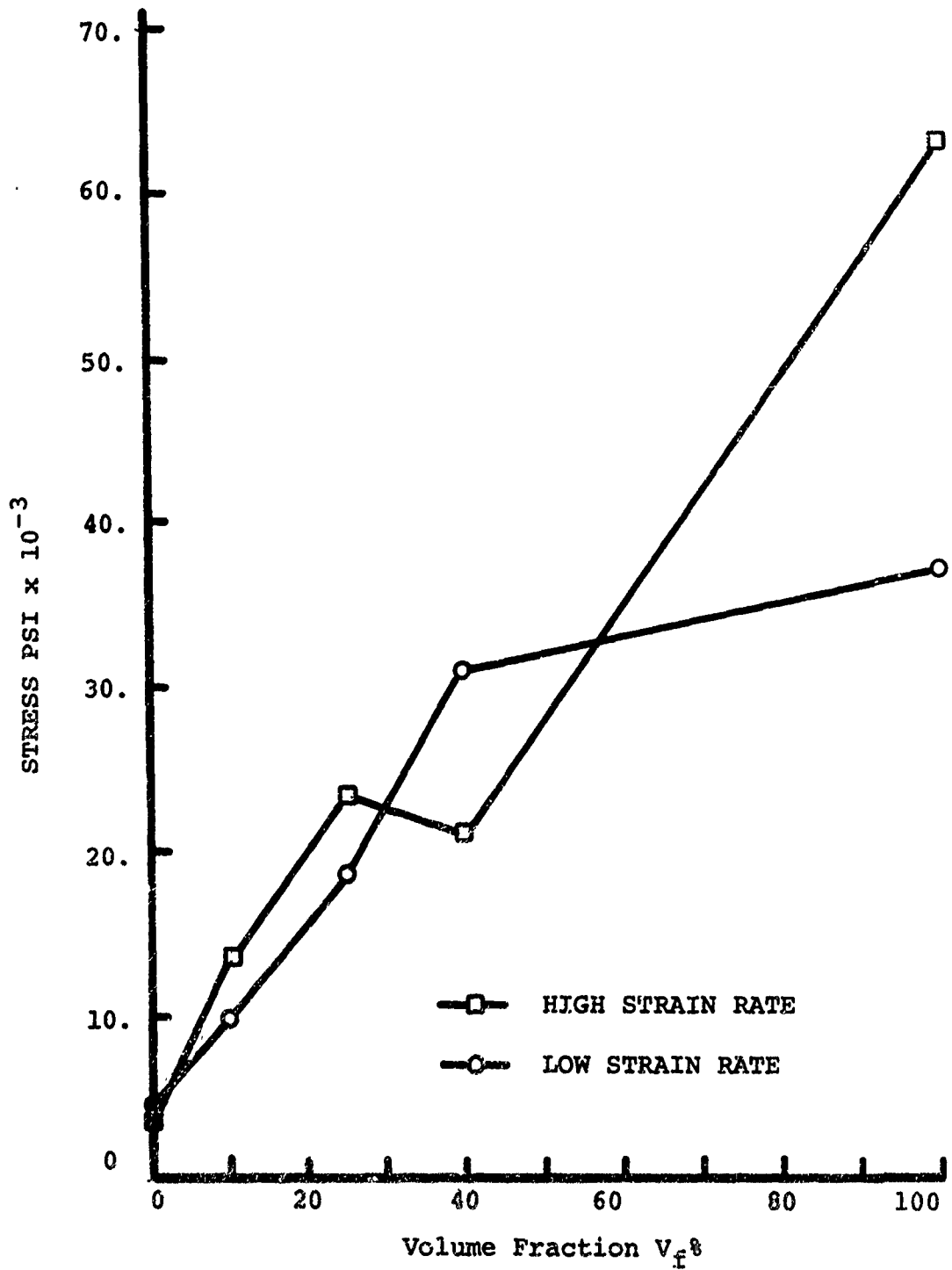


Figure 19. Stress Versus Volume Fraction at One Percent Strain for High and Low Strain Rates
Wire Diameter = 0.004 Inch

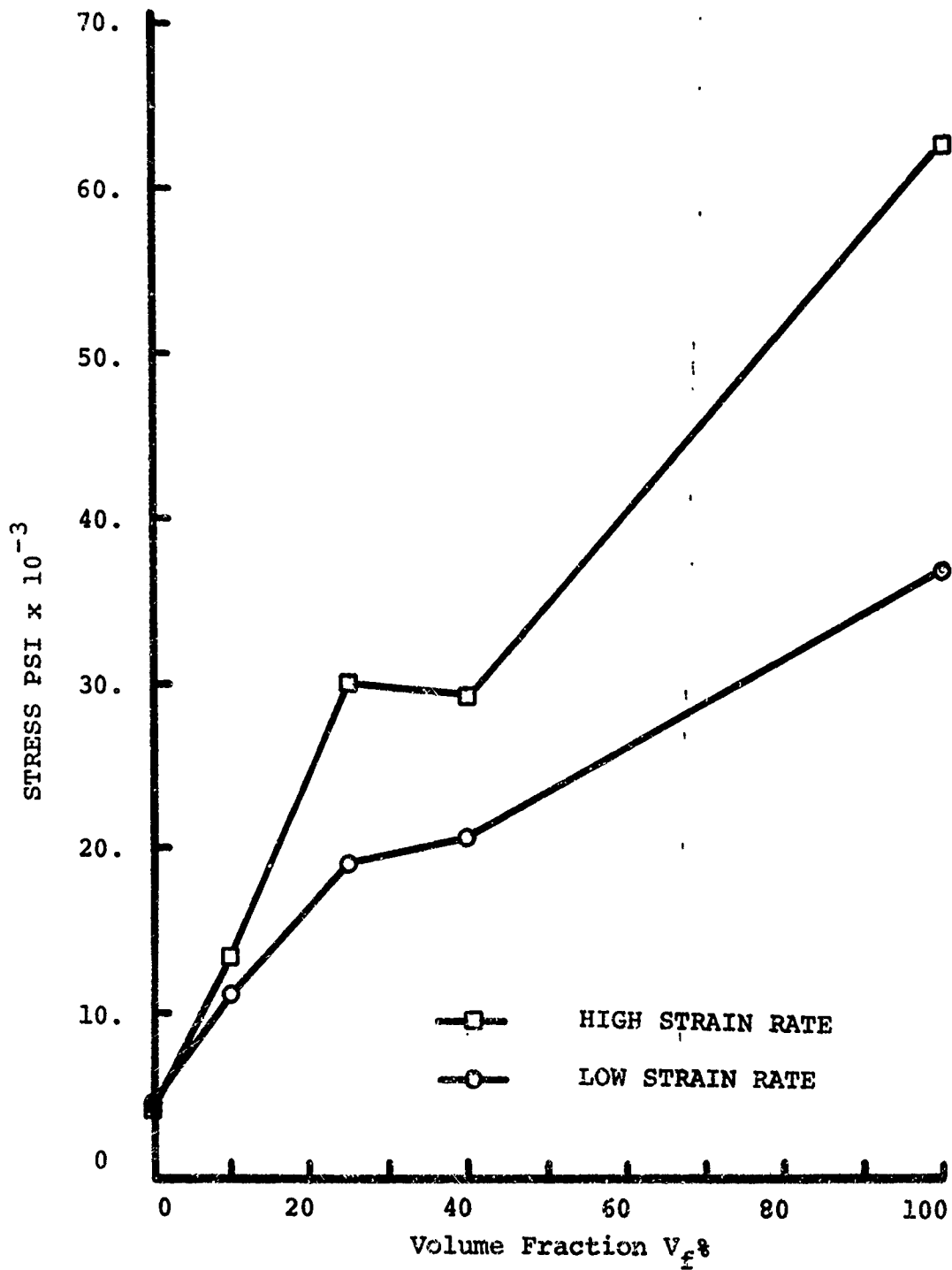


Figure 20. Stress Versus Volume Fraction at One Percent Strain for High and Low Strain Rates
Wire Diameter = 0.008 Inch

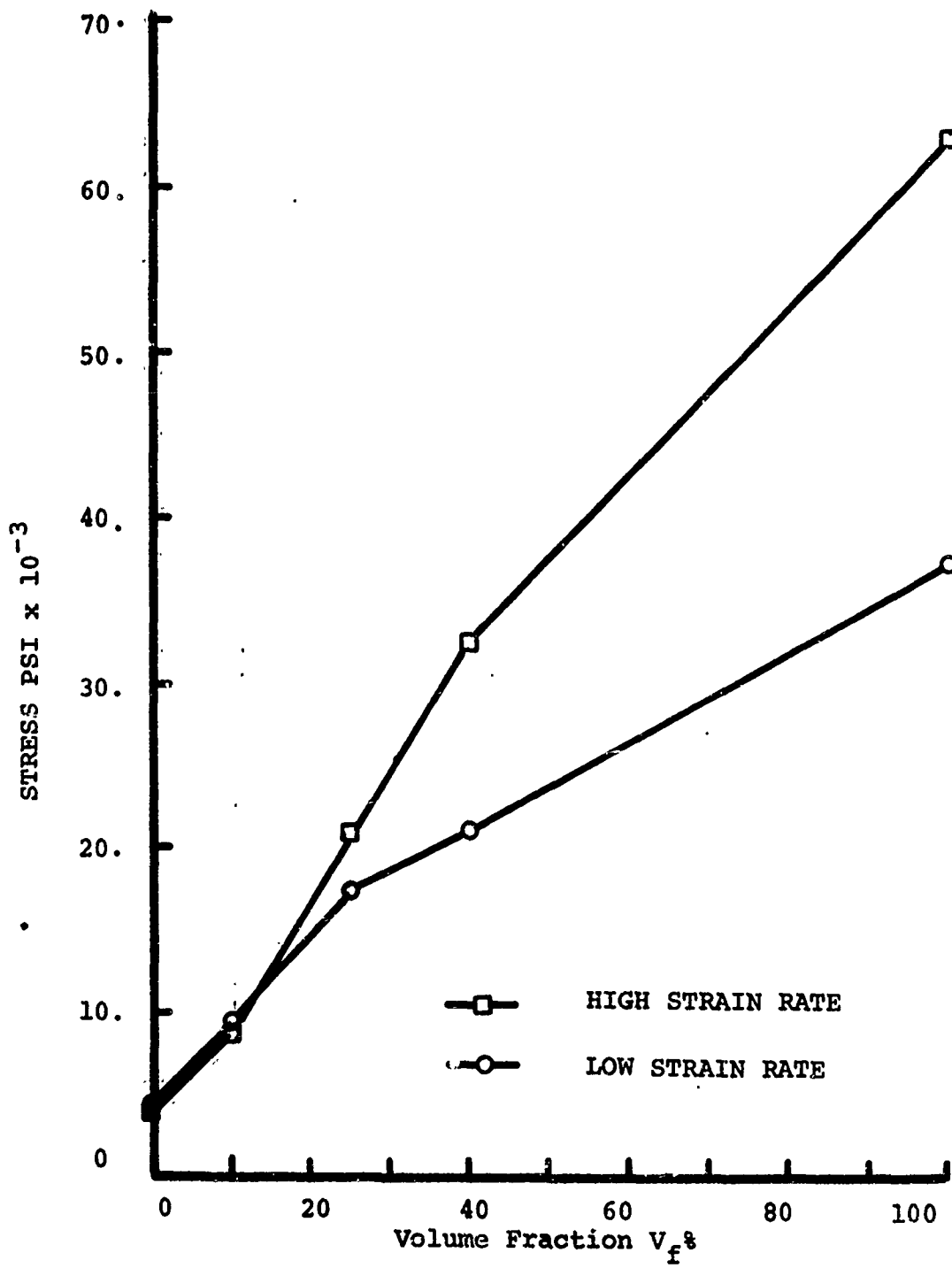


Figure 21. Stress Versus Volume Fraction at One Percent Strain for High and Low Strain Rates
Wire diameter = .008 Inch

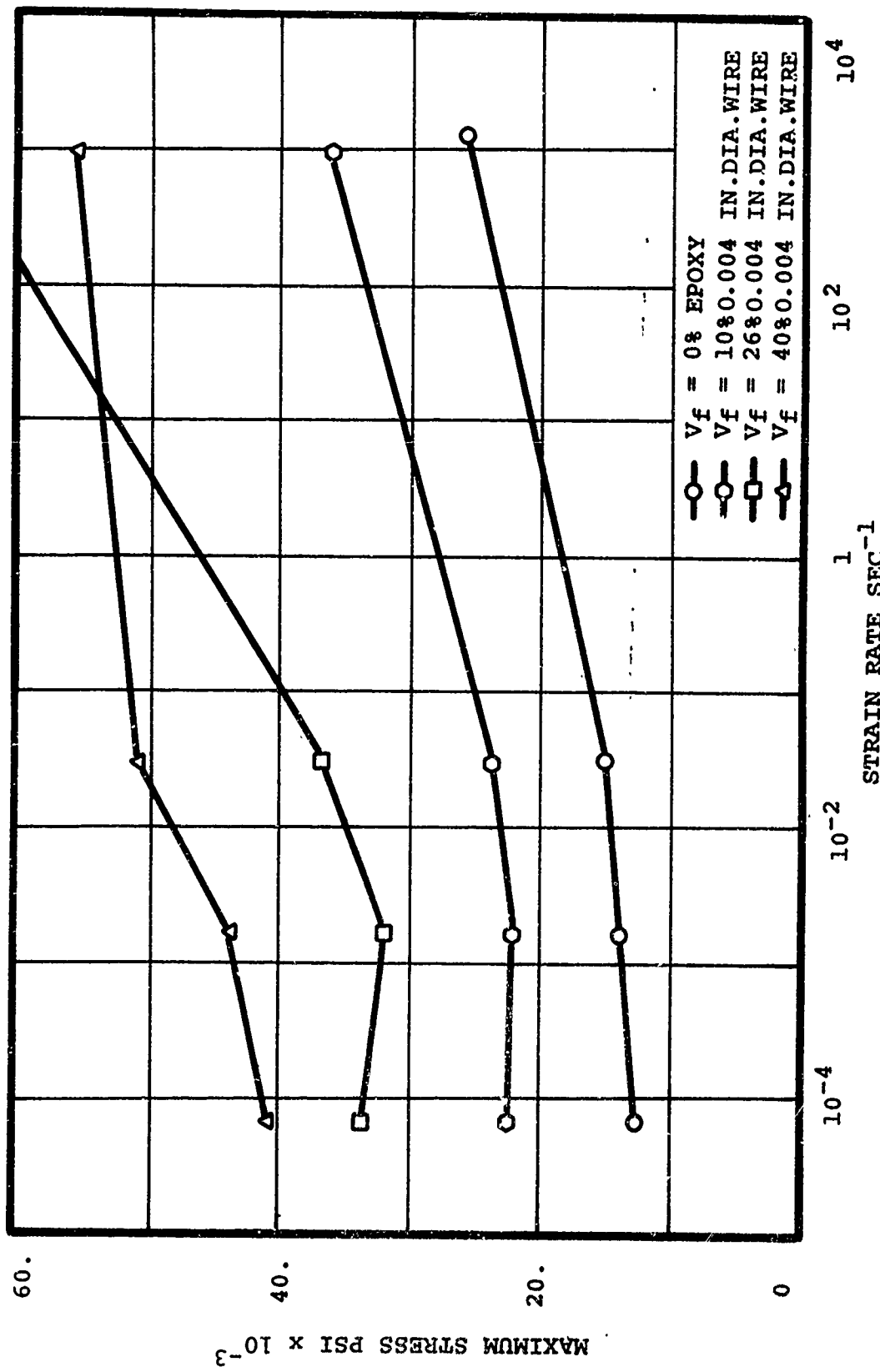


Figure 22. Maximum Stress Versus Strain Rate for Steel-Epoxy Composites Varying Volume Fraction Wire Diameter = 0.004 Inch

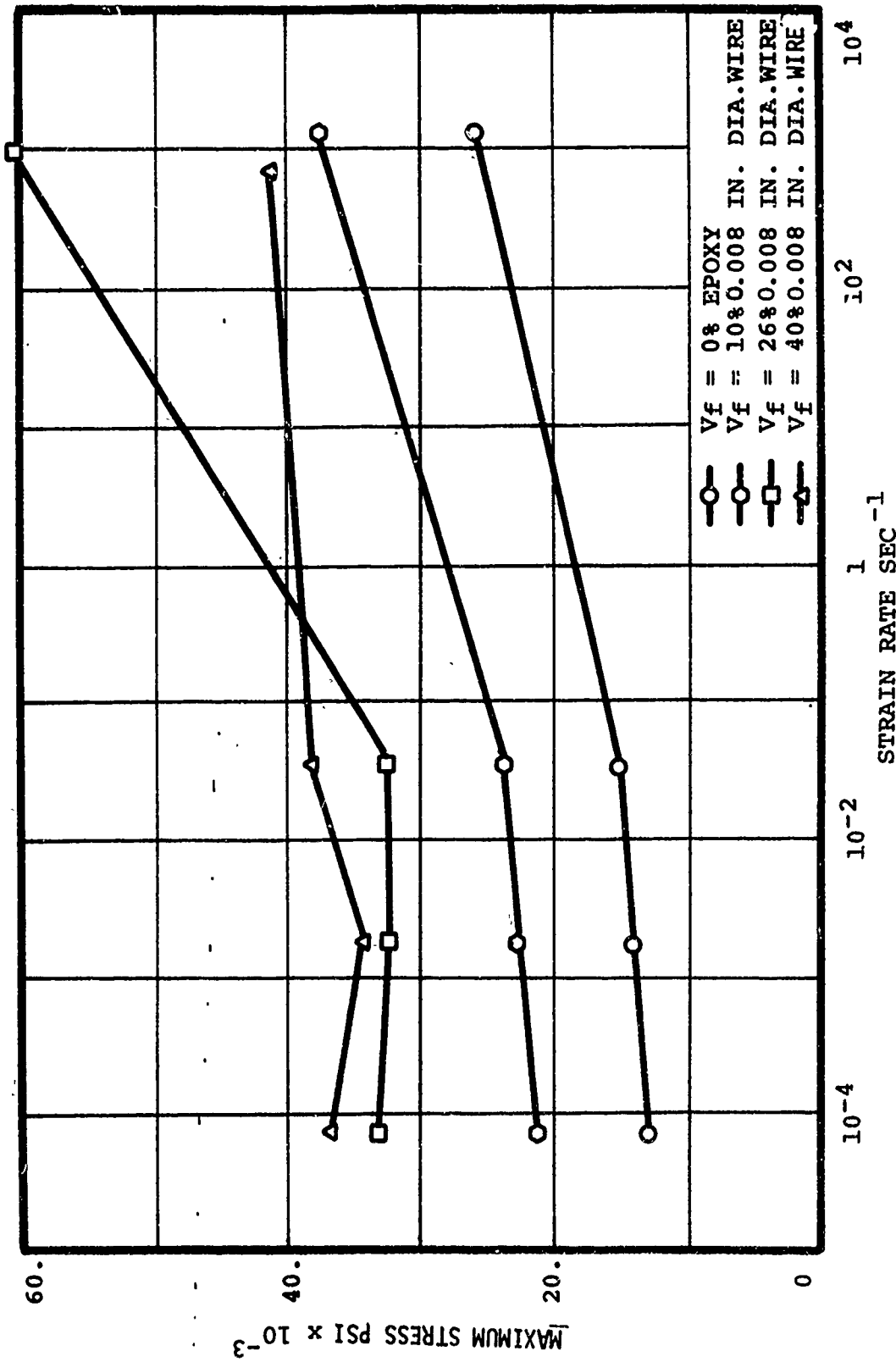


Figure 23. Maximum Stress Versus Strain Rate for Steel-Epoxy Composites Varying Volume Fraction Wire Diameter = 0.008 Inch

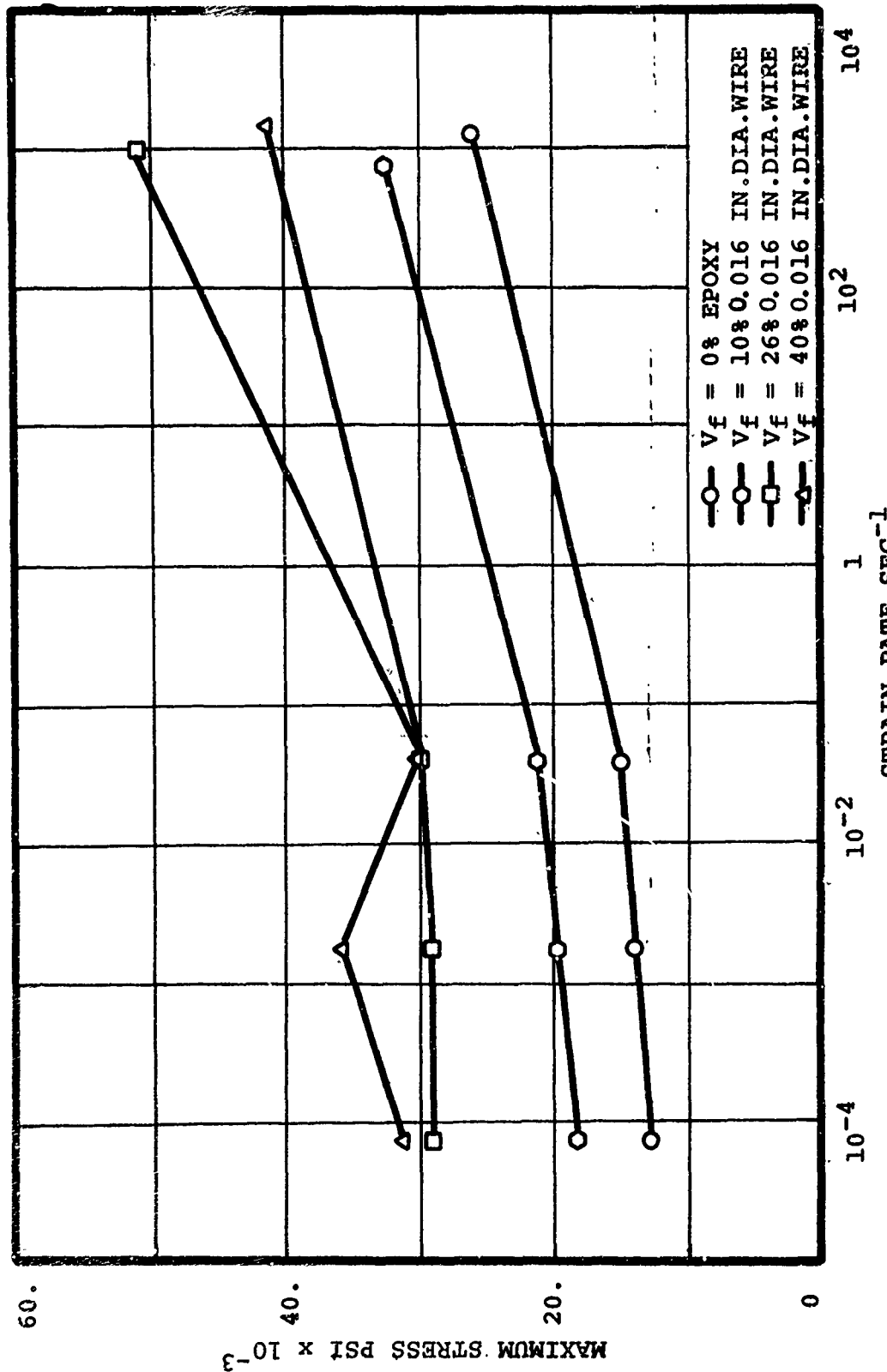


Figure 24. Maximum Stress Versus Strain Rate for Steel-Epoxy Composites Varying Volume Fraction Wire Diameter = 0.016 Inch

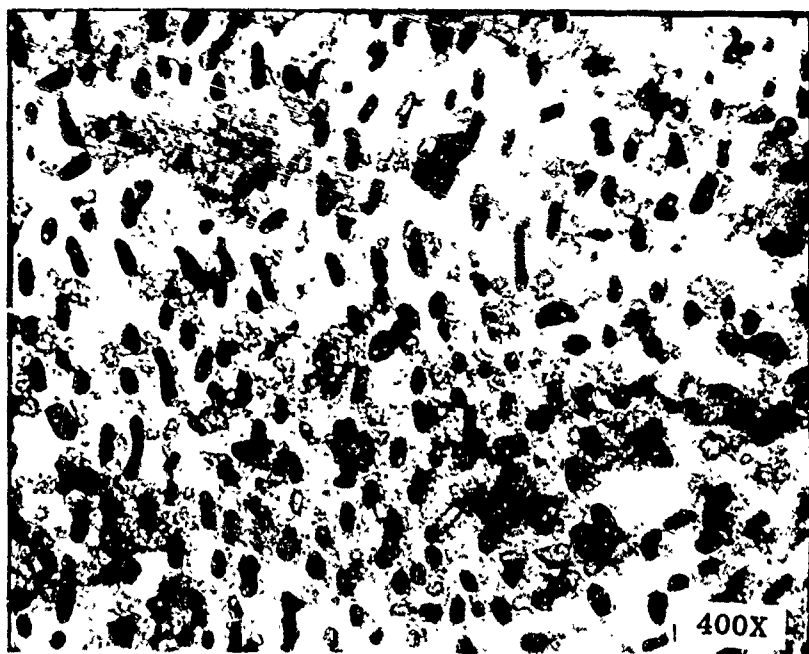
For completeness in the fabrication procedures established for the steel-epoxy system, several composite plates were made by extending the cylindrical specimen fabrication scheme described in Reference 1. Layered plate specimens were fabricated, utilizing alternating layers of spaced steel wires. An abbreviated description of the test procedure and response of such a system under dynamic impact loading is discussed in the Appendix. Such experimental studies in a subsequent program would be of value in investigating material behavior as related to scabbing, spall and plug formation phenomena. Further, such studies could be utilized directly for correlation with theoretical terminal ballistic investigation being conducted for the Armament Laboratory and reported on in References 10 through 12.

2.2 Aluminum-Nickel (Al_3Ni system represents one variety)

In References 1 and 13, a description of the metallurgical techniques used to prepare metal matrix type composites, using controlled solidification principles, was discussed. In this process the submicron size reinforcing phase is grown in-situ in the matrix, thus avoiding problems associated with mechanical and chemical interfiber bond formation. The present program has included tests of one such uniaxially reinforced type system consisting of two specific microstructures or morphologies. Each microstructure is representative of fast and slow rates of controlled solidification and, in particular, for the present specimens the rates were 11 cm/hr. and 0.6 cm/hr. The associated microstructures for the two solidification rates are shown in Figure 25. It has been found⁽¹⁴⁾ that as the solidification rate increases there is a corresponding tendency towards rod-like formation in a cell-type structure. This is also observed in Figure 25. Other types of eutectic systems may have plate-like reinforcements as exemplified by the Al-CuAl₂ system and discussed in Reference 6.



(a) Solidification Rate 11 Cm/Hr.



(b) Solidification Rate 0.6 Cm/Hr.

Figure 25. Al_3Ni Microstructures

The compressive stress-strain curves for the rod and plate-like reinforced specimens are shown in Figures 26 and 27. It is observed that the rod-like reinforced specimens were capable of sustaining higher stress values for both the low and high strain rate tests. Furthermore, both types of reinforced systems displayed what appears to be an unstable upper yield point. This is further documented in the associated Hopkinson Bar stress-strain data and is compared with the matrix response shown in Figure 28. This phenomena appears more pronounced for the rod or whisker type reinforcement and is not evident in available tensile data⁽¹³⁾. This instability can be associated with sudden load transfer during rotation and/or fracture of the rods and plates to the matrix phase. This localized type of failure phenomena for various strain rates is documented in Figure 29. As in the case of the steel epoxy-type system, a localized shear failure associated with a finite band width is observed. A further documentation of the developing localized deformation occurring for the Hopkinson Pressure Bar tests is shown in Figure 30. A check of the actual strain rate sensitivity was investigated by examining the stress versus strain rate behavior for the two types of specimens tested. Figure 31 shows some of the data obtained for one percent strain. It is observed that there may be some material strain rate dependency at the lower rate levels but that this effect appears negligible.

2.3 Copper-Tungsten

Two types of copper-tungsten systems have been considered in the present investigation. These consist of copper jacketed tungsten rods fabricated by press fitting the tungsten rod in an undersized copper jacket, while the second type specimen consists of oriented and ordered filaments surrounded by a copper matrix. The latter system was produced by the technique of liquid infiltration. A detailed description of the fabrication scheme used for this system is presented below. Table II lists the fabrication methods presently used for continuous filament reinforced composite systems and is included for reference purposes. It is important to note that most data reported elsewhere for copper-tungsten systems has been obtained for specimens fabricated by the liquid infiltration method indicated in Table II. However, the systems studied had a random distribution of reinforcing fibers^(15,16,17) rather than the ordered array in the specimens of this program. A primary

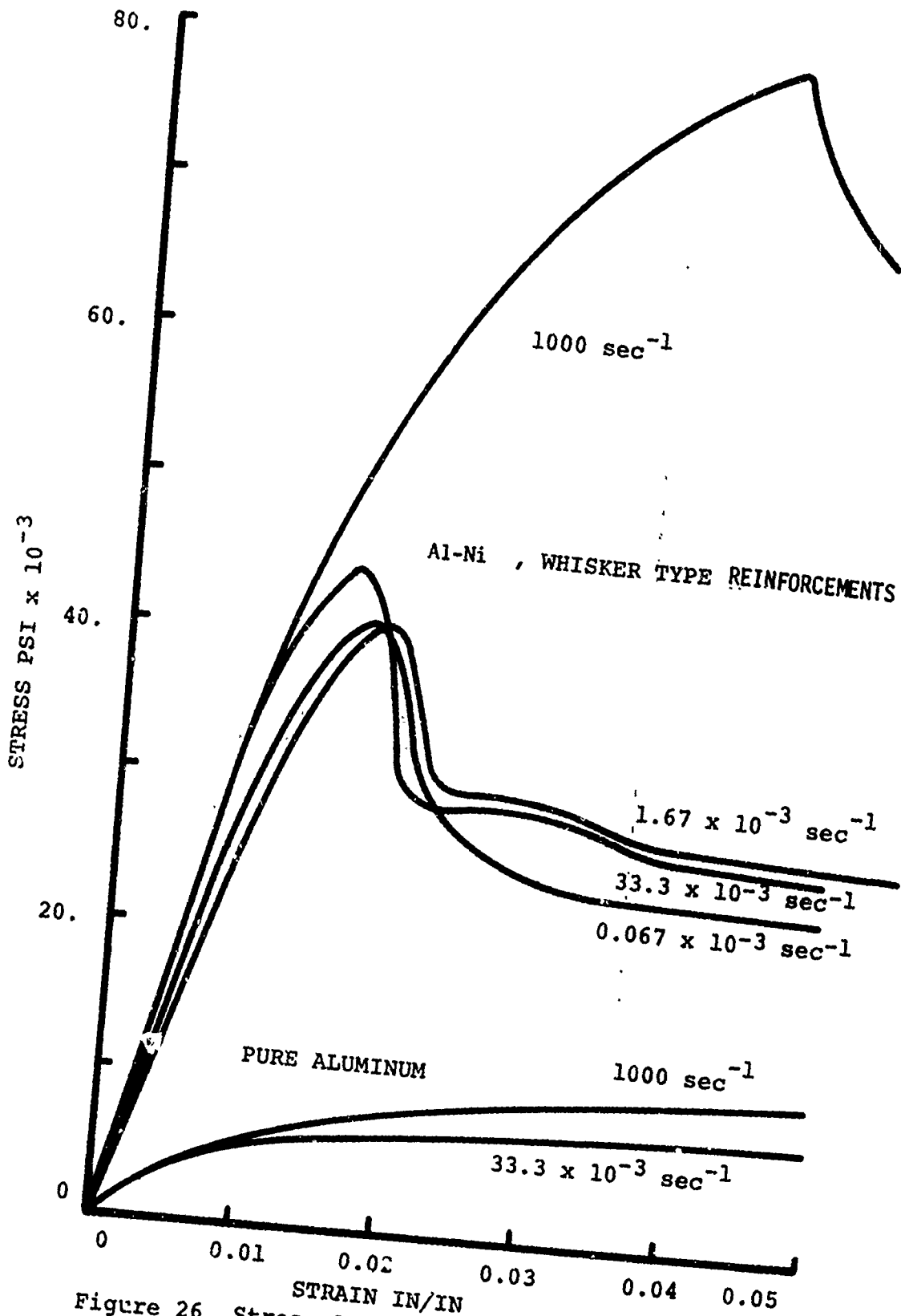


Figure 26. Stress-Strain Curve for Aluminum-Nickel Composite, Whisker-Type Reinforcement

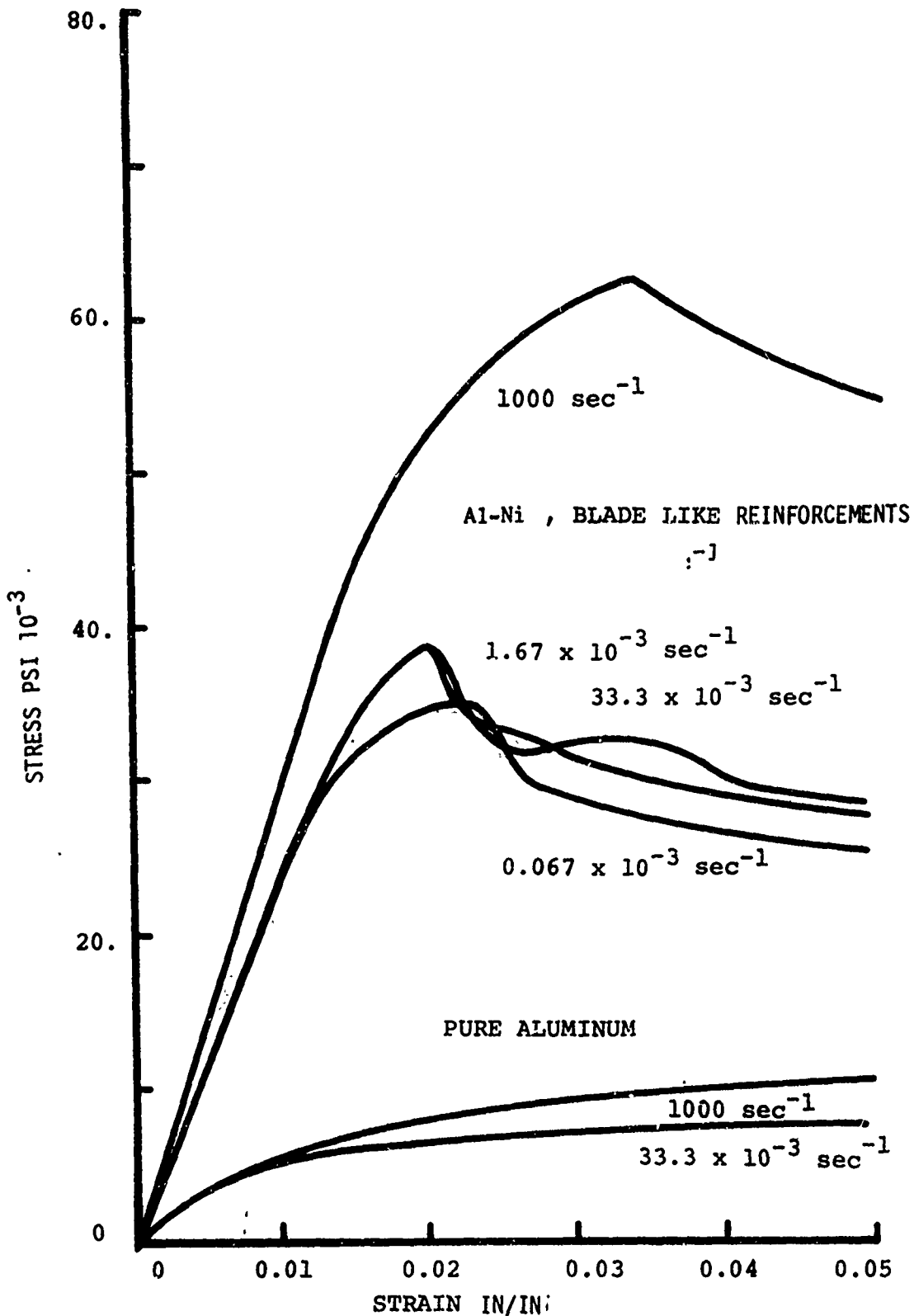


Figure 27. Stress-Strain Curve for Aluminum-Nickel Composite, Plate-Like Reinforcement

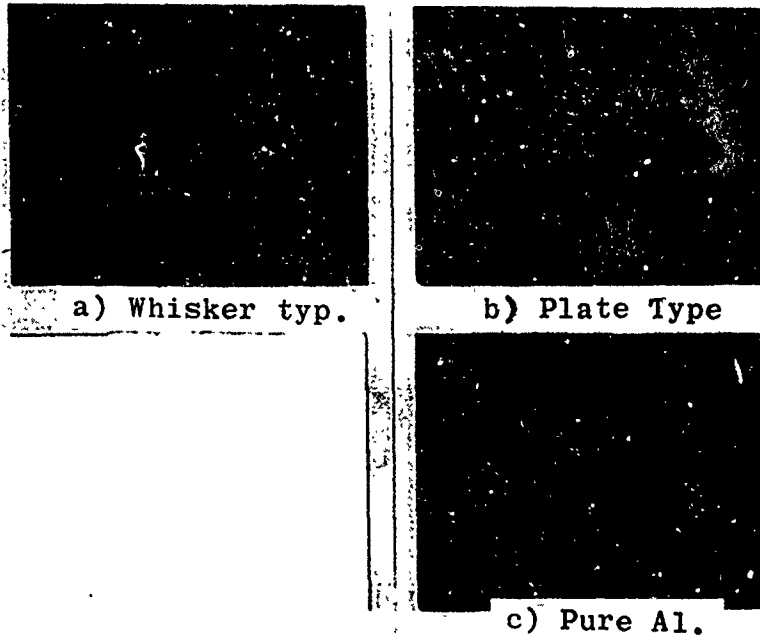


Figure 28. Hopkinson Bar Stress-Strain Curves for Aluminum-Nickel Composites

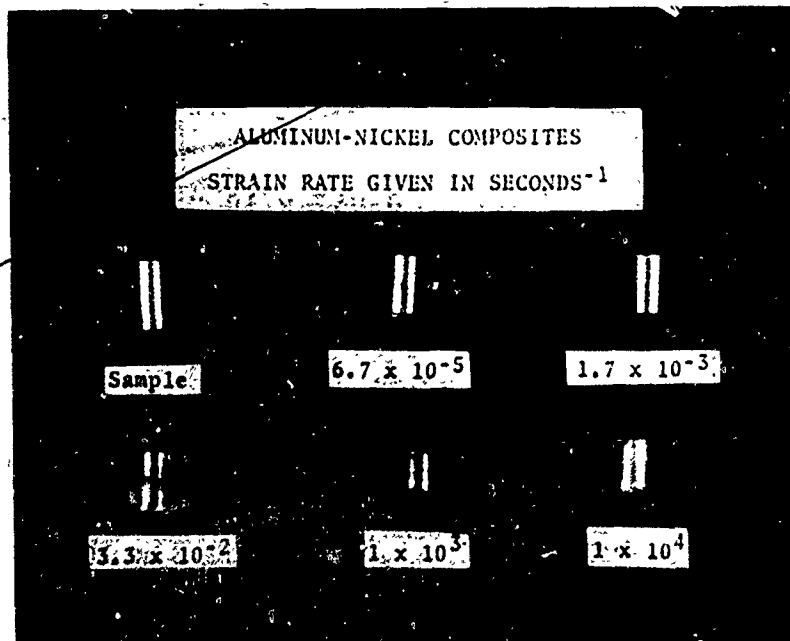


Figure 29. Aluminum-Nickel Composites Failure Modes for Given Strain Rates

objective of studying the two types of systems was to compare the resultant dynamic and failure properties of single rod reinforced composite systems of equal volume percent rod reinforcement versus distributed fiber systems. Experimental results comparing these systems is included in the following paragraphs and also in Section III.

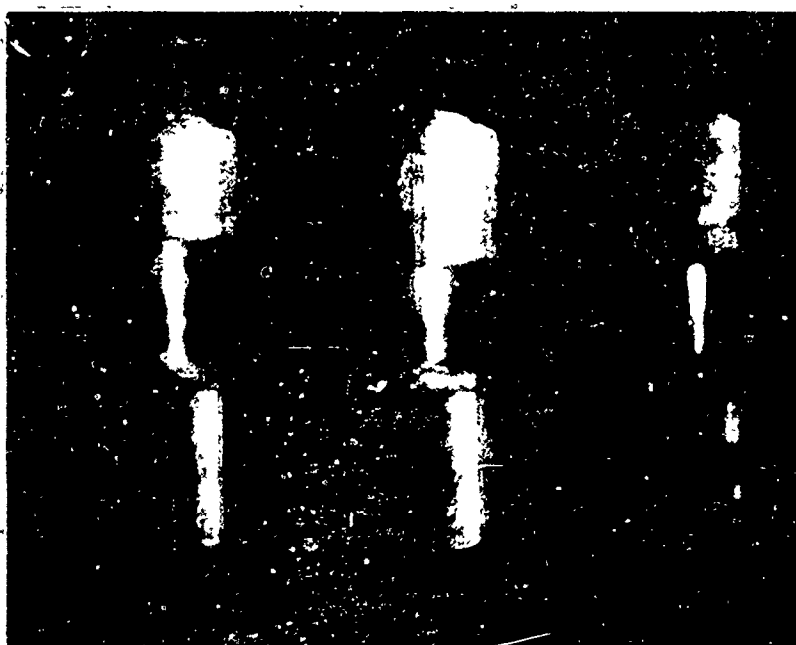


Figure 30. Deformation Behavior of Aluminum-Nickel Composites, Hopkinson Bar Test

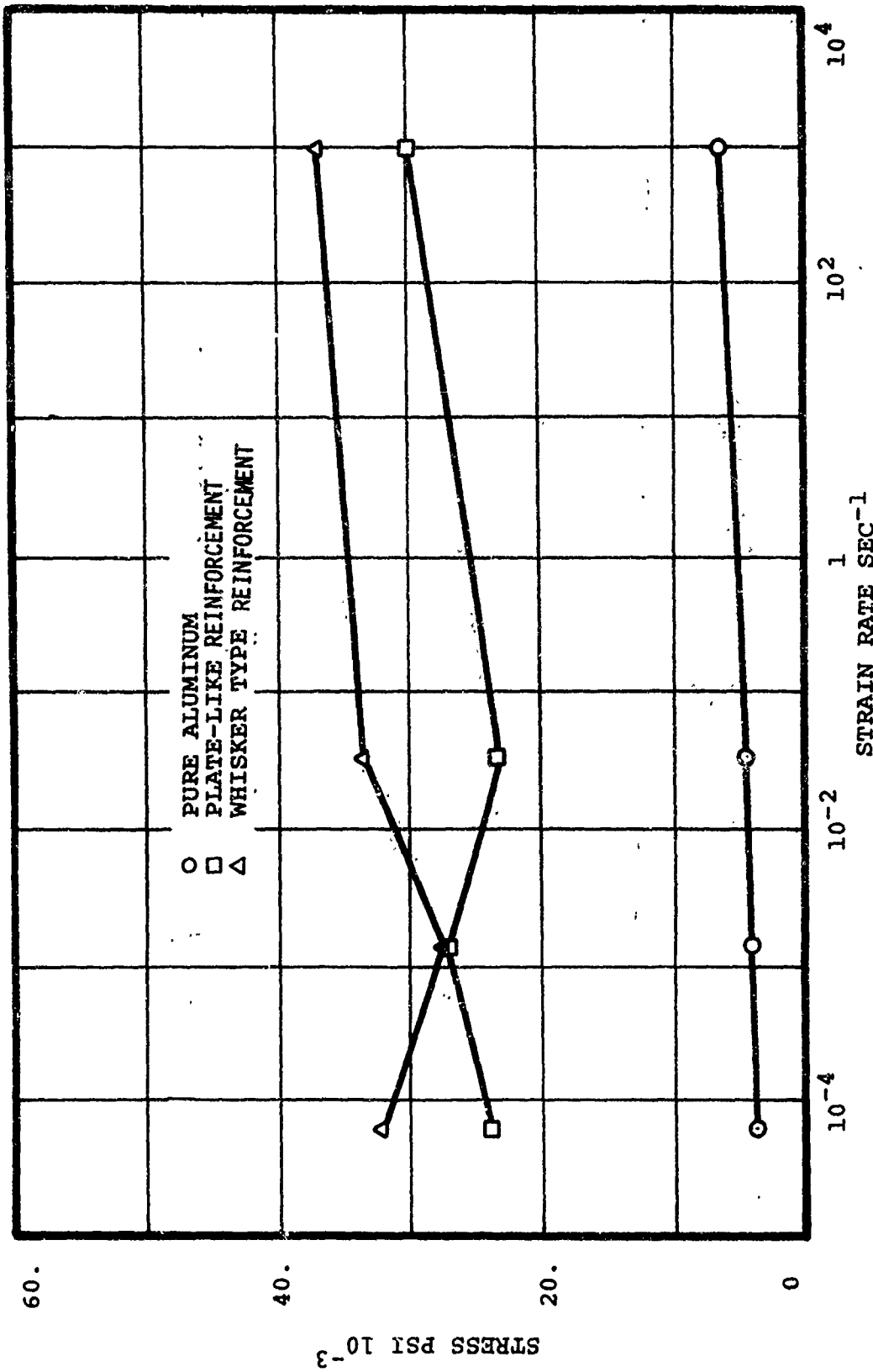


Figure 31. Stress Versus Strain Rate at One Percent Strain Aluminum-Nickel Composite and Pure Aluminum

TABLE II. FABRICATION METHODS FOR STABLE SYSTEMS

		Matrix						
		Al	Cu	Mg	Ni	Ag	Ti	W
Filament	B	LI HE PB ED P ER.		LI PB	HE ED		PB ER HE	CVD
	Borsic (Silicone vapor depos- ited on Boron filaments)	PB P					PB	
	W	HE	LI ED		LI HE S ED ER	LI S		P CVD
	Mo		LI		S ER		S ER	
	Ta		LI					
	Steel					LI		
	Stainless steel	PB						
	SiC	PB ED P			HE ED		PB HE	
	SiO ₂	PB						
	Be	CVD PB					PB	

LI - Liquid Infiltration HE - High Energy Rate Form
 PB - Hot Pressure Bond ER - Extrusion and Rolling
 S - Press and Sinter ED - Electrodeposition
 P - Plasma Spray CVD- Chemical Vapor Deposition

(Courtesy of Max Goldstein, Senior Materials Engineer, Battelle Memorial Institute)

2.3.1 Fabrication Process

The tungsten filament-copper matrix composite specimens were fabricated in three stages; that is, filament lay-up, matrix infiltration, and machining. The filament lay-up was accomplished by winding tungsten filaments (GE Type 218) on a mandrel as discussed in detail in Reference 1 and will be omitted in this report. Figure 32 shows a typical mandrel assembly and also one prepared for the infiltration process.

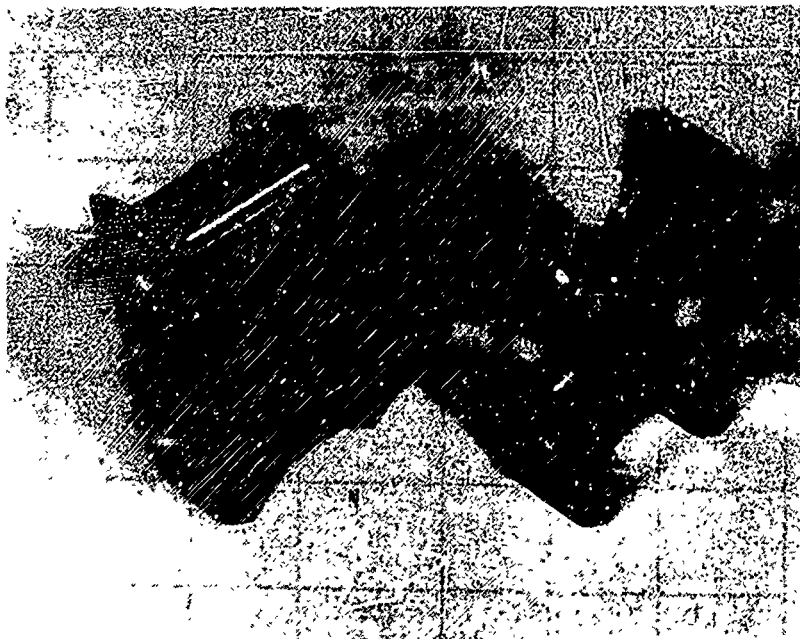


Figure 32. Winding Mandrel for
Tungsten-Copper Specimens

Two variations of vacuum infiltration were used to place the filaments in the copper matrix. In each case, either solid copper pellets or a one-half inch rod of 99.79% purity was used as the matrix material. For each prepared specimen, the wound mandrel, spacers, crucible, and copper were cleaned thoroughly and degreased by trichlorethylene vapor before the infiltration process was begun. After cleaning, the wound mandrel, spacers, and copper were placed in the crucible as shown in Figure 33.



Figure 33. Crucible and Winding Mandrel, with Spacers, for Fabrication of Tungsten-Copper Specimens by Liquid Infiltration

For the first infiltration method the open mandrel was placed in a vacuum furnace (Astro Model 4040) and the pressure reduced to 10^{-6} mm Hg. The furnace was then brought up to a temperature of 2200°F in thirty minutes and held at that temperature for one hour. The furnace power was then turned off and the crucible allowed to cool in the vacuum atmosphere.

This method produced considerably large porosity in the composite system. This porosity was attributed to improper cooling, and poor heat conduction from the steel mandrel, which caused the copper to remain molten near the center of the mandrel and produce shrinkage voids in the filament array.

The mandrel was then modified and a cooling coil was placed at the bottom of the crucible to produce directional solidification so that the upper portion of the copper solidified last. This method produced rather void free specimens.

For the second method a top (as shown in Figure 33) was welded to the crucible, after charging it with copper, and the vacuum tube was attached to a mechanical vacuum pump. The pressure was reduced to 100 microns of mercury and the crucible was lowered into a vertical furnace preheated by a Kanthol heating element to a temperature of 1800°F. The heating was continued for three hours up to 2200°F and held at that temperature for one hour. A cooling of the bottom of the crucible was accomplished by blowing room temperature gas directly on the bottom of the crucible. The cooling gas was directed on the crucible with the power on for about fifteen minutes or until the crucible temperature dropped below the melting point of the copper. The power was then disconnected and cooling gas continued for an additional fifteen minutes. The crucible was then allowed to cool for twenty-four hours with the vacuum pump still attached. Again this method produced relatively void free specimens.

The machining of the specimens was accomplished by first sawing away the top and bottom portions of the crucible and facing the ends of the crucible and mandrel down to the side plate screw center lines. These screws may be seen on the side plates of Figure 32. The spacer material was then sawed away and the mandrel was split by sawing down the center line of the mandrel inner core. At this stage the remaining two blocks of tungsten-copper composite were milled down to approximately 0.44 x 1.63 x 1.50 inches and then cut by a diamond embedded friction wheel into six rectangular pieces of dimensions 0.44 x 0.51 x 1.50 inches. These six pieces were then turned in a lathe to approximately 0.400-inch diameter by the use of a carbide-tipped tool. The final machining consisted of grinding these six cylindrical specimens to a diameter of 0.382 ±0.001 inch, cutting them into specimens approximately 0.5 inch long, and grinding the ends flat to produce final test specimens of 0.382 x 0.5 ±0.001 inch.

Measurements of the machined specimens were taken and recorded along with the weight of each specimen. Typical cross sections of the specimens produced are shown in Figure 34.

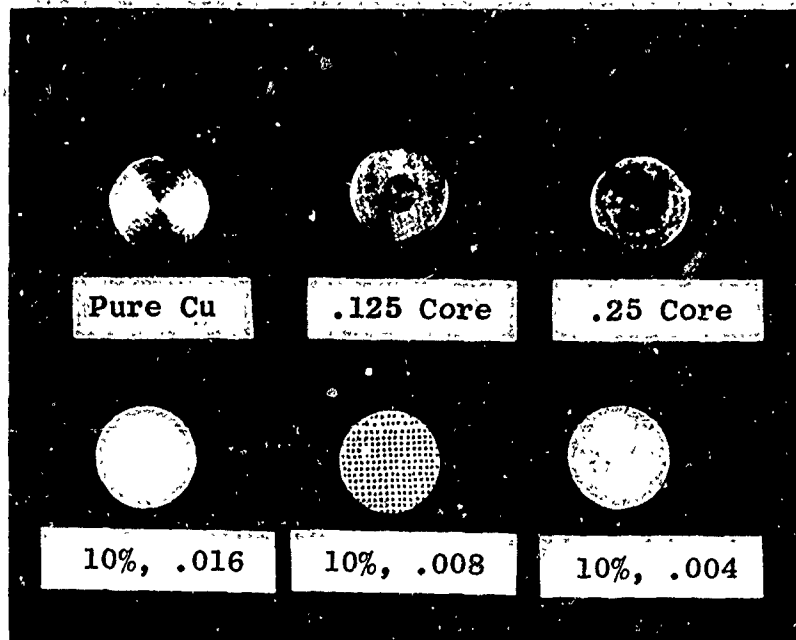


Figure 34. Cross Section View of Tungsten-Copper Specimens

2.3.2 Material Properties Data

Both the copper jacketed tungsten specimens and fiber reinforced samples were tested using the Hopkinson Pressure Bar. The test equipment was modified by mounting hardened 1095 steel wafers, nominal thickness 0.062 inch, Brinell Hardness 400, to the transmitter and receiver bars of the test equipment. This modification was necessitated by the high strength characteristics of the copper-tungsten specimens and several other high modulus composites tested. The transmitter and receiver bars were tested with wafers attached and without insertion of test specimens in order to check if use of such wafers produced observable deformations.

Dynamic stress-strain data for the two types of copper-tungsten composites tested are shown in Figure 35. Also shown in Figure 36 a and b are the constituent dynamic properties of the copper matrix and tungsten rod.

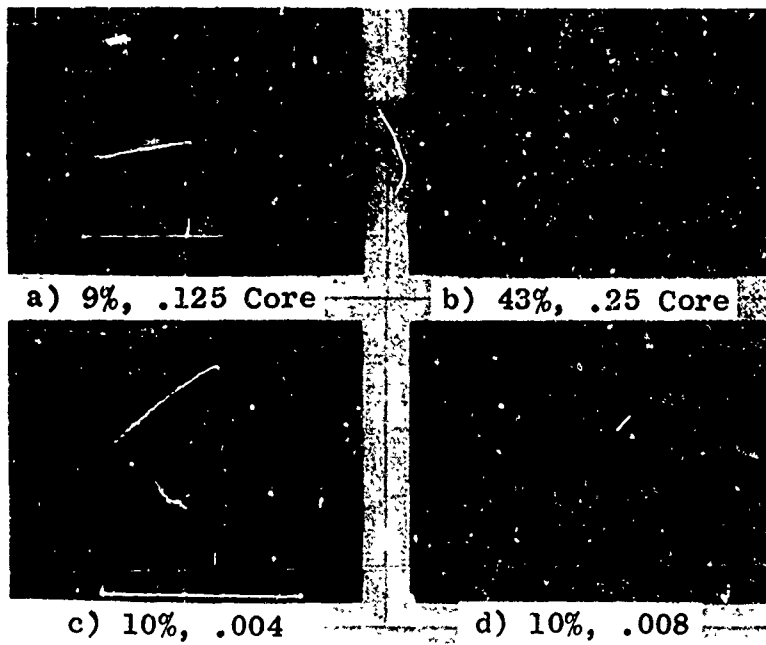


Figure 35. Dynamic Stress-Strain Curves V_f in Percent and Wire Diameter in Inches

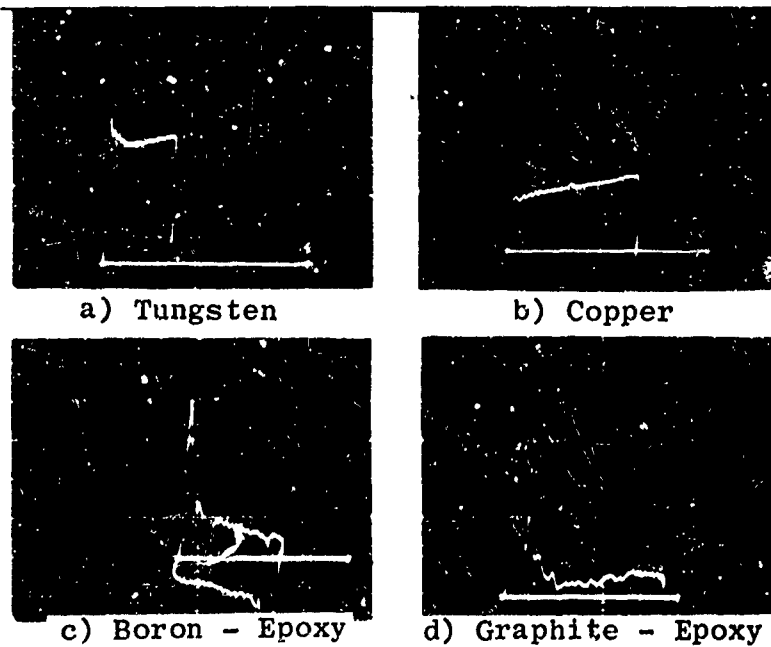


Figure 36. Dynamic Stress-Strain Curves Tungsten-Copper

In Figure 35 c and d the dynamic response of spaced ten percent volume, 0.004-inch and 0.008-inch ductile tungsten filaments embedded in a copper matrix, is shown. Space limitations precluded the insertion of the data obtained for ten percent volume; 0.016-inch tungsten wire. For constant volume percent and increasing wire size it is observed that an upper yield point occurs as in the case of the aluminum-nickel matrix system. This trend has been observed for unordered brittle tungsten reinforced copper specimens, for constant wire size and increasing volume percent of reinforcement in Reference 17.* The occurrence of the upper yield point coincides with an observed change in failure mode, that is, from a barreling type failure for the 0.004 wire to localized shear failure for 0.008 and 0.016-inch filamentary specimens.

For the copper jacketed specimens an upper yield point was not discernible (Figure 35 a and b). Furthermore, for the one-eighth inch tungsten rod system, equivalent volume fraction of ten percent, a comparison with results for the equivalent volume tungsten filament reinforced system shows considerably less overall strength with increasing strain. For large rod reinforcements, one-quarter of an inch tungsten rod, equivalent to forty-three percent volume fraction, the composite system behaves as essentially pure tungsten.

2.4 Other Systems

In addition to the aforementioned systems, some high performance composites of current interest in Air Force systems development were dynamically compression tested on the Hopkinson Pressure Bar. The two composites tested were a boron-epoxy, sixty-five percent volume fraction, 0.004-inch diameter filamentary system and a graphite-epoxy, fifty percent volume fraction system reinforced by British manufactured Morganite I graphite fibers. The boron-epoxy system was relatively void free while the graphite-epoxy was fairly porous. Dynamic stress curves for the specimens are shown in Figure 36 c and d. Both specimens showed a brittle elastic response to failure, with dynamic stress-strain characteristics resembling E-glass fiberglass as discussed in Reference 1.

*Tests in this reference were performed at the, low strain rates.

2.5 Conclusions and Implications

In the present investigation a wide variety of composite type specimens have been studied at varying compressive loading conditions. The principal conclusions which can be drawn from the compressive properties tested are:

- (1) Dynamic compressive response of composites, both qualitative and quantitative, is significantly different from the response in conventional, low speed engineering testing. Thus, in composites, strain rate is usually significant and depends on the individual composite constituent properties, geometric arrangement, and volume fraction of reinforcements.
- (2) In some cases, composite strain rate sensitivity is significantly different from that of the constituents.
- (3) Compressive failure modes for low strain rate testing are varied and distinct from tensile failure modes, depending upon constituent materials, geometry and volume fraction of fiber distribution.
- (4) Theoretical prediction of low strain rate compressive failure modes for metal matrix systems is reasonably successful whereas it has not been successful for non-metal matrix systems.
- (5) Matrix shear as well as interfiber spacing and bond strength are observed as important design criteria for compressive load failure.

Some implications of these results in regard to potential design criteria for impacting solid systems are:

- (1) Low speed compressive failure modes can be controlled for certain composite systems based on matrix and constituent properties data.
- (2) Since composites are highly rate sensitive, dynamic as well as static test results are essential to predicting impact processes.

- (3) Mechanical properties obtained at varying strain rates are essential input to designing systems where wave propagation is significant. In addition, such basic information for composite systems is directly useful as input for projectile-target interaction studies developed for monolithic systems and considered for Air Force application in References 10 through 12.
- (4) Even though individual constituent properties are not attractive for certain applications, these constituents should not be discounted as not being effective in composite combinations.

SECTION III

FAILURE/FRACTURE CHARACTERISTICS

In order to study the failure (excessive deformation)/fracture characteristics of composite specimens, a series of experiments involving the impacting of flat ended cylindrical projectile (specimens) against essentially rigid targets has been performed. Such tests for determining impact properties of monolithic materials has been surveyed in Reference 18 and more recently explored for single phase metals at room and elevated temperatures in References 19 and 20. Several important specimen failure characteristics, particularly critical specimen velocity and qualitative fracture behavior of composites, based on visual records, were studied.

The experimental equipment devised for projecting the specimens has been comprehensively described in Reference 1 and involves an air gun assembly a shielded massive target, and appropriate supporting equipment. The principal monitoring equipment consists of a TRW high speed image converting camera which can be used to photograph the impact event in a series of three to five photographs over varying interframes delay times. The experimental set-up is discussed and shown in Reference 1 and the results for the various specimens are described below.

3.1 Steel Epoxy

It has been recognized, for example in Reference 18, that failure and/or fracture of monolithic materials may be varied and complex. The associated problems inherent with composite materials, however, is further complicated by the individual and combined influence of the constituent reinforcing elements. Further, the particular mode of failure/fracture for composite specimens is of importance. For the steel-epoxy composites, two distinct types or stages of failure were identified. The first stage was associated with filament delamination/debonding characterized by the onset of permanent bending or buckling of individual filaments and occurs at that point of the stress-strain curve for which the composite maximum stress is first attained. This latter value has been correlated with the horizontal tangent to the stress-strain curve. The second distinct stage of failure observed was complete fracture and fragmentation of the specimen. For this case, the first observable fragmentation was considered sufficient to define failure.

To correlate the dynamic properties data with the failure/fracture dynamics studies conducted using impacting specimens, several theoretical approaches were evaluated and are further described in Reference 1. Based on the observed data, a simple energy criterion was established for correlating dynamic Pressure Bar data with the gas gun experiment. Comparisons of theory with experiment are shown in Figures 37 and 38, which are comprehensive descriptions of previously established data discussed in Reference 1. The solid curves represent the calculated prediction, while actual test results are shown as data points for the various specimens. It is observed that two critical velocities are shown, V_p representing the critical velocity for initiation of failure stage one, as previously discussed, and V_f the velocity associated with failure stage two.

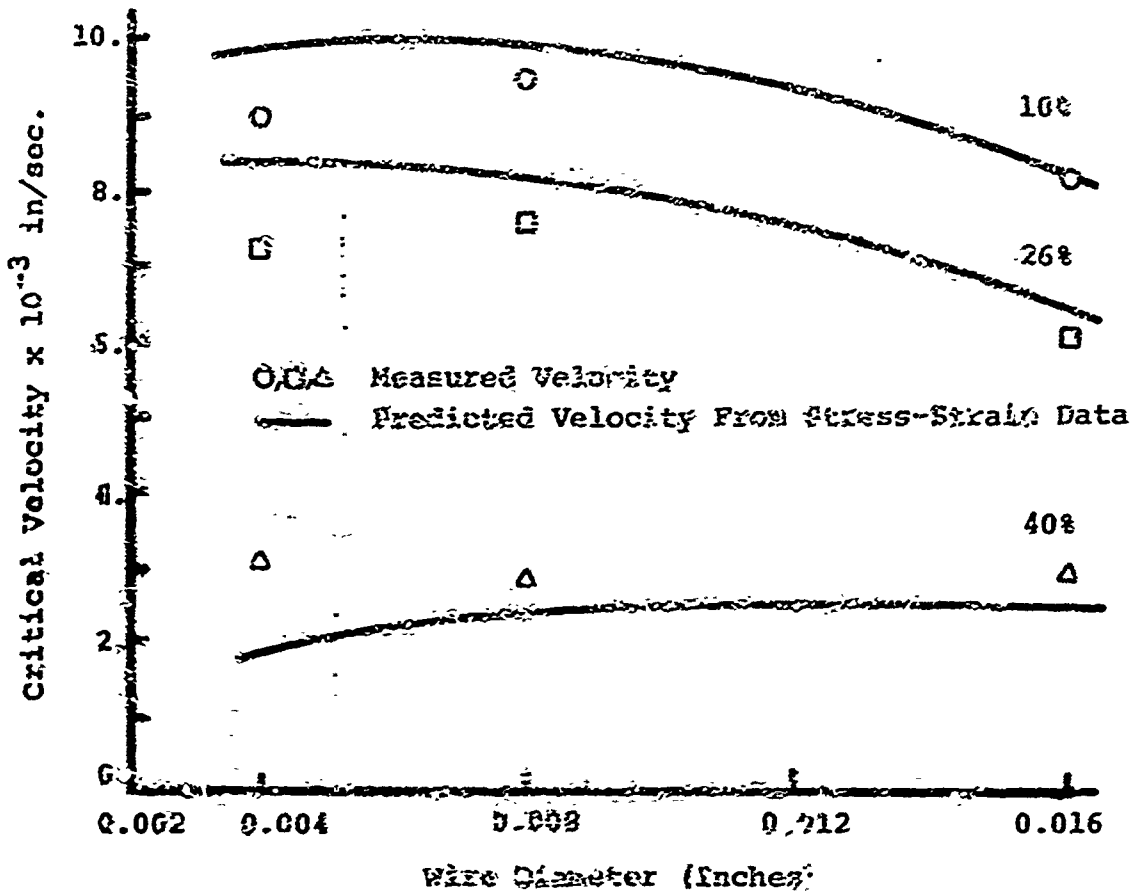


Figure 37. Critical Fracture Velocity Versus Wire Diameter for Steel-Epoxy composites $V_f = 10\%, 26\%, 40\%$

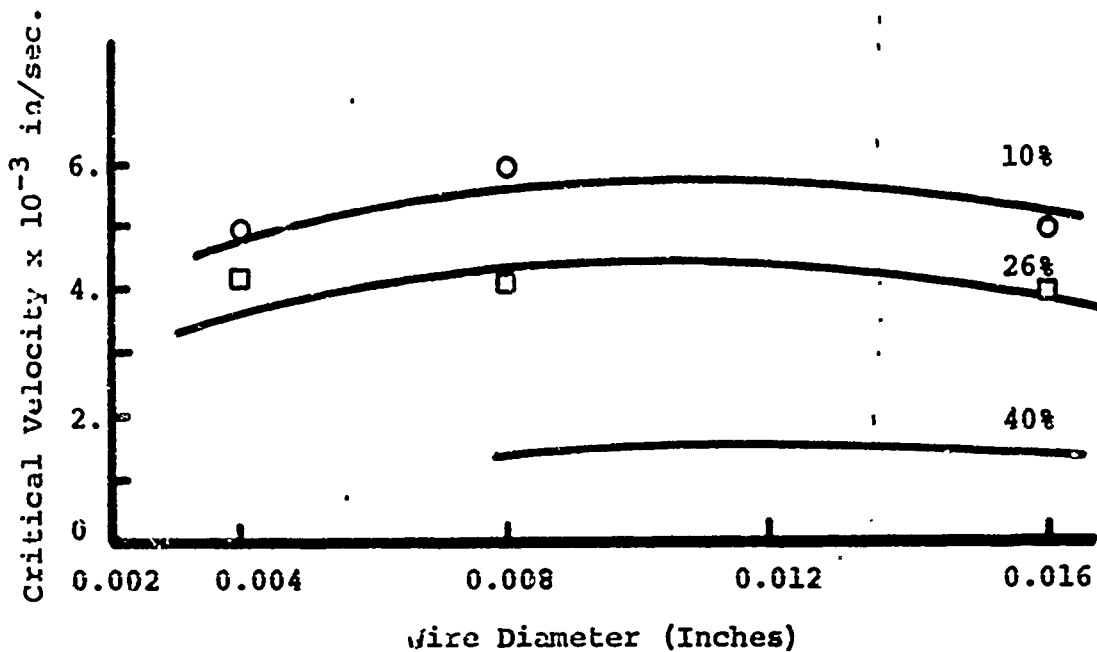


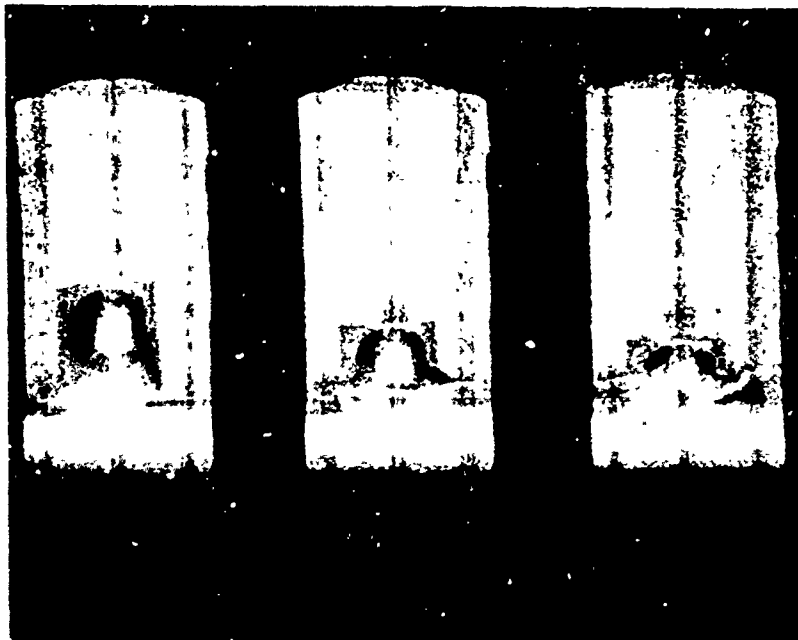
Figure 38. Critical Plastic Flow Velocity Versus Wire Diameter for Steel-Epoxy Composites $V_f = 10\%$, 26% , 40%

Data obtained provided good correlation between predicted and actual test results for early specimen failure and ultimate specimen fracture. The experimental points shown represented bracketed data for impact velocities since a completely precise determination was not obtainable within the present program. It is noted that experimental data for the critical velocity V_p for the forty volume percent specimens is absent. This is due to the increased embrittlement of the steel-epoxy specimens with increase in volume percent of reinforcing filament such that only specimen fracture could be observed. This effect is evident in the mechanical properties data described in paragraph 2.1, Section II, and is further correlated with results shown in Figures 37 and 38. In both results for V_p and V_F there appears to be an optimum wire size for a particular volume percent of reinforcement which will generally yield an optimum critical velocity.

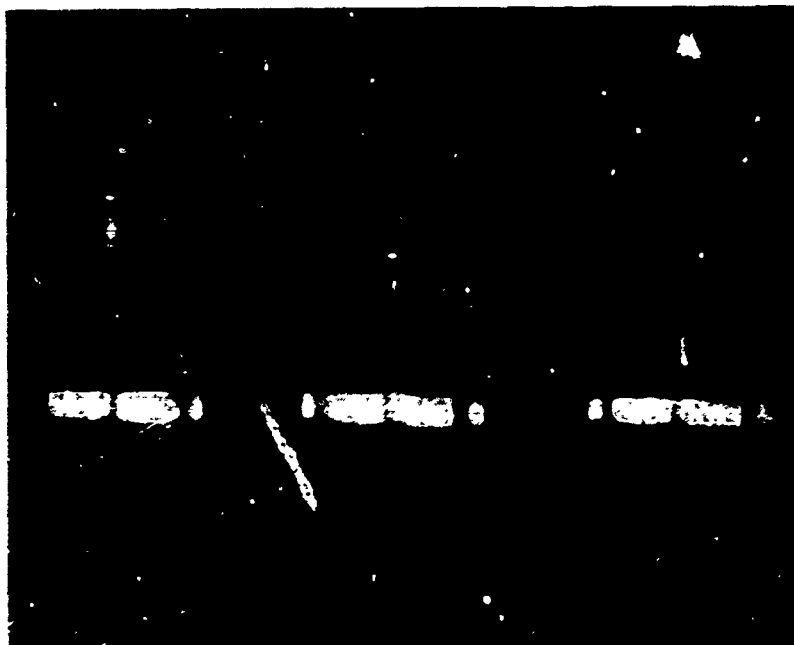
Documentation of defined V_p and V_f have been described in Reference 1, using post impact deformation photos along with photo sequences of the actual impact event at the target area. Comparing the dynamic failure/fracture characteristics as obtained from strain rate data with that obtained from gun tests, it is observed that for low volume percents of reinforcement at the various wire sizes tested and for low speed impact, a comparable local deformation was observed. However, as the impact velocity was increased, comparable to increased strain rate, specimen fracture associated with segmented fragments was obtained.

3.2 Aluminum-Nickel

As mentioned in paragraph 2.2, Section II, this composite system is representative of a metal matrix reinforced material having several basic microstructures. Unlike the man-made composite system described above, distinguishable modes of failure/fracture are not discernible. For the present system the definition of failure properties is defined in terms of a dynamic yield stress as measured by observable plastic deformation. As in the preceding discussion a relationship between the pressure bar test results and impact tests from the air gun assembly was sought. The dynamic deformation characteristics of the material specimens tested in the Hopkinson Pressure Bar are shown in Figure 30, while typical target impact sequences are shown in Figure 39. A summary of the post impact results for the specimens along both the transverse and longitudinal sections are also shown in Figures 40 and 41. Since failure for these specimens is associated with excessive plastic deformation in the impact zone, the analytical techniques discussed in References 18 through 20 for single phase materials were examined in relation to the composite systems. The property of particular interest to evaluate for this system was the dynamic compressive yield stress obtained by measuring the extent of the plastic deformation zone for various impact velocities. Since the deformation patterns obtained here resemble those for monolithic aluminum, Taylor's analysis was used to predict the dynamic yield stress from deformation measurements of post yielded specimens. It was found that this technique predicted the lower yield stress consistently and reliably to within several percent.



(a) Whisker Type Reinforcement, Impact Velocity = 19,050 In/Second



(b) Plate-Like Reinforcement, Impact Velocity = 16,000 In/Second

Figure 39. Dynamic Target Impact Behavior of Aluminum-Nickel

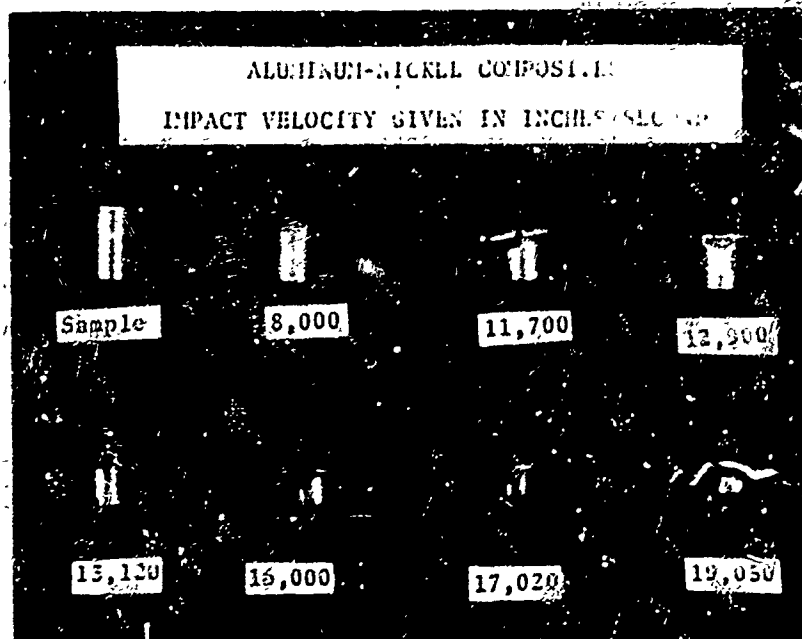


Figure 40. Dynamic Deformation at Various Impact Velocities
Aluminum-Nickel Composites Side View $V_f = 11\%$

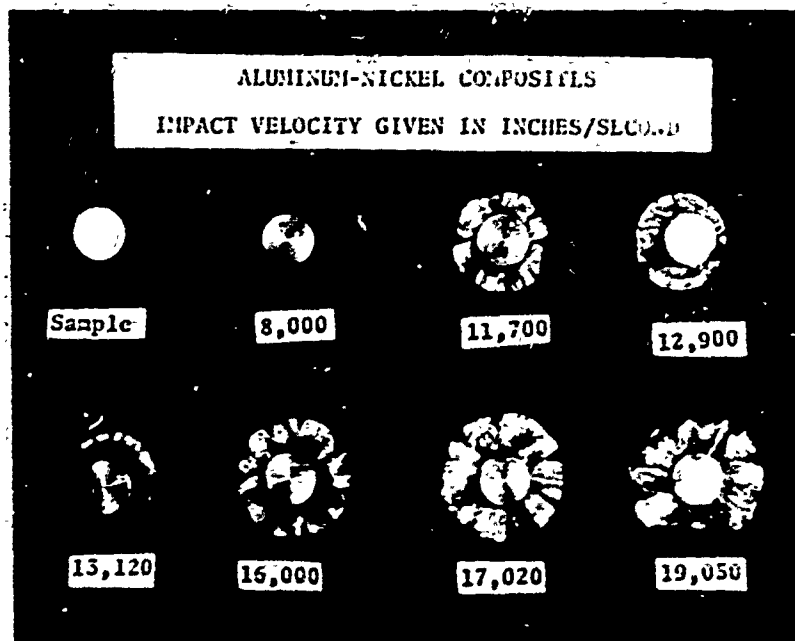


Figure 41. Dynamic Deformation at Various Impact Velocities
Aluminum-Nickel Composites End View $V_f = 11\%$

3.3 Tungsten-Copper

The two types of fabricated tungsten-copper specimens have been impact tested to examine their failure characteristics. As in the preceding metal matrix system, failure is defined in terms of excessive plastic deformation. Some typical target impact sequences for the tungsten-copper fiber system are shown in Figure 42 while post impact results for both types of specimens tested are shown in Figures 43 and 44. Examination of the filament reinforced specimens reveals that continuous deformation between the filaments and matrix has occurred. Further, this deformation is confined to the impacted end with the rigidly structured fiber arrangement following a symmetrical deformation pattern. For the tungsten rod reinforced system (Figure 44) virtually all the visible deformation occurs in the matrix materials.

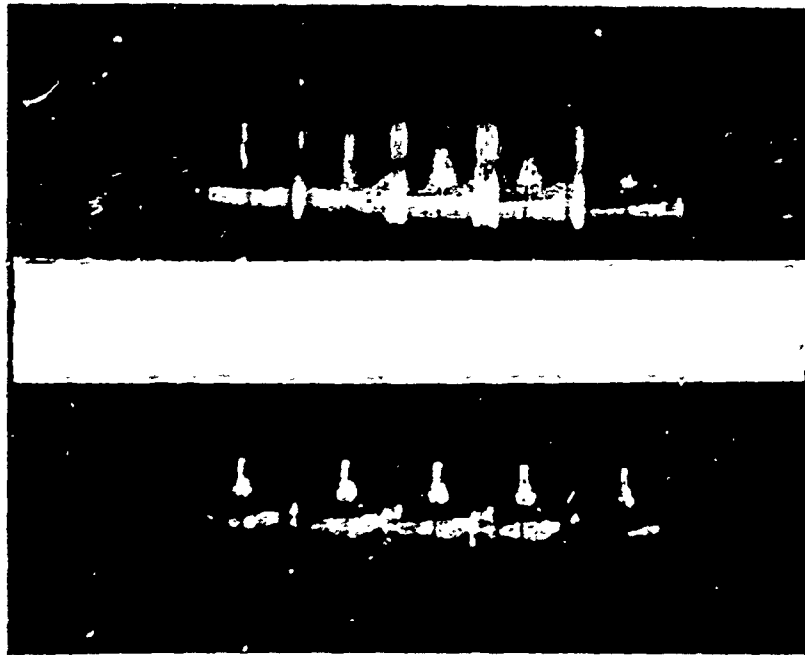


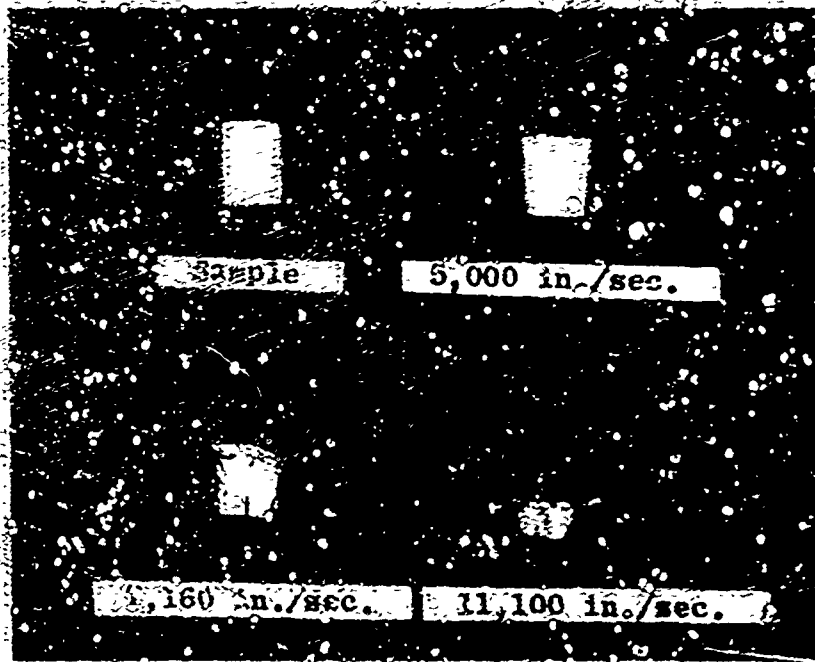
Figure 42. Dynamic Target Impact Behavior of Tungsten-Copper Composites

In order to relate the impact studies to the dynamic stress-strain behavior, the analytical techniques proposed by Taylor and Hawkyard (References 18 through 20) have been used. Using the initially observed yield stress from the dynamic stress-strain relations, agreement to within ten percent of Taylor's model has been obtained. Further, the dynamic stress appears to follow a rule of mixtures prediction for this type of composite systems as shown in Figure 45.

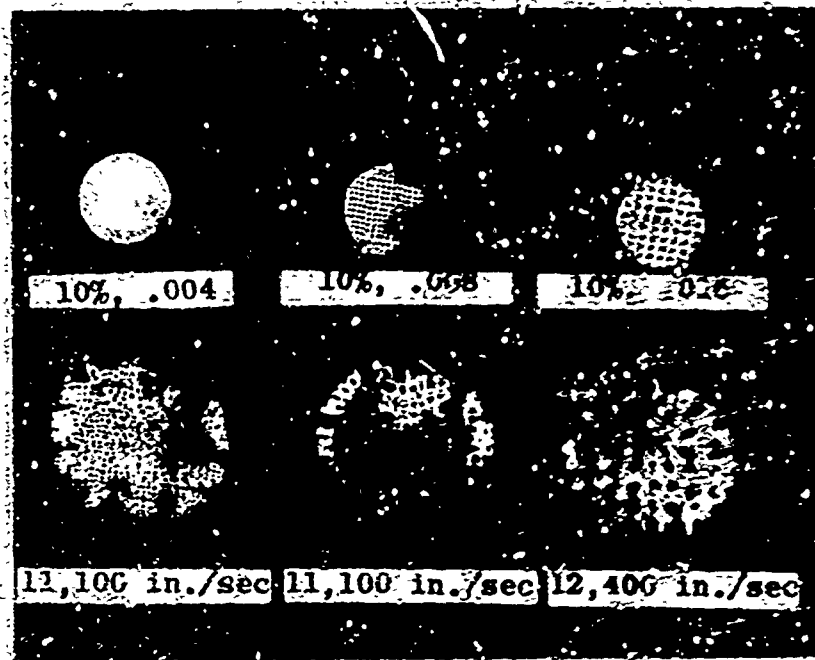
3.4 Other Systems

Both the boron-epoxy and graphite-epoxy systems were impact tested in order to correlate with previous dynamic testing and model systems. A series of impact tests on these specimens revealed failure by separation and delamination. Since both systems contained brittle reinforcements in a brittle matrix, the failure model developed for the steel-epoxy and and fiber-glass systems was used as a predictor for estimating the failure velocity, that is, the velocity at specimen separation. Using the simple energy criterion of equating impact energy to dynamic stored energy, calculated results agreed to within ten percent accuracy for both types of systems. Some typical post impact sequences for the boron-epoxy and graphite-epoxy specimens are shown in Figure 46, where the upper half of the photograph shows the factured boron composite and the bottom half the graphite system. In addition, Figure 47 shows a summary of the various composite systems impact tested in the velocity range of 6,000-7,500 in/sec. The specimens of the top row as shown are impacted pure epoxy, aluminum, Al_3Ni , and copper. The essentially pure metal matrix materials, that is, aluminum and copper, showed a more extensive plastic region in comparison to the localized deformation of the aluminum-nickel system for essentially the same impact velocity.

The second row shows an impacted tungsten-copper filament reinforced specimen, a one-quarter inch tungsten rod reinforced specimen, a one-eighth inch tungsten rod specimen, and a steel fiber reinforced epoxy specimen impact tested at approximately 7,000 in/sec. The first, second and fourth specimens are ten percent volume fraction reinforced composites. It is noted that the tungsten-copper specimens show considerable matrix deformation.

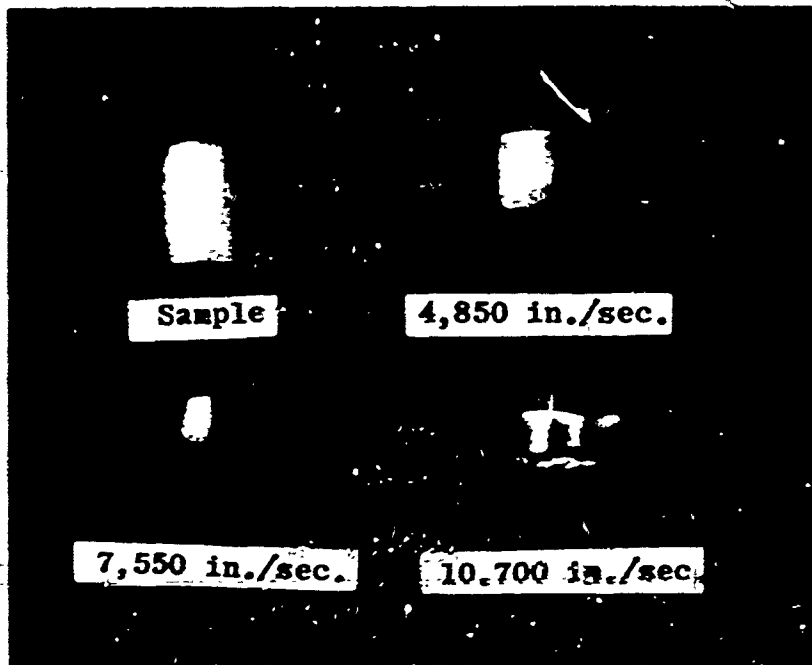


(a) Side View

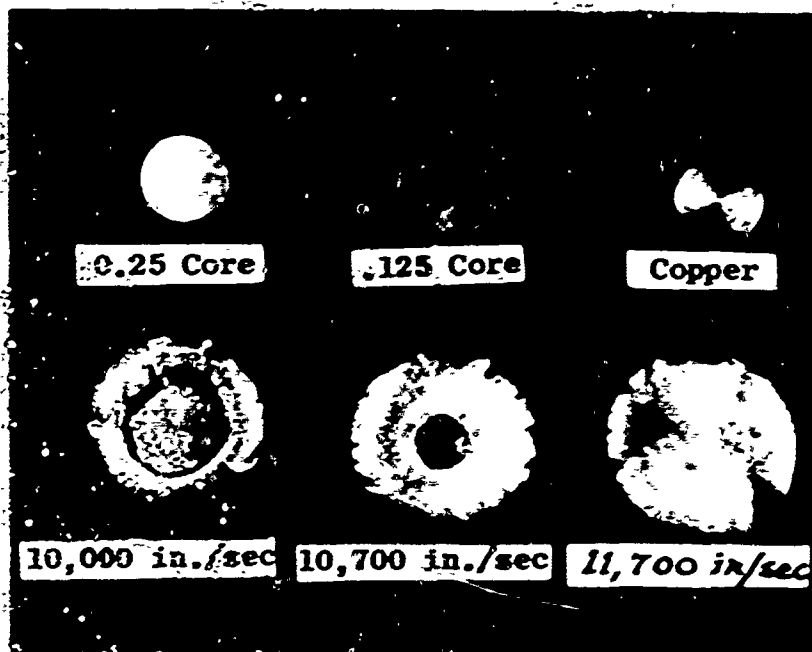


(b) End View

Figure 43. Dynamic Deformation at Various Impact Velocities
Tungsten-Copper Filament Composites $V_i = 10\%$



(a) Side View



(b) End View

Figure 44. Dynamic Deformation at Various Impact Velocities
Tungsten-Copper Rod Reinforced Composites $V_f = 10\%$

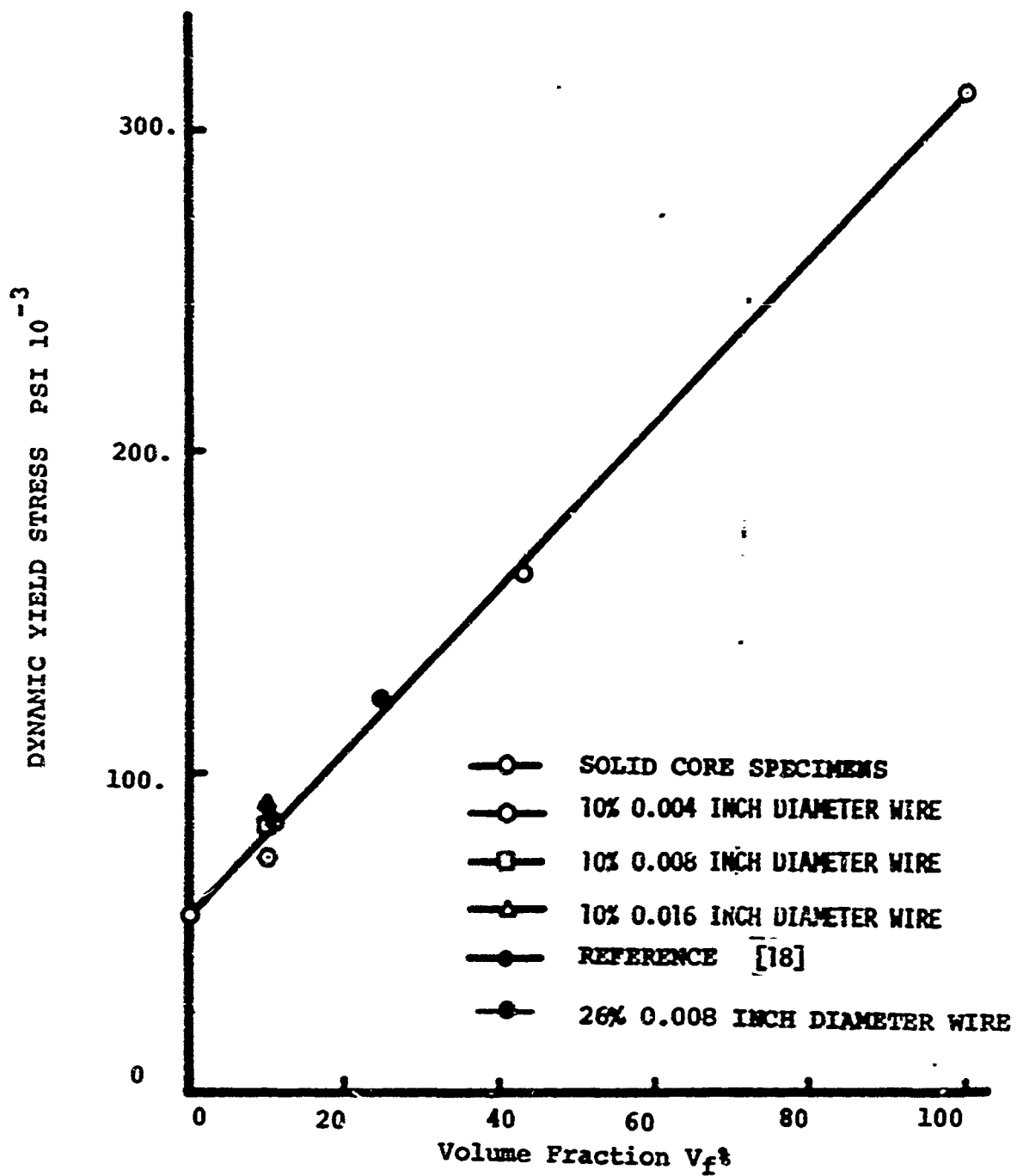


Figure 45. Dynamic Stress Versus. Volume Fraction for Tungsten-Copper Composites

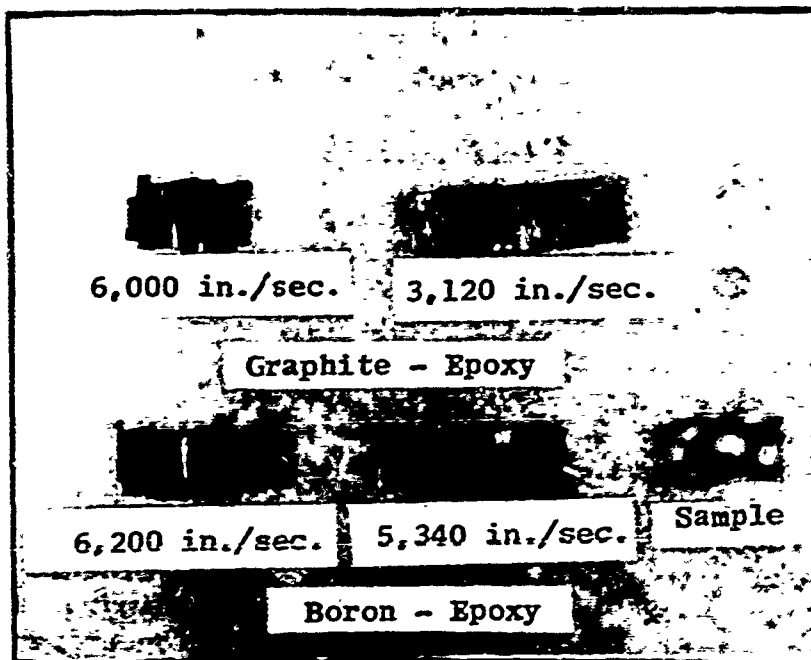


Figure 46. Dynamic Deformation at Various Impact Velocities Graphite-Epoxy and Boron-Epoxy

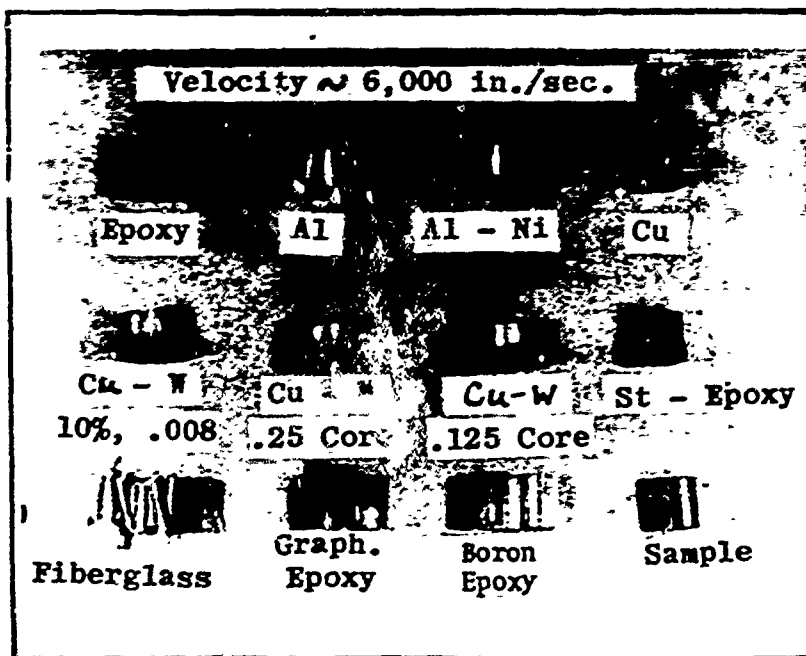


Figure 47. Dynamic Deformation Summary

The last row consists of brittle fiber reinforced epoxy matrix composites, reading from left to right, fiberglass, graphite, boron, and a typical undeformed specimen. All of these specimens fractured by separation and delamination.

3.5 Conclusions and Implications

Conclusions reached on the failure/fracture characteristics of projected composite specimens during impact studies are:

- (1) Consistent failure/fracture characteristics of composites can be determined for ductile and brittle matrix systems. For ductile matrix systems, failure by excessive deformation, defined in terms of dynamic yield stress or the extent of plastic yielding can be determined from the theoretical analysis presented in Reference 18. For brittle matrix systems a simple kinetic energy criterion has been found meaningful for predicting specimen separation and delamination and is defined by a critical impact velocity, V_F .
- (2) To predict composite failure/fracture behavior, knowledge of system response to dynamic loading in the principal loading mode is necessary.
- (3) Composite impact failure/fracture characteristics are not necessarily coincident with observed failure/fracture in low speed testing.
- (4) Ductile reinforced non-metal matrix systems impact tested can behave similarly to brittle reinforced non-metal matrix systems depending upon filament volume fraction and spacing.
- (5) Limited information indicates that the rule of mixtures can predict dynamic strengths for certain composite systems.

- (6) Concentrating the volume fraction of reinforcement into a single equivalent reinforcement, as opposed to ordered distribution, does not alter the apparent dynamic yield stress. The mode of failure, however, is changed from an overall uniform mushroomed deformation for distributed filaments to essentially matrix shear for a concentrated reinforcement. The apparent controlling factor in the deformation process appears to be the radial matrix-reinforcement stress.

The principal implications of these results in regard to potential behavior of composite projected specimens are:

- (1) A variety of failure/fracture modes utilizing composite specimens is possible. A design trade-off to achieve desired ductile-brittle material fracture behavior can be made by proper selection and combination of materials.
- (2) For brittle matrix impacted specimens, segmented fractures are obtainable in various numbers of segments, depending upon the geometric distribution and number of reinforcing filaments. This suggests the strong possibility of controlling the nature and location of fracture by proper design of the constituent element geometry.
- (3) For concentrated rod reinforced ductile matrix systems, the failure modes obtained suggest the design potential of utilizing the matrix as a simple binder for penetration and controlled fragmentation of the reinforcing elements.
- (4) Composite projectiles offer an approach to optimizing penetration of both softer and harder targets. This approach probably should be investigated separately in a clearly design-oriented program.

SECTION IV

WAVE PROPAGATION STUDIES

4.1 Introduction

In impact processes, energy may be transmitted large distances from the point of impact through stress waves and may cause considerable damage at distances remote from the impact point. In addition, the response of solid systems to explosive and impulsive loadings is often highly dependent on the strength and shape of stress waves generated as well as geometrical and material factors. It is therefore expected that in attempts to predict and to control the location and extent of fracture and other forms of damage during impact and impulsive loading processes, that the behavior of stress waves would be an important factor.

Composite materials clearly offer a number of promising advantages in the design of projectiles, explosive containers and impact resisting systems. There are, however, new questions and new problems which arise in the use of composites in these applications. Thus, although questions of speed, attenuation, and dispersion of waves in homogeneous metals are relatively well understood, very little knowledge is available for the behavior of stress waves in composites.

Some analytical studies related to this area for both layered and fiber reinforced materials have appeared in References 1, 21, 24 and 25. Further, some studies on the high speed shock Hugoniot problem have been discussed in References 26, 27 and 28. Experimental results for composite systems are quite limited. Some observations of test results for the elastic modulus of composites using longitudinal wave propagation tests for fixed volume percent and reinforcing filament size systems are found in Reference 29. More recent results on glass-epoxy and boron-epoxy systems determined from vibration studies are discussed in Reference 30.

The principal purposes of the program of tests reported in this section have been to determine, for rods of a representative composite material, the basic composite parameters influencing wave speeds in the composites, the spatial distribution of the dissipation of energy as waves traverse the rods, and the changes in shape or dispersion of the waves. In particular, as a first step in understanding the behavior of waves in composites, an examination has been made of the accuracy with which a rule of mixtures-type approach predicts the wave speeds, attenuation and dispersion of waves in steel reinforced epoxy composites. Since dynamic fracture is sensitive to the amplitude and shape of the stress waves causing it, results of these studies will help in attempts to use the unique capabilities of composites to provide for control of the location of fracture and to seek to create coalescence or cohesion of waves to accomplish various purposes.

4.2 Fabrication Process

Cylindrical rods 0.400 inch in diameter and 30 to 48 inches long were fabricated as follows. Type 304 soft stainless steel reinforcing wires in sizes 0.008 inch and 0.016 inch diameter were stretched to their yield point in an aluminum mold as shown in Figure 48. The relative position of wires in each layer was controlled by wrapping them around the accurately spaced pins shown outside the end of the rod section. Spacing between layers was controlled using shims.

When all reinforcing wires were accurately positioned and tensioned, the mold and wires were cleaned in a trichlorethylene vapor degreaser and then potted in an epoxy resin consisting of 100 parts Epon 828 resin with 12 parts Shell Agent 400 hardener. The mold was then covered and cured for two hours at 150°F.

The square cross section rod was then removed from the mold, machined round in a lathe, the ends ground perpendicular to the axis of the rod, and strain gages attached as appropriate.

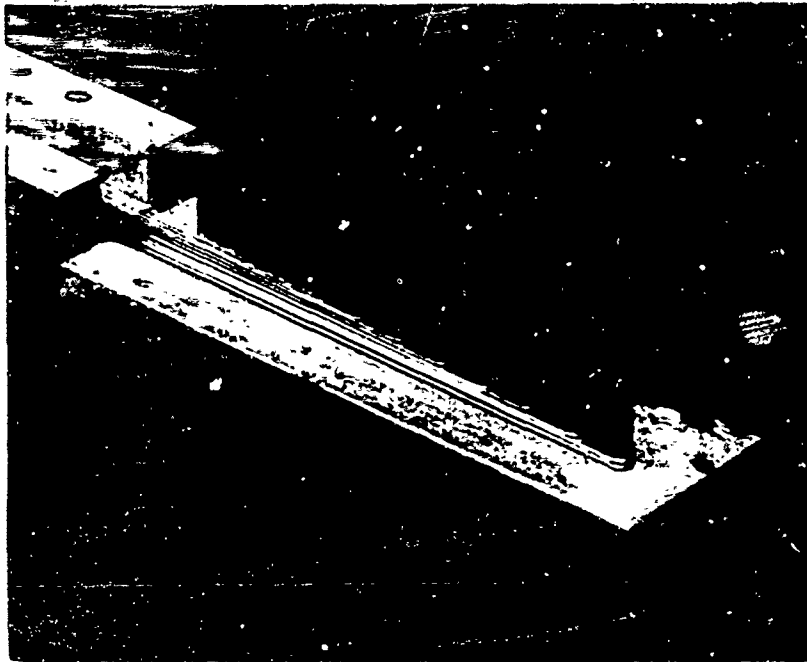


Figure 48. Aluminum Mold Used for Fabrication of Steel-Epoxy Composite Rods

The accuracy of the packing of the reinforcing wires is shown in Figure 49. These illustrations are typical of the packing accuracy both at the ends and throughout the length of the rod. The accuracy at central sections of the rod could be checked optically by looking laterally through the layers and rows of wire reinforcements.

The specimens were instrumented using BLH-FAE-06J-12S6 foil strain gages attached to the epoxy rods with Eastman 910 cement. The size of the gages insured that several filaments passed under each gage. The current through the gages was limited to five milliamps in order to eliminate heating in the vicinity of the gage. A Wheatstone bridge circuit using three dummy gages was used and the results displayed on a Tektronix 502A oscilloscope and recorded with a Polaroid camera.

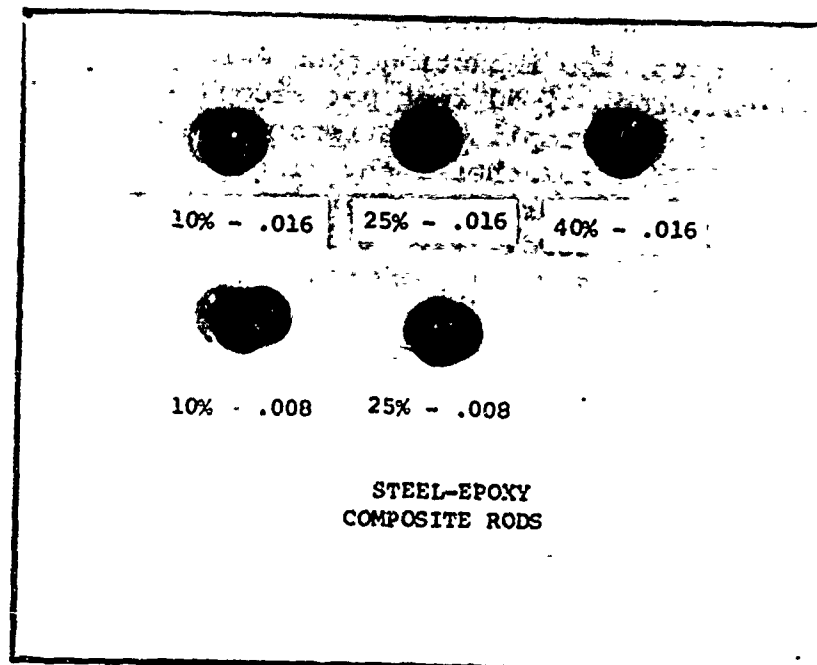


Figure 49. End View of Fabricated Composite Rods

The instrumented rods were next carefully aligned with the bore of an air gun which is described in Reference 1. To insure alignment, one end of the bar was inserted approximately 0.25 inch into the vented muzzle of the gun and the rods were supported at the 1/4 and 3/4 points by 1/8-inch wide teflon rings providing a loose slip fit.

Stress waves were initiated in the rods by impact with homogeneous bars propelled by the air gun. The solid steel specimens were impacted using a six-inch long steel bar of approximately 0.382-inch diameter. The composite and solid epoxy specimens were impacted by a 3-3/16 inches long by 0.382 inch diameter epoxy rod. To insure that slight misalignment would not significantly influence test results, the ends of the impacting bars were rounded slightly with the center crowned to extend 0.003 to 0.005 inch past the outside diameter.

For these tests, the impacting rods were propelled at velocities in the order of 50 feet per second and therefore produced relatively low amplitude stress waves with strains in the order of 750 microinches/inch. The exact impact velocity was adjusted to provide an appropriate pulse size on the oscilloscope being used. Figure 50 shows a specimen set up in the gun muzzle ready for testing.

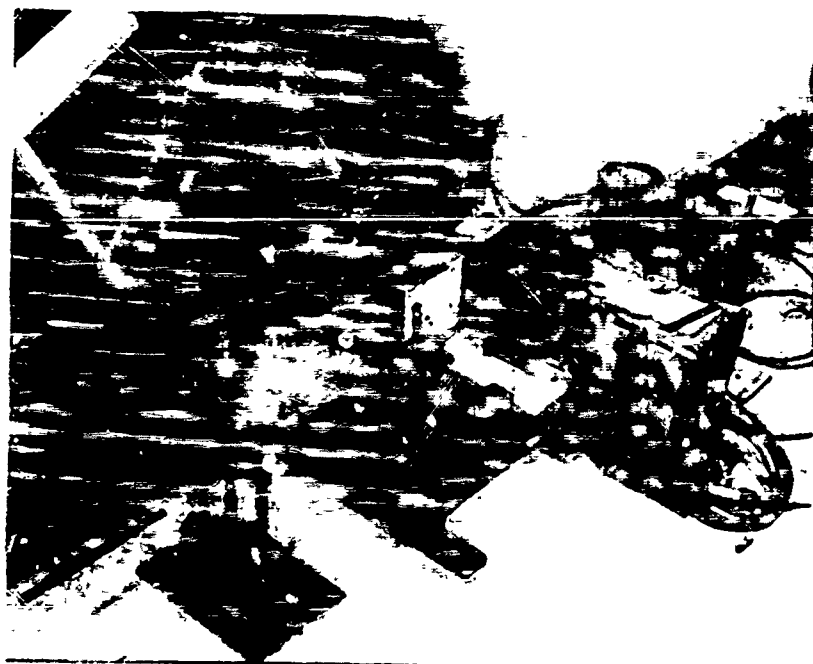


Figure 50. Experimental Test Set-Up for Wave Propagation Studies

4.3 Wave Speeds

The principal purposes of these tests were to determine if essentially one-dimensional waves propagated longitudinally in axially reinforced composites with varying wire size and volume percent reinforcement would be drastically changed, and if they would propagate with a velocity predicted by a rule of mixtures-type formula: Where E_f and E_m are the moduli of the filament and matrix,

$$C_c = \sqrt{\frac{E_f V_f + E_m V_m}{\rho_f V_f + \rho_m V_m}}$$

Essentially square pulses of approximately 100 microseconds duration were introduced into the rods by the impact process described in the previous section. Figures 51 through 54 show the raw photographic data on which the conclusions of this and the following two sections are based. Table II gives, in tabulator form, the experimentally observed wave speeds in pure epoxy, steel and a variety of composite rods, plus the rule of mixtures predictions of the wave speed in the composites based on the experimentally observed speeds in steel and epoxy. Figure 55 provides a graphic display of the accuracy with which the rule of mixtures predicts the wave speeds in these composites.

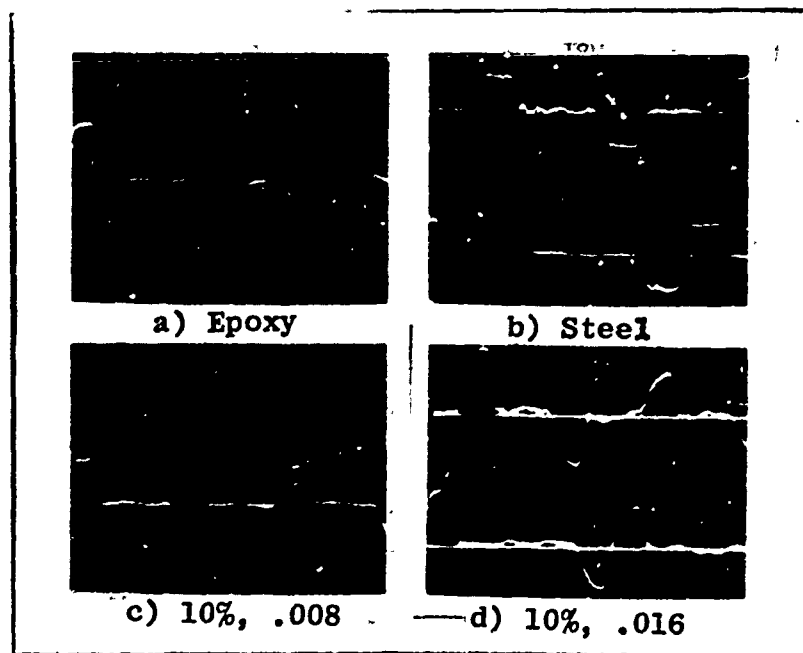


Figure 51. Experimental Wave Propagation Results
 V_f in Percent and Wire Diameter in Inches

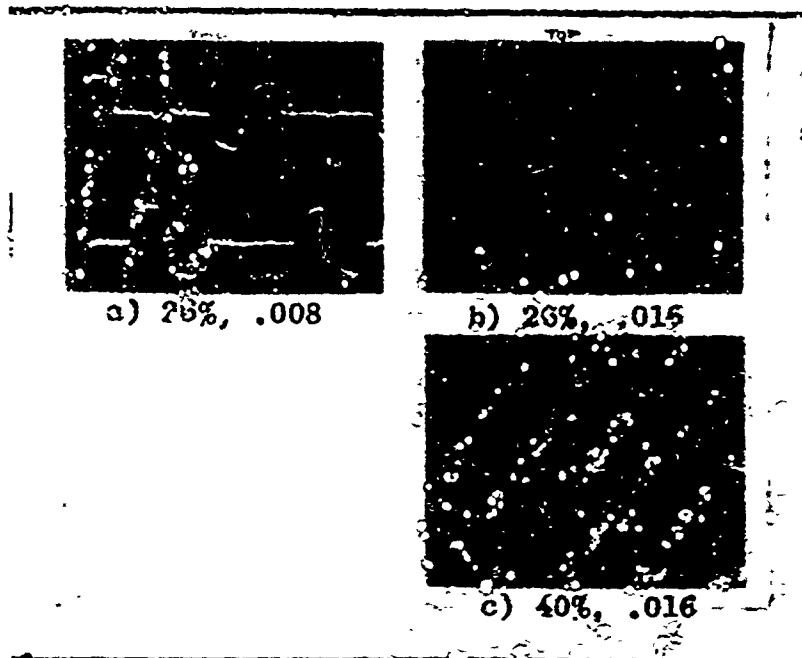


Figure 52. Experimental Wave Propagation Results
 V_f in Percent and Wire Diameter in Inches

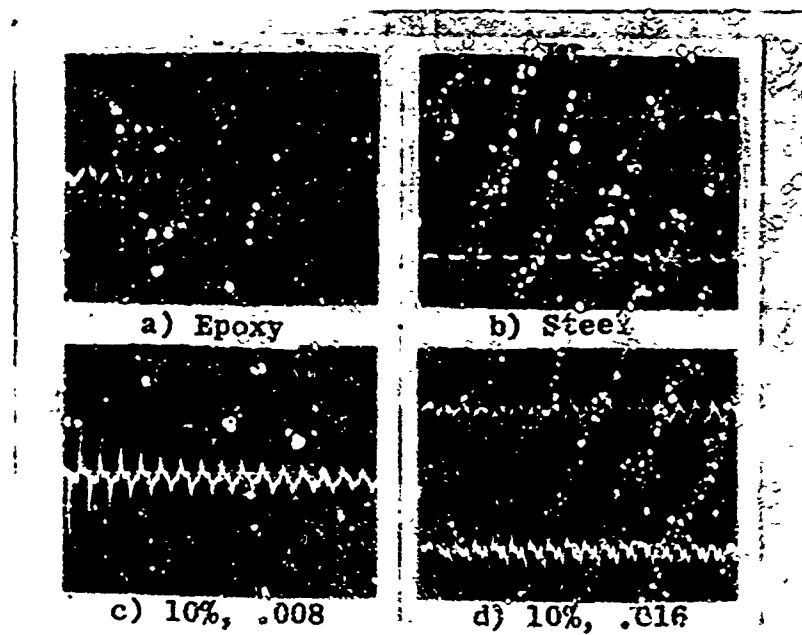


Figure 53. Experimental Wave Propagation Results
 V_f in Percent and Wire Diameter in Inches

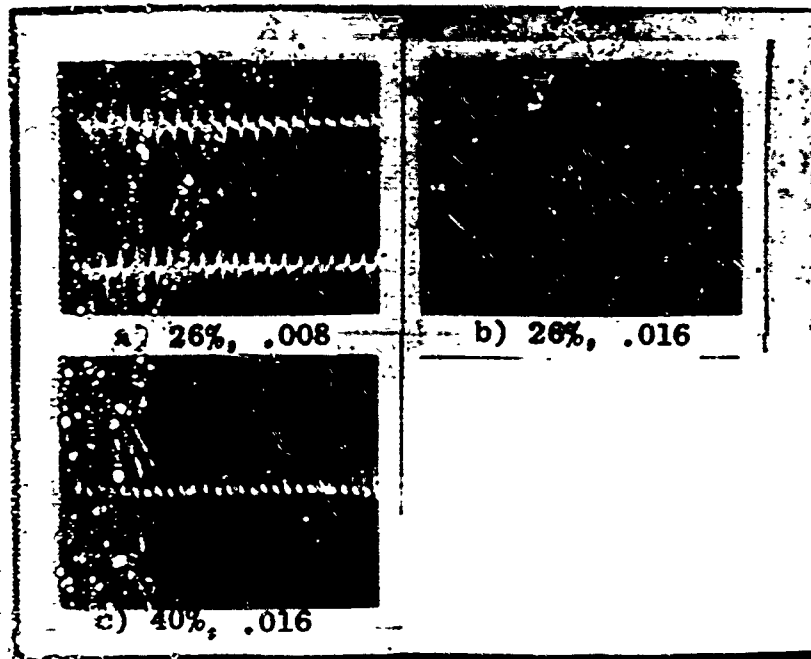


Figure 54. Experimental Wave Propagation Results
 V_p in Percent and Wire Diameter in Inches

TABLE III. WAVE SPEEDS OF TEST SPECIMENS

Spec.	Experimentally Observed In/Sec.		Rule of Mixtures In/Sec.
	Initial	Avg for 1000 In.	
Steel	197,300	197,300	197,300
Epoxy	72,220	73,500	75,220
10%-0.008	137,800	142,000	142,500
26%-0.008	152,400	178,500	171,000
10%-0.016	143,600	147,800	139,600
26%-0.016	172,900	179,000	167,400
40%-0.016	188,000	193,300	183,000

The wave speeds presented in Table III and Figure 55 involve an average of tensile and compressive wave speeds since at least one wave reflection was involved in each test. A careful examination of the data indicates that there is a consistent difference between tensile and compressive wave speeds with the speeds in tension being somewhat higher than the speeds in compression. The wave speeds appeared to be slightly amplitude dependent, also, with higher speeds corresponding consistently to lower amplitudes. These differences are shown in Table III and Figure 55.

The wave speeds determined here were computed using measured distances between points of maximum slope on the pulses observed in Figures 51 and 52. Overall, an instrumentation and measurement accuracy of plus or minus two percent is believed reasonable.

4.4 Amplitude Attenuation and Wave Dispersion

It is expected that stress waves traveling along composite rods would both attenuate and disperse. The attenuation will be considered first.

The ratio of change in amplitude to current amplitude per unit distance wave travel was chosen as the most appropriate measure to be used. Information was extracted from the raw data of Figures 53 and 54 and is presented in Table IV in tabular form and graphically in Figure 56. The solid curve of Figure 56 represents a rule of mixtures' prediction of the attenuation factor between the values for pure steel and pure epoxy. Except for the 0.016 wire, 40% volume fraction, the rule of mixtures' predictions are seen to be quite good.

TABLE IV. WAVE ATTENUATION FOR TEST SPECIMENS

Spec.	Attenuation in $^{-1} \times 10^3$
Steel	0.317
Epoxy	1.040
10%-0.008	0.791
26%-0.008	0.586
10%-0.016	0.807
26%-0.016	0.626
40%-0.016	0.303

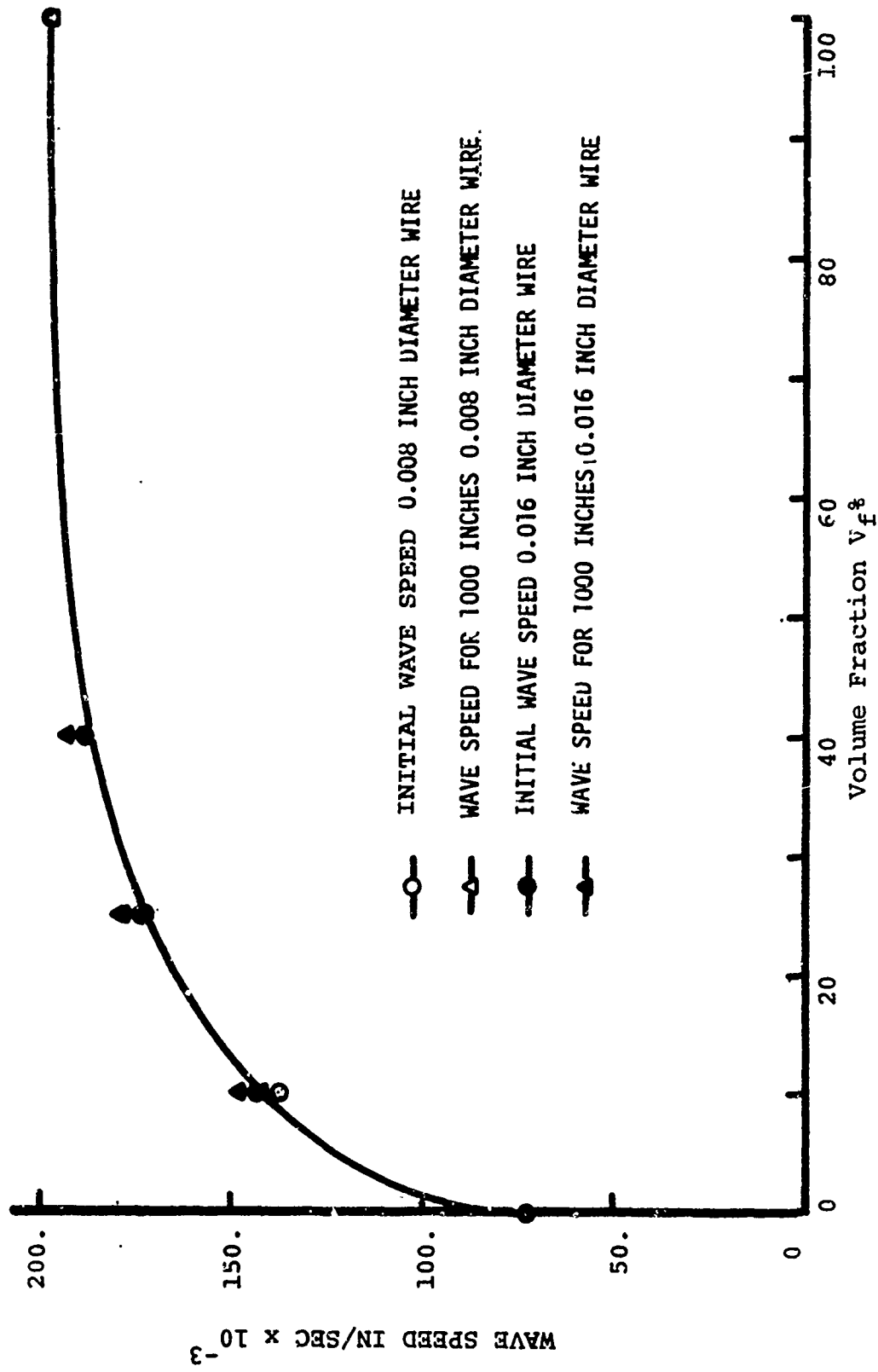


Figure 55. Rule of Mixtures Prediction for Composite Wave Velocities

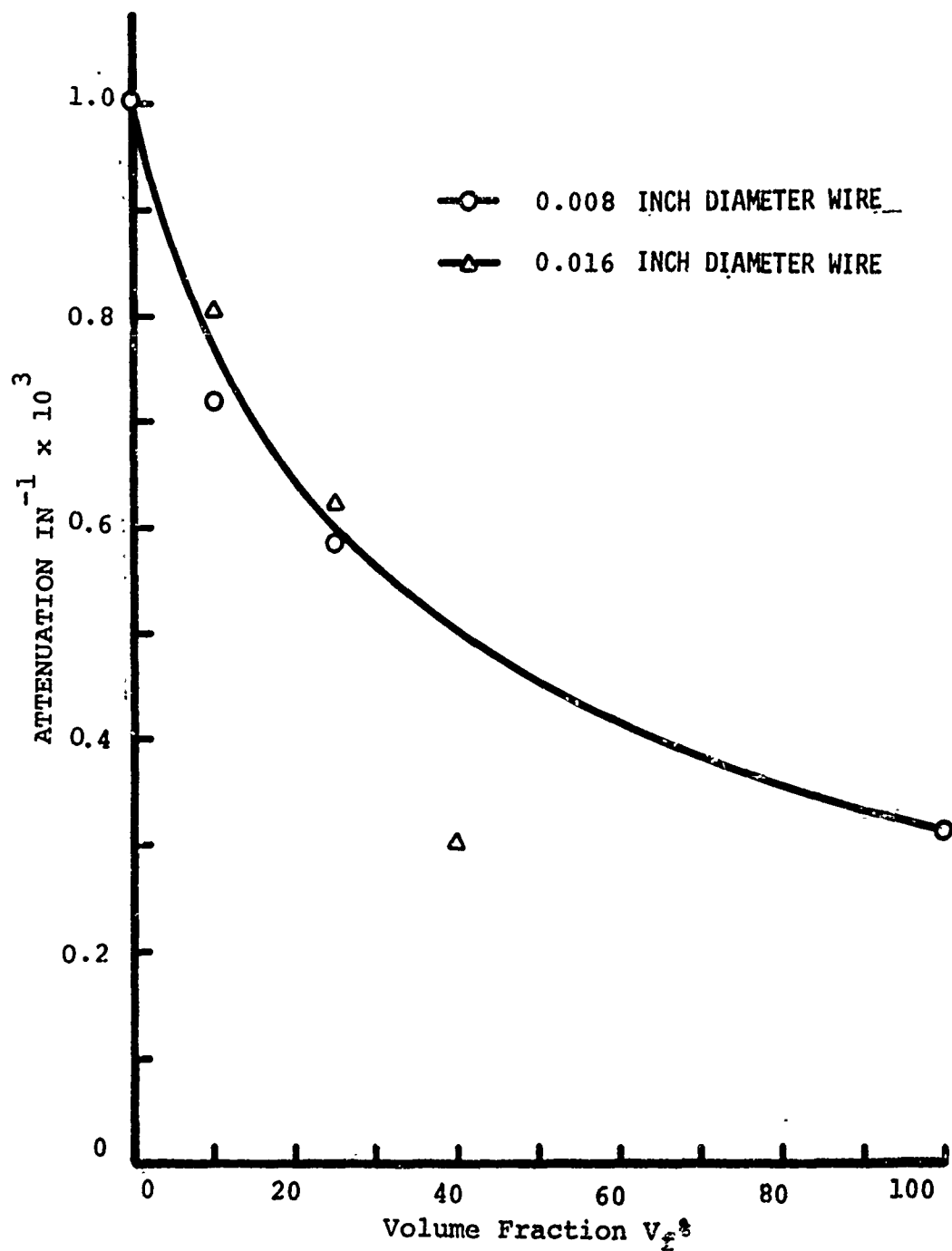


Figure 56. Rule of Mixtures Prediction for Composite Attenuation

The results presented in Table IV and Figure 56 involve approximately 20 traverses of the rod with reflections at each end. Since a relatively large number of reflections are involved, it is reasonable to inquire as to their participation in the attenuation. Since, however, no unique contribution of reflections to attenuation is expected in the all steel and pure epoxy rods, all ends being ground square to the same accuracy, and since the rule of mixtures does predict with good accuracy most of the results of the composite tests, it is believed valid to assume that reflection attenuation plays a minor role compared to the attenuation taking place during the traverse of waves along the rods. No reasonable explanation has been advanced for the relatively low attenuation of the 0.016-inch fibers - 40% reinforcement rod and in view of the consistency of other results, this result is considered to be in error.

The dispersion and shape change of pulses was also considered. It was not possible to obtain meaningful quantitative data regarding dispersion from the data of Figures 53 and 54 and therefore only qualitative observations and conclusions can be made. In studying the change of shape and dispersion of pulses the stress versus time at a single point has been measured. The pulses initiated in all tests were relatively square and thus symmetric. In all cases the amplitude gradually diminished as was discussed earlier in this section. In addition, the waves consistently dispersed or spread out in time and space. For the steel rods, as expected, these effects were small and the results symmetrical. For the epoxy, much larger changes took place but the results were again symmetrical. In the case of the composite rods, however, a consistent change in shape leading to a non-symmetrical pulse was observed. Consistently, the peak amplitude shifted toward the following part of the pulse and away from the beginning of the pulse. Further, at large distances, in the order of 1,000 inches or more, for the composite rods the shapes changed sufficiently drastically that individual pulses became difficult or impossible to identify.

For relatively early times and short distances, therefore, the most significant result regarding pulse shape change and dispersion is the unexpected change in shape and peak shift present in the composite rods but not present in either the all steel or all epoxy rods. Since the initial pulse shapes and specimen machining accuracy were similar for all specimens, this result is believed to be intrinsic in the composite nature.

4.5 Conclusions and Implications

The principal conclusions which can be drawn from this work regarding the propagation of small amplitudal pulses along axially reinforced long cylindrical rods, are:

- (1) Wave speeds are accurately predicted by a rule of mixtures approach using speeds in pure matrix and pure reinforcing material for reference.
- (2) Tensile waves propagate at somewhat higher rates than compressive waves.
- (3) Wave speeds are somewhat amplitude dependent with lower amplitudes propagating at higher speeds.
- (4) The amplitude attenuation of waves is accurately predicted by a rule of mixtures approach using the attenuation factors for pure steel and pure epoxy as reference.
- (5) Attenuation during the reflection process at a free end is negligible compared to attenuation during propagation over distances in the order of 30 inches.
- (6) Significant dispersion takes place in the composite rods and in contrast to the pure epoxy and pure steel, peak amplitude is retarded for the composites leading to non-symmetrical pulse shapes.

The implications of these results regarding the behavior of projectiles and impacted and impulsively loaded solid systems are as follows:

- (1) Since the attenuation of waves in the composites can be expected to be significantly larger than the attenuation in equivalent structural metals, the stress waves created by projectile impact of impulsive loading will be less dangerous and damaging at significant distances from the impact or loading point and therefore damage is expected to be more localized.

- (2) Since dynamic fracture is sensitive to pulse shape, the fact that in these composites the shape changes from symmetrical to non-symmetrical in a relatively short propagation distance, indicates the possibility of using pulse shape change as another tool in attempts to control the location and nature of fracture.
- (3) Thus, in summary, for composites materials, in addition to control of geometry and strength distribution, modification of material attenuation rates and modification of pulse shapes may be used as additional variables in attempts to design and control the extent, nature and location of fracture.

APPENDIX

PRELIMINARY PLATE IMPACT TESTS

In the present investigation, principal attention has been focused on dynamic material properties and associated wave propagation phenomenon. This has involved developing fabrication procedures for representative composite systems in order to test ordered array type specimens in the laboratory. One system which has been extensively tested following developed fabrication procedures is the steel-epoxy system for which cylindrical compression type and long bar specimens have been fabricated. An extension of the fabrication scheme for producing compression specimens has been developed in order to produce plate specimens. The main objective of this development was to demonstrate fabrication feasibility of finite size composite plate systems based on previously developed controlled fabrication schemes for small sized specimens. Furthermore, with the capability of producing such plate specimens, the practically important problem of studying projectile-target interaction could be examined. In relation to current Air Force Armament Laboratory programs, such studies could yield direct experimental data for comparison with presently developed computer codes for monolithic materials as reported on in References 10 through 12.

In order to test the plate specimens, a special holding attachment as shown in Figure I-1 has been developed for penetration type studies. Also included in this figure is a cross sectional view indicating the layered structural arrangement of steel fiber reinforcement. In this ordered arrangement a seven layer lay-up is shown, wound with adjacent layers perpendicular. Alternate fiber arrangements including additional fiber layers and orientations are obtainable using the present winding apparatus.

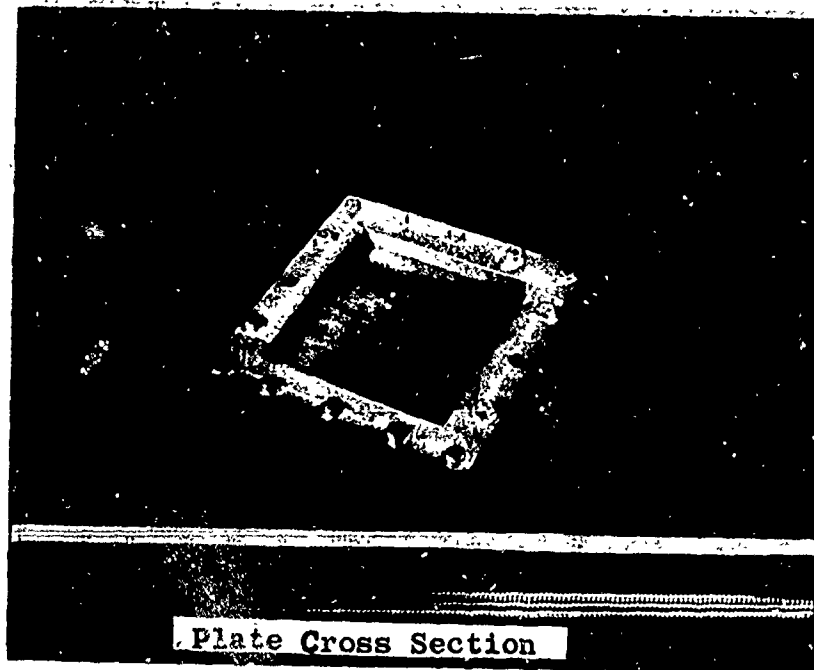


Figure I-1. Composite Plate Mounted for Impact Test

In order to evaluate the projectile-target interaction and failure phenomena an adaptive fixture was inserted into the air gun assembly described in Reference 1. A flat-ended steel projectile of 0.382-inch diameter was then fired at the composite target assembly at a velocity of 400 in/second. This firing velocity penetrated the target assembly, and a photograph of this post-impact composite target assembly is shown in Figure I-2. The localized penetration and failure, as indicated from the wave propagation and dispersement tests, is evident in this Figure.

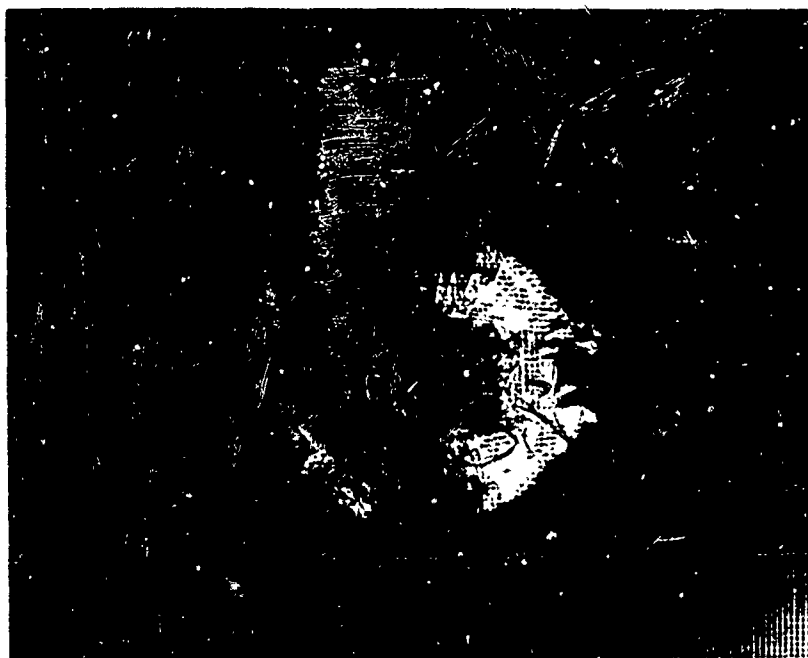


Figure I-2. Fracture Pattern of Penetrated Composite Plate

In summary, the experimental investigation discussed above has demonstrated:

- (1) Capability of fabricating layered plate assemblies with ordered reinforcements.
- (2) Feasibility of modifying the present air gun assembly for projectile-target interaction studies.
- (3) Feasibility of obtaining experimental target interaction data for composite systems as input for correlation studies with wave propagation data and existing numerical computations technique as discussed in References 10 through 12.
- (4) Potential application of composite projectile-target interaction parameters to allow prediction and control of the nature, location, and timing of fracture of projectile during impact. Thus, information on control of trajectories of fractured segments for subsequent penetration could be evaluated for short range application.

REFERENCES

1. Sierakowski, R. L., Nevill, G. E., Jr., Ross, C. A., and Jones, E. R., "Studies of the Ballistic Impact of Composite Materials," AFATL-TR-69-99, Air Force Armament Laboratory, Eglin Air Force Base, Florida, July 1969, UNCLASSIFIED.
2. Sierakowski, R. L., Nevill, G. E., Jr., Ross, C. A., and Jones, E. R., "Experimental Studies of the Dynamic Deformation and Fracture of Filament Reinforced Composites," Proceedings 11th AIAA/ASME Structures, Structural Dynamics, and Materials Conference, Denver, Colorado, 22-24 April 1970, UNCLASSIFIED.
3. Moncunill de Ferran, E., and Harris, B., "Compression Strength of Polyester Resin Reinforced with Steel Wires," Journal of Composites Materials, Volume 4, page 62, 1970, UNCLASSIFIED.
4. Rosen, B. W., "Mechanics of Composite Strengthening," Fibre Composite Materials, ASM, 1964, UNCLASSIFIED.
5. Foye, R. L., "Compression Strength of Unidirectional Composites," Paper presented at AIAA Meeting, 1966, UNCLASSIFIED.
6. Yue, S. F., Crossman, F. W., Vidoz, A. E., and Jacobson, M. I., "Controlled Microstructures of Al-CuAl₂ Eutectic Composites," Transactions AIME, Volume 242, page 2441, 1968, UNCLASSIFIED.
7. Lager, J. R., and June, R. R., "Compressive Strength of Boron-Epoxy Composites," Journal of Composite Materials, Volume 3, page 48, 1968, UNCLASSIFIED.
8. Pinnel, M. R., and Lawley, A., "The Role of the Interface Region on the Mechanical Behavior of Metal--Matrix Composites," ONR-TR-3, Drexel University, Pennsylvania, February 1970, UNCLASSIFIED.

REFERENCES (Continued)

9. Lindholm, U. S., and Bessey, R. L., "A Survey of Rate Dependent Strength Properties of Metals," AFML-TR-69-119, Air Force Materials Laboratory, Wright-Patterson Air Force Base, Ohio, April 1969, UNCLASSIFIED.
10. Sedgwick, R. T., "Theoretical Terminal Ballistic Investigation and Studies of Impact at Low and Very High Velocities," AFATL-TR-68-61, Air Force Armament Laboratory, Eglin Air Force Base, Florida, April 1969, UNCLASSIFIED.
11. Sedgwick, R. T., "Theoretical Investigation of Metallic Perforation by Kinetic Energy Projectiles," AFATL-TR-69-54, Air Force Armament Laboratory, Eglin Air Force Base, Florida, April 1969, UNCLASSIFIED.
12. Sedgwick, R. T., "Numerical Solution of Ballistic Impact," AFATL-TR-69-73, Air Force Armament Laboratory, Eglin Air Force Base, Florida, June 1969, UNCLASSIFIED.
13. Lemkey, F., Hertzberg, R., and Foxd, J., "The Microstructure, Crystallography, and Mechanical Behavior of Unidirectionally Solidified Al-Al₃Ni Eutectic," Transactions AIME, Volume 233, page 334, 1965, UNCLASSIFIED.
14. George, F. D., Ford, J. A., and Solkind, M. J., "The Effect of Fiber Morphology on the Tensile Behavior of Al₃Ni Whisker Reinforced Aluminum," in ASTM Special Technical Publication, page 427, 1967, UNCLASSIFIED.
15. Jech, R. W., McDaneis, D. L., and Weeton, J. W., "Fiber Reinforced Metallic Composites," Proceedings 6th Sagamore Ordnance Materials Research Conference, 1959, UNCLASSIFIED.
16. McDaneis, D. L., Jech, R. W., and Weeton, J. W., "Stress-Strain Behavior of Tungsten Fiber-Reinforced Copper Composites," WASA-TR-D-1881, WASA-Lewis, Ohio, 1963, UNCLASSIFIED.

REFERENCES (Continued)

17. Kelly, A., and Tyson, W. R., "Tensile Properties of Fiber-Reinforced Metals: Copper/Tungsten and Copper Molybdenum," Journal of Mechanics and Physics of Solids, Volume 13, page 329, 1965, UNCLASSIFIED.
18. Nicolas, T., "The Mechanics of Ballistic Impact--A Survey," AFML-TR-67-208, Air Force Materials Laboratory, Wright-Patterson Air Force Base, Ohio, July 1967, UNCLASSIFIED.
19. Hawkyard, J. B., Eaton, D., and Johnson, W., "The Mean Dynamic Yield Strength of Copper and Low Carbon Steel at Elevated Temperatures from Measurements of the "Mushrooming" of Flat-Ended Projectiles," International Journal of Mechanical Sciences, Volume 10, page 929, 1968, UNCLASSIFIED.
20. Hawkyard, J. B., "A Theory for the Mushrooming of Flat-Ended Projectiles Impinging on a Flat Rigid Anvil, Using Energy Considerations," International Journal of Mechanical Sciences, Volume 11, page 313, 1969, UNCLASSIFIED.
21. Achenbach, J. D., and Herrmann, G., "Dispersion of Free Harmonic Waves in Fiber Reinforced Composites," AIAA Journal, Volume 6, page 1832, 1968, UNCLASSIFIED.
22. Achenbach, J. D., Hemann, J. H., and Ziegler, F., "Tensile Failure at Interface Bonds in a Composite Body Subjected to Compressive Loads," AIAA Journal, Volume 6, page 2040, 1968, UNCLASSIFIED.
23. Puppo, A., Fenb, Ming-Yuan, and Haener, J., "Micro-dynamics of Wave Propagation," AFML-TR-68-311, Air Force Armament Laboratory, Wright-Patterson Air Force Base, Ohio, 1968, UNCLASSIFIED.
24. Armenakas, A. E., "Propagation of Harmonic Waves in Composite Circular-Cylindrical Rods," Journal of the Acoustical Society, Volume 47, page 822, 1970, UNCLASSIFIED.

REFERENCES (Concluded)

25. Kinslow, R., "Stress Waves in Laminar Materials," Bulletin of the American Physical Society, Volume 15, page 192, 1970, UNCLASSIFIED.
26. Chou, Pei-Chou, "Introduction to Wave Propagation in Composite Materials," in Composite Material Workshop, Technomic Publishing Company, Connecticut, 1968, UNCLASSIFIED.
27. Tsou, F. K. and Chow, Pei Chi, "Analytical Study of Hugoniot in Unidirectional Fiber Reinforced Composites," Journal of Composite Materials, Volume 3, page 500, 1969, UNCLASSIFIED.
28. Torvik, P. J., "Shock Propagation in a Composite Material," Journal of Composite Materials, Volume 4, page 236, 1970, UNCLASSIFIED.
29. Albott, B. W. and Broutman, L. J., "Stress-Wave Propagation in Composite Materials," Experimental Mechanics, Volume 6, page 383, July 1966, UNCLASSIFIED.
30. Tauchert, T., and Moon, F., "Propagation of Stress Waves in Fiber Reinforced Composite Rods." Proceedings 11th AIAA/ASME Structures, Structural Dynamics, and Materials Conference, Denver, Colorado, 22-24 April 1970, UNCLASSIFIED.

UNCLASSIFIED

Security Classification

DOCUMENT CONTROL DATA - R & D

(Security classification of title, body of abstract and indexing annotation must be entered when the overall report is classified)

1. ORIGINATING ACTIVITY (Corporate author) Department of Engineering Sciences and Mechanics, University of Florida Gainesville, Florida		2a. REPORT SECURITY CLASSIFICATION UNCLASSIFIED	
3. REPORT TITLE FOLLOW-ON STUDIES ON THE BALLISTIC IMPACT OF COMPOSITE MATERIALS		2b. GROUP	
4. DESCRIPTIVE NOTES (Type of report and inclusive dates) Final Report - July 1969 to July 1970			
5. AUTHOR(S) (First name, middle initial, last name) R. L. Sierakowski C. A. ROSS G. E. Nevill, Jr. E. R. Jones			
6. REPORT DATE August 1970	7a. TOTAL NO. OF PAGES 96	7b. NO. OF REFS 30	
8a. CONTRACT OR GRANT NO. F08635-58-C-0115	9a. ORIGINATOR'S REPORT NUMBER(S)		
b. PROJECT NO.	9b. OTHER REPORT NO(S) (Any other numbers that may be assigned this report) AFATL-TR-70-87		
10. DISTRIBUTION STATEMENT This document is subject to special export controls and each transmittal to foreign governments or foreign nationals may be made only with prior approval of the Air Force Armament Laboratory (ADLRD), Eglin AFB, Florida 32542.			
11. SUPPLEMENTARY NOTES Available in DDC		12. SPONSORING MILITARY ACTIVITY Air Force Armament Laboratory Air Force Systems Command Eglin Air Force Base, Florida	
13. ABSTRACT Studies have been conducted on both metal matrix and non-metal matrix reinforced systems. Emphasis has been placed on fabricating high quality and reproducible specimens from each of these primary groups. In addition, tests have been conducted on specimens received from industrial sources, which are of current practical interest. Mechanical properties tests have been conducted using a conventionalinius Olser and (Lit Popkinson Pressure Bar System, in order to investigate composite strain rate sensitivity and load carrying capability. Further, failure/fracture studies have been conducted by projecting the various composite specimens at a rigid elastic target. Analytical criteria have been utilized in order to establish predictable trends in composite failure/fracture characteristics for potential application to terminal ballistics design. Finally, studies of wave propagation, attenuation, and dispersment have been conducted in order to establish criteria for evaluating energy transfer and absorption properties of composites as well as varying wave speed, for failure by controlled fragmentation.			

GG 1473

UNCLASSIFIED

Security Classification

UNCLASSIFIED

Security Classification

14 KEY WORDS	LINK A		LINK B		LINK C	
	ROLE	WT	ROLE	WT	ROLE	WT
Dynamic Compressive Behavior						
Wave Propagation Behavior						
Unidirectional Reinforced Composite Specimens						
Metal Matrix Reinforced Systems						
Non-Metal Matrix Reinforced Systems						
Failure/Fracture Studies						
Ballistic Impact						

UNCLASSIFIED

Security Classification